ELSEVIER

Treatise on Process Metallurgy

Volume 3: Industrial Processes, Part A

Editor-in-Chief
Seshadri Seetharaman

Co-editors-in-Chief
Alexander McLean
Roderick Guthrie
Sridhar Seetharaman

VOLUME 3

TREATISE ON
PROCESS METALLURGY
Industrial Processes, Part A

VOLUME 3

TREATISE ON
PROCESS METALLURGY

Industrial Processes, Part A

Editor-in-Chief

SESHADRI SEETHARAMAN
Royal Institute of Technology
Stockholm, Sweden

Co-editors-in-Chief

ALEXANDER McLEAN
Department of Materials Science and Engineering
University of Toronto,
Toronto, Ontario, Canada

RODERICK GUTHRIE
McGill Metals Processing Centre,
Montreal, Quebec, H3A 2B2, Canada

SEETHARAMAN SRIDHAR
Royal Academy of Engineering / Tata Steel Research Chair
in Low Carbon Materials Technologies
University of Warwick
Coventry, UK

Amsterdam • Waltham • Heidelberg • London • New York • Oxford
ELSEVIER Paris • San Diego • San Francisco • Sydney • Tokyo

Elsevier
The Boulevard, Langford Lane, Kidlington, Oxford OX5 1GB, UK
225 Wyman Street, Waltham, MA 02451, USA

British Library Cataloguing in Publication Data
A catalogue record for this book is available from the British Library

Library of Congress Cataloging in Publication Data
A catalog record for this book is available from the Library of Congress

Volume 3 SET ISBN: 978-0-08-096988-6
PART A ISBN: 978-0-08-100000-7
PART B ISBN: 978-0-08-100001-4

For information on all Elsevier publications
visit our website at store.elsevier.com

Printed and bound in United Kingdom.
14 15 16 17 10 9 8 7 6 5 4 3 2 1

This book is dedicated to the Memory of former Chief Co-editor Professor Masanori Iwase, Kyoto University, Japan

January 10, 1948 to September 29, 2011

Professor Masanori Iwase, known to his friends as "Masa," was a beacon of knowledge with respect to the thermochemistry of metallurgical systems. He graduated from Kyoto University with his Bachelor's Degree in 1971, obtained his Master's Degree in 1973, and his Doctor of Engineering Degree in 1979, by which time he had already published 14 papers. From 1979 through 1981, he was a Post-Doctoral Fellow with Professor Alexander McLean's Group within the Department of Metallurgy and Materials Science at the University of Toronto. He was appointed Associate Professor in the Department of Ferrous Metallurgy, now the Department of Energy Science and Technology, at Kyoto University in 1985 and became Full Professor in 1996. On several occasions he served as Department Chair. He held visiting Professorships at the University of Toronto, the University of New South Wales, and the Royal Institute of Science and Technology in Stockholm and was granted the title of Honorable Professor by North Eastern University in China. He was a member of the International Editorial Board of "Transactions of the Iron and Steel Society of AIME" and "High Temperature Materials and Processes." He presented numerous courses on metallurgical chemistry to steelmaking engineers and researchers in Japan and countries overseas. He published over 200 technical papers and 2 books and obtained over 30 patents. He had a strong interest in the development of electrochemical sensors for the measurement of the chemical potentials of species in molten copper as well as in molten iron and steel and steelmaking slags. He was the inventor of a "Silicon Sensor" and an "FeO Activity Determinator" both of which are manufactured commercially and currently utilized by a number of steel companies in different parts of the world. In the area of slags, he made a number of major contributions by combining excellent experimental measurements with a sound knowledge of thermodynamics. During his later years, he was deeply engaged in the environmental problems associated with the metallurgical industries and conducted studies on waste incineration in the blast furnace. His research findings on the reduction of steelmaking slag volume and fluorspar consumption have been applied within several steel plants in Japan. In recognition of his many achievements, he received the Silver Medal Award from the Japan Institute of Metals in 1991 and the Nishiyama Memorial Award from the Iron and Steel Institute of Japan in 1993. During his last days, he was Co-Editor-in-Chief for this Treatise on Process Metallurgy. May it serve as a tribute to his numerous contributions.

David R. Gaskell, (1940 – 2013)

A Memorial Tribute

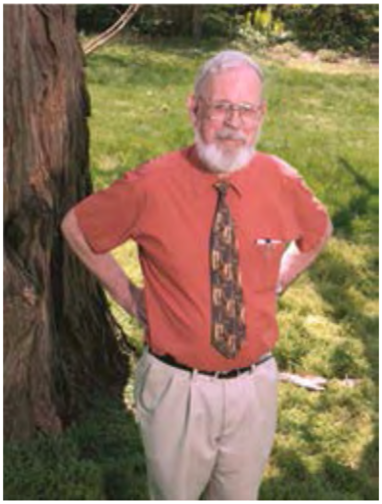

David Robert Gaskell was born in Glasgow, Scotland where he attended Glasgow University and The Royal College of Science and Technology. He received his B.Sc. and A.R.C.S.T. with First Class Honors in Metallurgy and Technical Chemistry in 1962 after which he spent two years working in England with the chemical industry. He married Sheena Morrow in 1964 and they had three children, Sarah, Claire and Drew. Shortly after their marriage they immigrated to Hamilton, Canada where David conducted graduate studies at McMaster University under the supervision of Professors R. G. Ward and A. McLean. His Ph.D. degree was awarded in 1967 with a thesis entitled: "The Densities of Liquid Silicates Containing Iron Oxide at 1410°C." Following his Doctoral studies, David joined the University of Pennsylvania as an Assistant Professor where he worked closely with Professor Geoff Belton. In 1982 he moved to Purdue University as a Professor of Metallurgical Engineering. During his career, Dr. Gaskell served as a Visiting Professor working with Dr. Charles Masson at the Atlantic Regional Laboratory of the National Research Council of Canada in Halifax, Nova Scotia (1975–1976) and as a Visiting Professor at the G.C. Williams Co-operative Research Centre for Extraction Metallurgy at the University of Melbourne (1995).

Professor Gaskell was gifted with an exceptional combination of intellect and curiosity and particularly enjoyed his teaching, his research and his discussions with students. He served as thesis advisor for numerous graduate students as well as faculty mentor for dozens of undergraduate student projects. He was the recipient on several occasions of the Schuhmann Best Teaching Award in Materials Engineering. Dr. Gaskell was a prolific writer with numerous publications in journals and conference proceedings. He was known internationally for his classic textbooks "Introduction to Metallurgical Thermodynamics", "An Introduction to the Thermodynamics of Materials", and "An Introduction to Transport Phenomena in Materials Engineering". He was also involved in professional activities, including the Metallurgical Society of AIME, Alpha Sigma Mu (President, 1985–1986) and the Iron and Steel Society Transactions International Advisory Board. In 1977 Dr. Gaskell was named a Distinguished Alumnus of McMaster University and in 2000 was the recipient of the John F. Elliott Memorial Lectureship Award from the Iron and Steel Society of AIME. At the time of his death, David was serving as one of four distinguished reviewers for this Treatise on Process Metallurgy. He will be remembered with great fondness by many friends around the world not only for his intellectual achievements, and they were many, but also for his laughter, his sense of fun and his ability to play the bagpipes.

CONTENTS

PART A

PART B

PREFACE

This book, "Treatise on Process Metallurgy", consisting of three volumes, aims to provide a comprehensive work that is intended to be a reference source for industrial and academic researchers and to provide material for teachers of process metallurgy. This effort was inspired by the successful series on Treatise for Physical Metallurgy by Robert Cahn and Peter Haasen published by Elsevier that has become a standard text found on the shelves of most academics and industrial metallurgists. We hope to mirror this success in the field of Process Metallurgy. This work is intended to provide the most pertinent contemporary developments within process metallurgy and offer a single complete collection of information on metal extraction processes from atomic level to industrial production.

The book is an important milestone in the development of technologies in metal extraction and refining that have evolved over the past millennia. After humans discovered fire and started using this energy source for metal extraction, the field of process metallurgy has grown from an art to an area of advanced technology. Growth has been significant over the past 200 years, and over the past five decades it has been exponential. Although there are books available describing well-defined aspects of the subject, it is rather surprising that we do not yet have a comprehensive volume which covers the broad spectrum of topics that constitute "process metallurgy". The current endeavor is aimed at addressing this deficiency.

An important phenomenon that has happened over the years is the separation of the subject of process metallurgy into ferrous and non-ferrous extraction processes. While the underlying principles are the same for both areas, the enormous impact of iron and steel on human civilization has given ferrous metallurgy a special place. Process design in the case of non-ferrous metals such as copper, lead and zinc, has often lagged behind that in iron and steelmaking. Over the course of time, the synergistic effects of the interactions between these two major areas of process metallurgy were lost. The present work is designed to bridge this knowledge gap.

Another development, which has manifested itself especially in Europe, is the division between "Theoretical Process Metallurgy" and "Applied Process Metallurgy". Fortunately, this division is not encountered to the same extent within Northern America. This division between theory and practice can be attributed in large part to the eagerness of industry to solve their immediate problems within tightly defined conditions and within the shortest possible time frame. As a consequence, in the absence of proper theoretical foundations, the solutions tend to be empirical in character and of limited applicability. In this context, it is worth emphasizing that no solution is generally applicable without proper theory, and no theory is particularly helpful, if it cannot be applied.

Another objective of this Treatise therefore, is to provide a bridge between fundamental concepts and practical applications.

The current work aims to present a comprehensive overview of the broad field of process metallurgy, bridging the above-mentioned gaps. It begins with a historical perspective of the development of metal extraction processes from the earliest of times to today's state-of-the art. There are thirteen chapters with about twenty five editors and eighty specialists, who have contributed to particular subject areas within which they

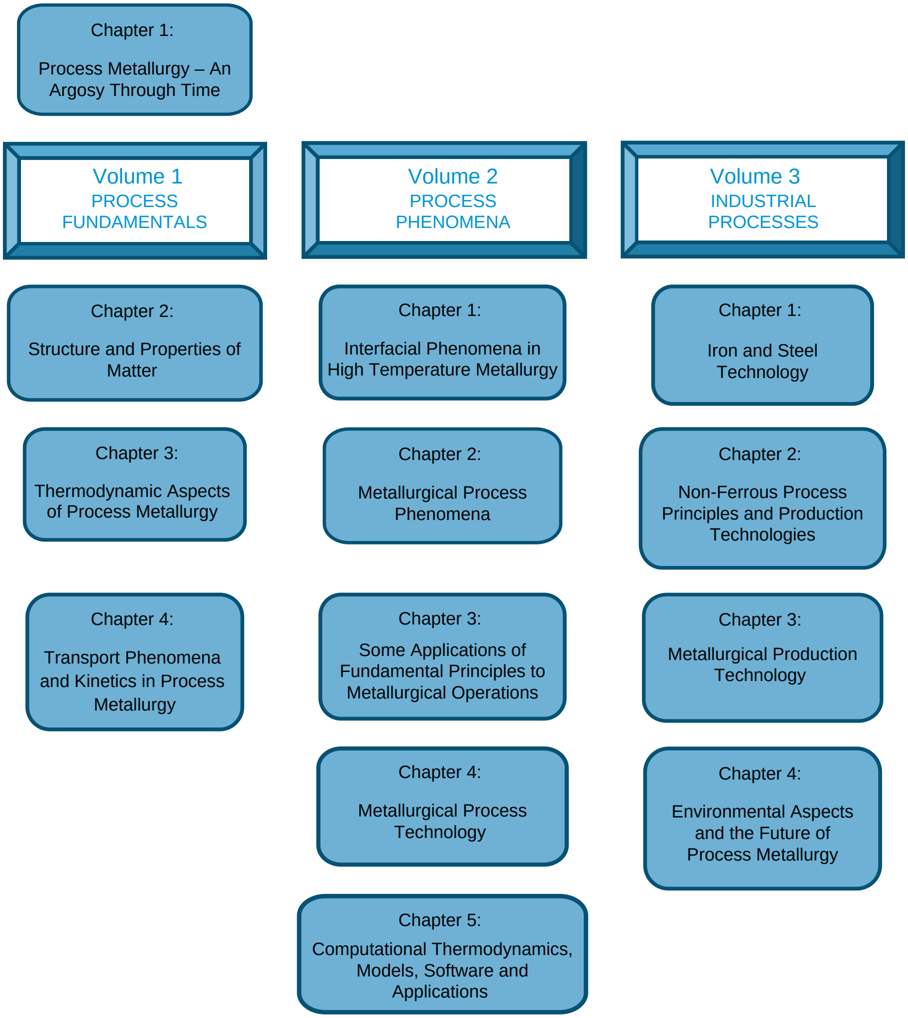

Figure. The flowchart of chapters in the Treatise.

are recognized experts. The development of the subject through these chapters is outlined in the following flow-chart.

The book is divided into three main streams. Following the first chapter which presents a birds-eye view of the history of metal extraction from stone-age to modern times, Chapters 2–4 present the process fundamentals. The second group of chapters on Process Phenomena, *viz*. Chapters 1–5, link the micro-modeling of process phenomena to macro-modeling of industrial processes, reactor technologies and computational models for process simulations. The third group deals with Industrial Processes. Chapters 1 and 2 present details of modern industrial practice for the extraction and refining of ferrous and non-ferrous metals respectively. Chapter 3 describes the design of metallurgical plants including the logistics, economics, intellectual property rights, upscaling and some case studies. The last chapter, Chapter 4, addresses the environmental problems existing today and the directions we should take for a better future. All chapters use the same nomenclature and symbols so that the reader can more readily see the links between related areas.

As the subject area is broad, the Treatise was designed as a multi-author work. The editors were asked to choose their contributors so that one red-thread passed through any particular chapter. While the potential problem of different schools of thought in each area had to be resolved, the editors took care that, where necessary, other schools of thought were presented, without causing confusion. The editors and contributors are from all parts of the world and formed a virtual forum of noted metallurgists who have worked in harmony for a period of more than two years. As the Board of Editors-in-Chief, it has been a distinct privilege to bring these leading members of the process metallurgy community together. We were also fortunate to obtain four world-famous metallurgists to review the chapters, so that their views could be implemented before the manuscripts were printed.

The publication of this Treatise is timely, as many of the present younger generation do not perceive Process Metallurgy as a "high-tech" area compared to more recent technologies, such as electronic-, bio- and nano-materials. The work is intended to show to the coming generations that Process Metallurgy is a continuously evolving subject area, like a flowing river, collecting tributaries from adjoining areas: sensor developments, signal processing, physical and mathematical modeling, automation, robotics and business management. It can be said, without exaggeration, that Process Metallurgy has had a major impact on the development of human civilization, and will continue to exert a powerful influence on metals production and the generation of advanced materials, for many decades to come.

The Board of Editors-in Chief expresses its deep gratitude to Staff Members at Elsevier who proposed the concept of a treatise on Process Metallurgy and who encouraged and assisted it throughout this activity. The generous support of Chief Editor, Seshadri Seetharaman, by the Swedish Steel Producers Association is also greatly appreciated. Finally, the Editors-in-Chief express their sincere thanks to the chapter editors, contributors and reviewers, for providing their valuable time and expertise, in order to bring this endeavor to a successful conclusion.

	Alexander McLean	Rod Guthrie	
Seshadri Seetharaman	Alexander McLean	Roderick Guthrie	Seetharaman Sridhar
Stockholm	Toronto	Montreal	Warwick

EDITOR IN CHIEF

Seshadri Seetharaman received his Ph.D. degree in Metallurgy from Indian Institute of Science, Bangalore, India, in the year 1971. He joined the Royal Institute of Technology, Stockholm, in 1973 as Senior Research Associate and became Associate Professor in 1981. Dr. Seetharaman was installed in the Chair of Theoretical Metallurgy in 1990 and he retired from this position at the end of 2010. Professor Seetharaman has about 350 peer-reviewed publications in leading journals in Metallurgy, about 150 conference presentations, and 10 patents. His major scientific interests are the fundamentals of Process Metallurgy that covers thermodynamics, transport phenomena, thermophysical properties of high temperature systems, and interfacial phenomena. He was also involved in the teaching of the above subjects.

Professor Seshadri Seetharaman has been nominated eight times as the best teacher in Materials Design teaching program at the Royal Institute of Technology. He has been awarded the President's Award in 1994 for meritorious contributions in teaching. He was selected as the best teacher of the Royal Institute of Technology in 2004.

Professor Seshadri Seetharaman has been awarded the Brimacombe Prize for the year 2010. He is an Honorary member of the Iron and Steel Institute of Japan, Honorary doctor at the Aalto University in Finland, Honorary Professor at the Metallurgical Academy of Ukraine as well as at The University of Science and Technology Beijing. He also received the Distinguished Alumni Award of the Indian Institute of Science, Bangalore, in the year 2013.

CO-EDITORS-IN-CHIEF

Alexander McLean

Following graduation with degrees in Applied Chemistry and Metallurgy from the Royal College of Science and Technology and the University of Glasgow, Dr. McLean spent 5 years at McMaster University before moving to Jones and Laughlin Steel Corporation in Pittsburgh. He joined the University of Toronto in 1970, and in 1984 the Ferrous Metallurgy Research Group was formed with Professor McLean as Director. He served as Department Chair from 1992 through 1997 and was appointed Professor Emeritus in 2002. He is an Honorary Member and elected Fellow of several organizations including AIME, The Iron and Steel Institute of Japan, the Royal Society of Canada, and the Canadian Academy of Engineering. He is a recipient of the Queen Elizabeth II Diamond Jubilee Medal and received Honorary Doctorates from the University of Miskolc and the University of Strathclyde. He has published extensively in the areas of iron and steelmaking and materials processing.

Roderick Guthrie

Roderick I.L. Guthrie, Ph.D. (Imperial College), ARSM, Eng., is the Macdonald Professor of Metallurgy and Director of the McGill Metals Processing Centre. An Honorary Member of ISIJ, Distinguished Member of AIST, Fellow of the Canadian Institute of Mining and Metallurgy, Fellow of the Royal Society of Canada, and Fellow of the Canadian Academy of Engineering, he is the author of two text books concerning *Engineering in Process Metallurgy* and *The Physical Properties of Liquid Metals*. The winner of the 2006 Killam Prize for Engineering, he was co-inventor of the successful LiMCA process for detecting inclusions in liquid metals, and also of the HSBC process for casting steel and aluminum alloy sheets. As a researcher, he has been keenly interested in the application of fluid flow, heat, and mass transfer phenomena in the description of metallurgical processes. A long-time consultant to the steel industry, Dr. Guthrie has worked in all segments of an integrated steelplant, from blast furnaces through steelmaking and hot rolling mills, to annealing and finishing lines.

Seetharaman Sridhar is currently the Tata Steel/RAEng Joint Chair for Research into Low Carbon Materials Technology. He was until recently the POSCO Professor of Steelmaking at Carnegie Mellon University and the co-director of the Industry–University Consortium, Center for Iron and Steelmaking Research (CISR) of which Tata is a member. He received his Ph.D. from the Massachusetts Institute of Technology and his undergraduate degree from the Royal Institute of Technology in Sweden.

His research and teaching interests lie in the physical chemistry of metal processing. He has published over 125 journal papers in the areas of secondary refining, casting and mold slags, coal gasification, oxidation, and hot-shortness. He has received the following best paper awards: Marcus Grossman Award from ASM, the Herty Award from ISS, The Spriggs Phase Equilibria Award from ACERS, and the Jerry Silver Award from AIST. He has also received the Friedrich Wilhelm Bessel Research Prize from the Alexander Von Humboldt Foundation and the NSF Career Award, both for his general contributions in research. As a teacher, he was recognized by the Benjamin Teare Teaching Award by Carnegie Institute of Technology, the Philbrook Prize by the MSE Department at CMU, and he was the recipient of the 2011 J.F. Elliott Lecturer Award for AIST. He is the editor for *AIST Transactions* and an associate editor for *Metallurgical and Metals Transactions A, B, and E*. He is also on the International Advisory Board for *Steel Research International* and *ISIJ International*.

CONTRIBUTORS TO VOLUME 3

P.S. Ananthanarayanan
Executive Director (Retired), Balmer Lawrie Ltd, Chennai, India

G. Balachandran
Scientist-F (Retired), Rare Earth Metals and Alloys Group, Defence Metallurgical Research Laboratory Kanchanbagh, Hyderabad, Andhra Pradesh, India

N. Balasubramanian
Center for Study of Science, Technology and Policy (CSTEP), Bangalore, India

Thomas Battle
Research and Development Technology Center, Midrex Technologies, Pineville, North Carolina, USA

Jean-Pierre Birat
European Steel Technology Platform (ESTEP), Bruxelles, Belgium

Bart Blanpain
KU Leuven Department MTM, Leuven, Belgium

Santanu Chakraborty
Visakhapatnam Steel Plant – Research and Development Division, RINL, Vishakhapatnam, Andhra Pradesh, India

A. Chychko
PEARL laboratory, Erasteel Kloster AB, Eramet group, Söderfors, Sweden (current) Material science and engineering department, Royal institute of technology, Stockholm, Sweden

Ichiro Daigo
Department of Materials Engineering, Graduate School of Engineering, The University of Tokyo

William G. Davenport
Department of Materials Science and Engineering, University of Arizona, Tucson, Arizona, USA

Rauf Hurman Eric
School of Chemical and Metallurgical Engineering, University of Witwatersrand, Johannesburg, South Africa

Michael L. Free
Department of Metallurgical Engineering, University of Utah, Salt Lake City, Utah, USA

Govind S. Gupta
Department of Materials Engineering Indian Institute of Science, Bangalore, India

Lauri Holappa
Department of Materials Science and Engineering, Aalto University, School of Chemical Technology, Espoo, Finland

Robert Hunter
Midrex Technologies, Charlotte, North Carolina, USA

Heikki Jalkanen
Department of Materials Science and Engineering, Aalto University, School of Chemical Technology, Espoo, Finland

Peter Tom Jones
KU Leuven Department MTM, Leuven, Belgium

Shin-ya Kitamura
Institute of Multidisciplinary Research for Advanced Materials, Tohoku University, Sendai, Japan

Eiki Kasai
Graduate School of Environmental Studies, Tohoku University, Japan

Takazo Kawaguchi
Process Research Laboratories, Nippon Steel & Sumitomo Metal Corporation

John Kopfle
Midrex Technologies, Charlotte, North Carolina, USA

S.S. Krishnan
Center for Study of Science, Technology and Policy (CSTEP), Bangalore, India

Seppo Louhenkilpi
Department of Materials Science and Engineering, Aalto University School of Chemical Technology, Espoo, Finland

Jorge Madias
Metallon, Buenos Aires, Argentina

Annelies Malfliet
KU Leuven Department MTM, Leuven, Belgium

Yasunari Matsuno
Department of Materials Engineering, Graduate School of Engineering, The University of Tokyo

Hiroyuki Matsuura
Graduate School of Frontier Sciences, The University of Tokyo, Japan

J.E.A. Maurits
Vancouver, Washington, USA

James McClelland
Research and Development Technology Center, Midrex Technologies, Pineville, North Carolina, USA

Ken Mills
Department of Materials, Imperial College, London, United Kingdom

Michael S. Moats
Department of Materials Science and Engineering, Missouri University of Science and Technology, Rolla, Missouri, USA

Michael Moats
Department of Materials Science and Engineering, Missouri University of Science and Technology, Rolla, Missouri, USA

Dong Joon Min
Materials Science and Engineering, College of Engineering, Yonsei University, Seoul Korea 120–749

Katsuhiro Nose
Institute of Industrial Science, The University of Tokyo

M. Nzotta
Process Development, Uddeholms AB, 6838 Hagfors, Sweden

Toru H. Okabe
Director, International Research Center for Sustainable Materials, Institute of Industrial Science, The University of Tokyo

M. Olivas-Martinez
Department of Metallurgical Engineering, The University of Utah, Salt Lake City, Utah, USA

Ray D. Peterson
Aleris International, Rockwood, Tennessee, USA

Kalevi Raipala
Rautaruukki Oyj (retiree), Tampere, Finland

John Rankin
CSIRO Process Science and Engineering, CLAYTON SOUTH VIC 3169, Australia

William J. Rankin
CSIRO Process Science and Engineering, Clayton, Australia

Koji Saito
Ironmaking Technical Division, Nippon Steel Corporation, Japan

S. Sarkar
Department of Metallurgical and Materials Engineering, Indian Institute of Technology, Madras, India

Lennart Scheunis
KU Leuven Department MTM, Leuven, Belgium

S. Seetharaman
Department of materials science and engineering, Royal institute of technology (KTH), 10044, Stockholm, Sweden

Il Sohn
Materials Science and Engineering, College of Engineering, Yonsei University, Seoul Korea 120–749

H.Y. Sohn
Department of Metallurgical Engineering, University of Utah, Salt Lake City, Utah, USA

Urvashi Srivastava
Research and Development Technology Center, Midrex Technologies, Pineville, North Carolina, USA

Alton T. Tabereaux
Alcoa Primary Metals, Muscle Shoals, Alabama, USA

Osamu Takeda
Graduate School of Engineering, Tohoku University

Hidetoshi Tanaka
Kobe Steel, Japan

L.D. Teng
Department of materials science and engineering, Royal institute of technology (KTH), 10044, Stockholm, Sweden

Fumitaka Tsukihashi
Graduate School of Frontier Sciences, The University of Tokyo, Japan

Tetsuya Uda
Department of Materials Science and Engineering, Kyoto University

Brinda K. Varma
Patent Attorney, Bangalore, Karnataka, India

Olle Wijk
Sandvik Materials Technology, Sandviken, Sweden

Yongxiang Yang
Department of Materials Science and Engineering, Delft University of Technology, Delft, The Netherlands

Jiayun Zhang
University of Science and Technology Beijing, China

ACKNOWLEDGEMENT

The Editors-in Chief express their sincere gratitude to
"Jernkontoret"- the Swedish Steel Producers' Association

for their generous support to Professor Seshadri Seetharaman towards the production of this book.

The support from the Iron and Steel Institute of Japan is gratefully acknowledged.

THE REVIEW COMMITTEE

The various chapters of the Treatise were distributed for review between the following internationally renowned metallurgists: Professors T. Emi (Japan), D. R. Gaskell (USA), D. C. G. Robertson (USA) and O. Wijk (Sweden). After the sad demise of Professor Gaskell, the review of his assigned material was completed by the Board of Editors-in-Chief and Dr. V.I. Lakshmanan (Canada). The Editors-in-Chief express their gratitude to the Reviewers for their invaluable contributions in improving the quality of the book.

CHAPTER 1

Iron and Steel Technology

Lauri Holappa
Department of Materials Science and Engineering, Aalto University, School of Chemical Technology, Espoo, Finland

Contents

CHAPTER 1.1

Ironmaking

Yongxiang Yang[a], Kalevi Raipala[b] and Lauri Holappa[c]
[a]Department of Materials Science and Engineering, Delft University of Technology, Delft, The Netherlands
[b]Rautaruukki Oyj (retiree), Tampere, Finland
[c]Department of Materials Science and Engineering, Aalto University, School of Chemical Technology, Espoo, Finland

1.1.1. INTRODUCTION

1.1.1.1. Early History of Ironmaking

In ancient times, iron was found as meteorite iron and used for ornaments and other small items. Then about 3500 years ago, people learned to produce iron in commercial amounts by reducing iron ore with charcoal in small furnaces, bloomeries. Where the technology was first invented, is not yet known.

The Iron Age began about 1200 BC. Iron was produced in small furnaces or even pits filled with charcoal and iron ore. The combustion air was blown with bellows. Even natural draft, especially on windy hillsides, was used. The bellows were driven by man power and that limited the height of the furnace to about 2 m. The hearth was about 0.5 m or less wide with one tuyere. When the hearth was full, the furnace was blown out, the hearth wall removed from one side and the iron lump pulled out from the hearth. The product from these furnaces was a solid block of malleable iron. The bloomery process was thus a direct method to produce steel from ore. The iron block contained various amounts of slag and therefore it had to be heated and hammered thoroughly to get the slag squeezed out from the block. The block was cut into smaller pieces and forged to tools and weapons or commercial blooms. The bloomery iron was unalloyed, low carbon steel. Blacksmiths were capable to carburize bloomery iron to get better hardness and strength. Bloomeries coexisted with blast furnaces till the end of nineteenth century, but with diminishing importance [1].

1.1.1.2. Beginning of Blast Furnace Era

Improvement of bellows and implementation of water wheels about 700–800 years ago made it possible to build higher furnaces and increase the blast volume. Increasing the blast volume made the combustion more intensive, which resulted in a slightly different process where the reduced iron was carbonized and melted. This blast furnace process is the oldest but still the main method to produce large quantities of molten raw iron, hot metal, and for steel making and foundry purposes.

Treatise on Process Metallurgy, Volume 3
http://dx.doi.org/10.1016/B978-0-08-096988-6.00017-1

The early blast furnace had about a 6 m × 6 m square formed stone foundation and 6–8 m high walls of stone blocks. The upper half of the walls could be also made of timber. In the middle of this housing was the round shaft pipe of (sand) stone masonry. The space between the shaft and housing was filled with sand [2].

The charcoal blast furnace had a slim shaft where charcoal and iron-bearing burden were charged on the top and air was blown in through one or more tuyeres in the lower part of the furnace. About 0.5 m below the tuyere was the bottom of the hearth with the tap hole. In some old constructions instead of a tap hole there was a dam of molten iron and slag. Descending iron oxides were reduced to metallic iron by the ascending gas, carbonized and melted to form hot metal. The gangue minerals and coal ash melted to form slag floating on the iron. The molten products were tapped at certain intervals. Iron was cast to pig iron in sand molds to be used for steelmaking or foundry purposes. Small castings could be made on the site by taking molten iron in a ladle to cast in a mold.

The inner profile of the first blast furnaces was akin to the bloomery furnace. Blast furnace people observed soon that if they built the middle part of the shaft (belly) wider, they could save charcoal and increase hot metal production. Improvement of bellows, introduction of water wheels, and invention of blowing machines made it possible to build higher and larger blast furnaces. The demand of charcoal was huge, so to set up a blast furnace was restricted by the governments.

There was no use for top gas and it was burned above the furnace top. It was merely a nuisance and health risk for the workers who charged the furnace by shoveling with ore and charcoal.

1.1.1.3. Development to Present Days

In the seventeenth century, the consumption of charcoal for iron production reached such proportions that in leading steel-producing regions like Britain and Sweden, the production capacity of the forests for charcoal was overdrawn. It was a necessity to find a new reducing agent and energy source for industrial and heating purposes.

1.1.1.3.1 From Charcoal to Coke

Coal was traditionally mined and used for industrial purposes but its use was limited by the sulfur it often contained. Coal was even tested for ironmaking but with poor success. At about the same time, however, the process to convert coal to coke was learned. Then Abraham Darby invented the use of coke in blast furnace in 1709 in England [3]. All coal was not suitable for blast furnace coke, which must have proper reactivity, but Darby was lucky to find such coke. Coke was cheaper than scarce charcoal and could replace it as blast furnace fuel. Coke was even stronger than charcoal and that is why it was possible to build higher and larger blast furnaces. Blast furnaces became big production units of cheap and high-quality hot metal for steelmaking. In this way invention of coke for BF accelerated the industrial revolution. The invention of coke replaced the use of charcoal almost totally. Nowadays the idea of "green or sustainable technology" has brought the use of charcoal and biomass in general to the spotlight. Such countries like Brazil have natural preconditions to produce charcoal, and they have significant iron and ferroalloys production based on charcoal.

Another remarkable invention was made by James Neilson in 1828 when he introduced preheating of the blast [1,4]. This invention saved a lot of fuel and increased blast furnace productivity. The first types of heaters were recuperative heat exchangers located on the top of the furnace. In the beginning, they were only some pipe loops above the top gas fire, but they were soon developed to form more effective recuperators. A blast temperature of 200 °C could already save 25% of charcoal.

In the 1800s, recovery of top gas improved the energy supply of the iron works remarkably. Top gas could be used in power plant to generate steam and electric power. Top gas was used also in hot stoves, regenerative heat exchangers, with which it was possible to preheat the blast to 1000 °C or more.

During the past three centuries, the construction of blast furnace has gone through many phases. The first big change was to lay the shaft from firebricks and reinforce the bricklayers with steel hoops. Because the bosh area eroded faster than the shaft, the shaft was laid on a lintel so that the bosh bricks could be replaced without removing the shaft. The bosh bricks were also cooled with cooling boxes with circulating water [5]. The next step was to cover the furnace with a gas-tight steel shell and equip the throat with gas-tight charging equipment, usually of bell type. The number of tuyeres increased with the size of the blast furnace and the tight steel shell made it possible to adapt high top pressure. Oxygen enrichment of the hot blast together with injection of coal powder, oil, and natural gas or waste plastics through the tuyeres is the latest steps in blast furnace technology [6].

The number of castings per day is 10 or less. At large blast furnaces with three or four tap holes, the casting is continuous. Still about 50 years ago, many blast furnace hearths were equipped with a separate cinder notch. Slag was tapped before iron casting when the slag level in the hearth reached the cinder notch. This technique was necessary because rich lumpy ores were scarce and slag rates were high.

Pig casting is not very common. It is used mainly for foundry grade iron or for surplus steelmaking iron for sale. Some plants use granulation or sand casting for surplus iron.

1.1.1.3.2 Ore Preparation

Roasting was also an important part of the ironmaking process. Iron ores contain compounds that should be removed before charging: bog ore and lake ore consisting of limonite ($FeO(OH) + nH_2O$), contained a lot of bound water, siderite ($FeCO_3$) contains CO_2 and almost all ores contain sulfur. Those unfavorable compounds were removed by roasting, which made also magnetite ores more reducible by oxidizing Fe_3O_4 to hematite, Fe_2O_3. The earliest roasting method was to roast the ores on a burning timber log bed. Special roaster furnaces were later developed, which used wood, coal fines, and later even top gas as fuel.

Nowadays roasting has been replaced by agglomeration processes: sintering or pelletizing. In sintering, ore fines and/or iron concentrate are mixed and heated in oxidizing atmosphere up to sintering temperature on a grate machine where ore grains fuse together. In pelletizing, the finely ground iron ore is rolled to pellets before firing in a kiln or on a grate machine.

1.1.1.4. Blast Furnace Process in Brief

1.1.1.4.1 Blast Furnace Process for Integrated Steelmaking

Steel is produced by using two types of raw materials: hot metal or pig iron, and steel scrap, and through two types of processes: basic oxygen furnaces (BOF) or basic oxygen steelmaking and electric arc furnaces (EAF). In BOF steelmaking, about 75% of iron comes from the hot metal produced by blast furnace process, the remaining 25% of the raw materials is steel scrap. EAF process uses 100% steel scrap in general, however, in some plants significant share of direct reduced iron (DRI) is used. Further, solid pig iron is used as "pure" raw material and carbon source in EAFs. The blast furnace–BOF route produces almost 66% total crude steel, and EAF route accounts for about 31%, while the blast furnace–open hearth process, which dominated steelmaking in the first half of the 1900s, had only a share of about 3% left [7].

The blast furnace process has been for the past two centuries the dominating ironmaking route to provide the raw materials for steelmaking industry. Nowadays, over 93% of the total iron production from ores is taking place via BF route. An alternative route for iron production is direct reduction, which is described more thoroughly in a separate chapter. Figure 1.1.1 illustrates the position of the blast furnace as well as direct reduction in the overall steelmaking process [8].

Blast furnace uses iron ore as the iron-bearing raw materials, and coke and pulverized coal as reducing agents and heat source, lime, or limestone as the fluxing agents. The main objective of blast furnace ironmaking is to produce hot metal with consistent quality for BOF steelmaking process. Typically the specification of steel works requires a hot metal with 0.3–0.7% Si, 0.2–0.4% Mn, and 0.06–0.13% P, and a temperature as high as possible (1480–1520 °C at the tapping). A modern large blast furnace has a hearth diameter of 14–15 m, and a height of 35 m with an internal volume of about 4500 m^3. One such large blast furnace can produce 10,000 tons of hot metal per day (THM/day). Figure 1.1.2 illustrates the modern ironmaking blast furnaces.

Since blast furnace process consumes a large amount of metallurgical coke, other ironmaking processes are being developed and are emerging as eventual future alternative ironmaking processes: smelting reduction and direct reduction where metallurgical coke can be replaced by pulverized coal or other gaseous reducing agents. The examples of commercial processes are MIDREX [9] as direct reduction process and COREX [10] as smelting reduction process.

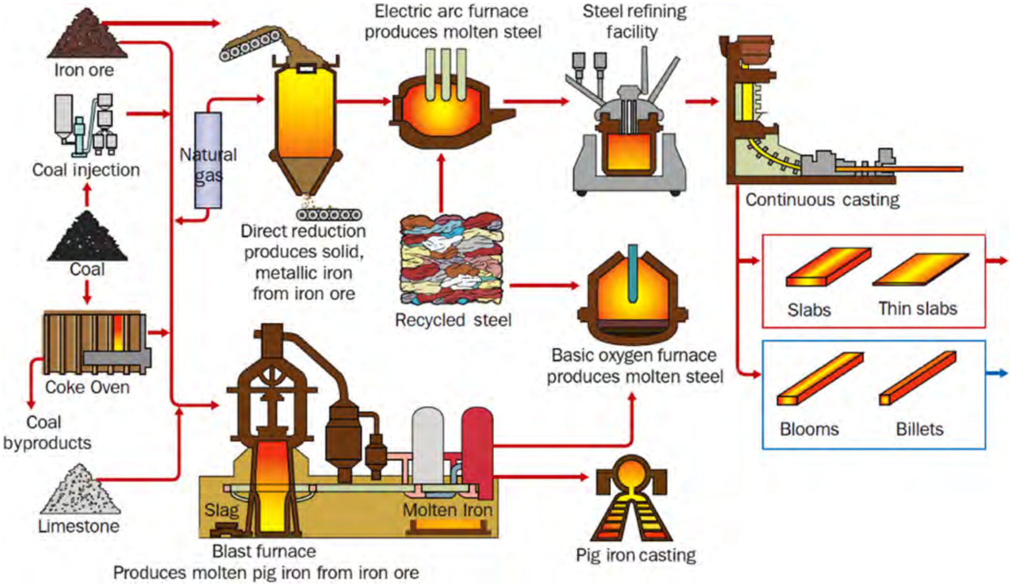

Figure 1.1.1 Illustration of ironmaking and steelmaking flowsheet [8].

Figure 1.1.2 Blast furnace No. 6 and 7 of Tata Steel in IJmuiden, The Netherlands. *Courtesy: Tata Steel Europe, IJmuiden (photographer: Vincent Bloothoofd).*

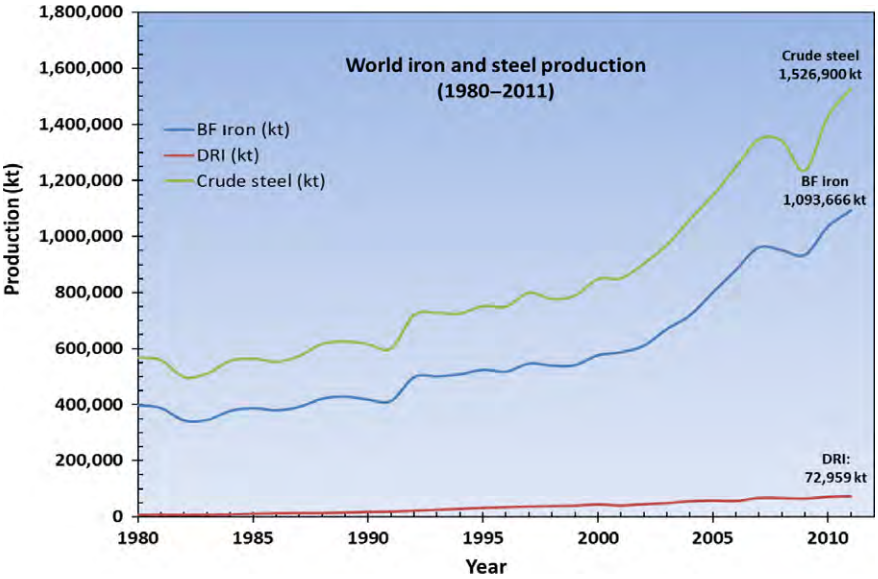

Figure 1.1.3 World iron and steel production: 1980–2011. *Data taken from World Steel Association [11].*

Annual hot metal production by blast furnace process, DRI, as well as crude steel from 1980 to 2011 is shown in Figure 1.1.3.

1.1.1.4.2 Blast Furnace Process Overview

The blast furnace is a continuously operating shaft furnace based on the counter-current flow principle. At the top coke and burden (sinter, pellets, lump ore, and flux) are charged in alternating layers. Charge materials descend under the influence of gravity. In the lower part of the furnace, hot blast from hot stoves is injected through tuyeres. In front of each tuyere, the hot blast reacts with the coke. Carbon monoxide is formed, and it ascends in the furnace and reduces the iron oxides in the ferrous ores. At the bottom of the hearth, the molten metal is collected. Besides hot metal a slag is formed that floats on top of the hot metal bath due to its lower density. Liquid hot metal (1500 °C) and slag (1550 °C) are tapped regularly. The products of the blast furnace process are carbon-saturated iron (hot metal), slag, top gas, and flue dust. Figure 1.1.4 illustrates the blast furnace processes [12].

1.1.1.4.2.1 Charging

The blast furnace is charged continuously with iron-bearing burden, slag formers, and coke. The iron burden consists of sinter, pellets, and/or lumpy ore in various proportions. Slag formers are usually limestone, BOF slag, and quartzite in small amounts to balance the slag rate and chemistry. Iron oxides are mainly Fe_2O_3, sometimes Fe_3O_4, with small

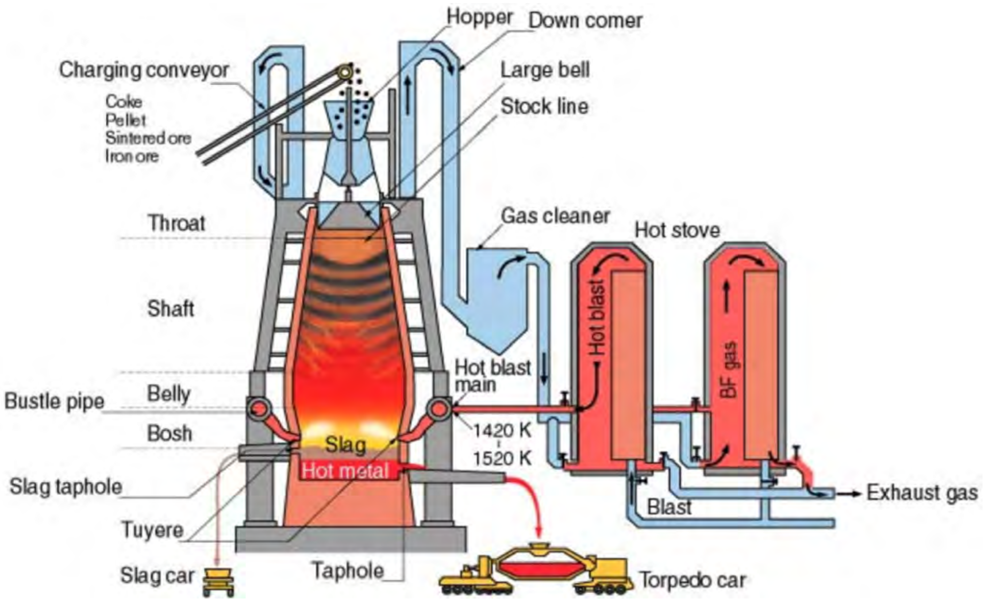

Figure 1.1.4 Illustration of blast furnace process [12].

amounts of FeO in agglomerates, and in gangue materials. In an ideal case, sinter and/or pellets are self-fluxing, or in other words they contain all slag formers in such amounts that no other slag formers are needed to make desired slag together with coke ash. Coke makes the basic source of energy and acts as a carbon reductant. Other sources of reducing agents are pulverized coal, hydrocarbons, waste plastics, or even biomass, which are injected through the tuyeres. Preheated blast (1200–1300 °C) of air or oxygen-enriched air brings an important amount of heat to the process.

1.1.1.4.2.2 Burden and Gas Movement

The oxygen in the hot blast reacts with the coke and pulverized coal in the belly and bosh of the blast furnace (raceway) to form a mixture of carbon monoxide and nitrogen. This gas mixture ascends in the furnace while exchanging heat and reacting with the ferrous materials (burden) descending from the furnace top.

The gas still with certain heating values is eventually discharged from the furnace top and recovered for use as fuel in the plant. During this process, the layer-thickness ratio of iron-bearing materials to coke charged from the furnace top and their radial distribution are controlled so that the ascending reducing gas can pass with appropriate radial distribution.

During the descent of the burden in the furnace, the iron-bearing materials are preliminarily reduced by carbon monoxide gas in the upper part of the furnace (indirect reduction). In the lower part of the furnace, carbon dioxide, produced by the reduction of the remaining iron ore by carbon monoxide is instantaneously reacted with coke (C) to form carbon monoxide (Boudouard reaction), which again reduces the iron oxide to metallic iron.

The overall sequence can be regarded as direct reduction of iron ore by solid carbon in the high-temperature zone from the lower part of the furnace. The reduced iron simultaneously carburized, melts, drips, and collects as hot metal at the hearth. The hot metal gets saturated with carbon in the hearth, then the hot metal and molten slag are discharged at fixed intervals (usually 2–5 h) by opening the tap holes and cinder notches in the furnace wall.

1.1.1.4.2.3 Blast Furnace Zones and Principal Reactions

The ironmaking process in the blast furnace is a heat and mass transfer process, and the furnace can be divided into different zones according to physical and chemical state of the feed and temperature. Figure 1.1.5 illustrates various zones of the blast furnace and feed distribution and materials flow [13]. Corresponding to each temperature interval, typical reactions will take place. The descending burden is dried and preheated during its descent by the ascending gas. The preheated blast is blown into the furnace through the tuyeres in the lower part of the furnace. Oxygen in the blast reacts with coke carbon to produce carbon monoxide and blast humidity reacts with carbon to produce carbon monoxide and hydrogen:

$$C + O_2 = CO_2 \tag{1.1.1}$$

$$C + CO_2 = 2CO \tag{1.1.2}$$

$$2C + O_2 = 2CO \tag{1.1.3}$$

$$C + H_2O = CO + H_2 \tag{1.1.4}$$

The role of nitrogen in the blast is to act as a heat carrier together with CO, CO_2, and H_2. The combustion space in front of the tuyeres is called the raceway. The adiabatic flame temperature in the raceway is about 2100–2300 °C. The ascending hot gas heats up the dripping iron and slag, which are collected in the hearth below the tuyere level and tapped at certain intervals. The ascending gas flows through the cohesive zone, also called softening–melting zone. Here iron and slag become soft, and they separate and melt down. The slag phase contains some unreduced iron oxide FeO. The reduction of this iron by solid carbon is called direct reduction:

$$C + (FeO) = Fe + CO \tag{1.1.5}$$

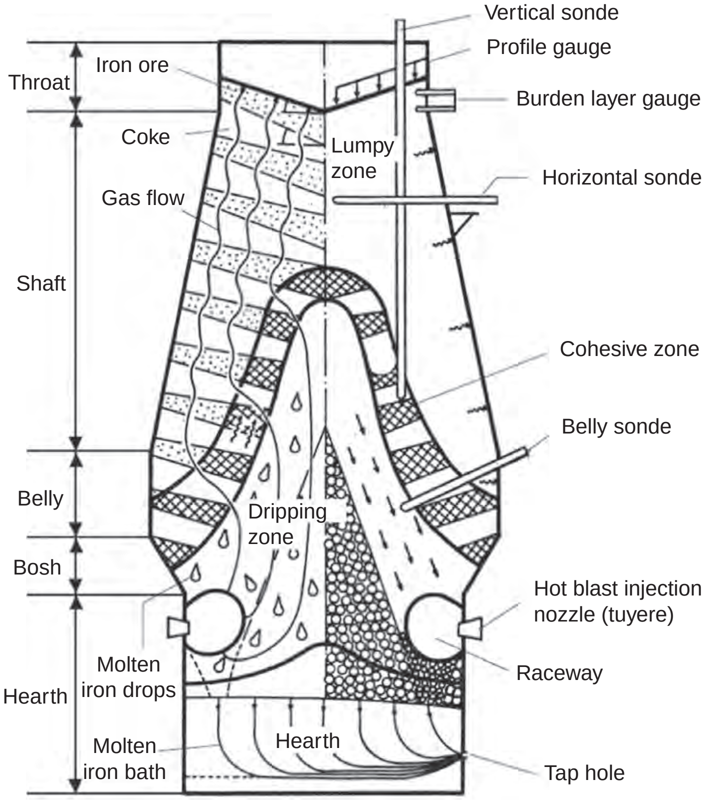

Figure 1.1.5 Illustration of various zones of blast furnace [13].

Above the cohesive zone, the gas heats up the burden. Carbon monoxide and hydrogen reduce iron oxide indirectly as gas–solid reactions:

$$CO + FeO = Fe + CO_2 \tag{1.1.6}$$

$$H_2 + FeO = Fe + H_2O \tag{1.1.7}$$

Carbon dioxide reacts with coke (carbon) (Boudouard reaction, or solution loss reaction):

$$CO_2 + C = 2CO \tag{1.1.2}$$

and water vapor reacts with coke in a similar way to generate reducing gases (water–gas reaction):

$$H_2O + C = CO + H_2 \tag{1.1.4}$$

These reactions diminish when gas temperature falls below 900 °C. Reduction reactions, increasing in CO_2 content and cooling of the gas continue along with its ascending.

The remaining heat content of the gas is used to dry and preheat the burden before the gas leaves the furnace top at 100–300 °C. The top gas is still a valuable fuel having a lower heating value of 3–4 MJ/Nm^3.

For burden materials, the first step after they have been charged is drying. The next steps are rapid preheating and start of reduction of iron oxides. Following reactions take place below 570 °C:

$$3Fe_2O_3 + CO = 2Fe_3O_4 + CO_2 \tag{1.1.8}$$

$$Fe_3O_4 + 4CO = 3Fe + 4CO_2 \tag{1.1.9}$$

and

$$3Fe_2O_3 + H_2 = 2Fe_3O_4 + H_2O \tag{1.1.10}$$

$$Fe_3O_4 + 4H_2 = 3Fe + 4H_2O \tag{1.1.11}$$

Above 570 °C, the reduction reactions are as follows:

$$Fe_3O_4 + CO = 3FeO + CO_2 \tag{1.1.12}$$

$$FeO + CO = Fe + CO_2 \tag{1.1.13}$$

and

$$Fe_3O_4 + H_2 = 3FeO + H_2O \tag{1.1.14}$$

$$FeO + CO = Fe + H_2O \tag{1.1.15}$$

After the relatively rapid heating to about 900 °C, the burden reaches the chemical reserve zone where the temperature difference between gas and solid is about 50 °C. At about 1000–1100 °C (depending on the chemical composition of the ferrous burden and the reduction degree), the burden comes to the cohesive zone. Iron oxides are mainly reduced to metallic Fe. The burden starts to soften. Iron and slag separate. The FeO content in slag phase can vary inside a large range, e.g., 5–25%. Metallic iron is carbonized by carbon in the coke and CO gas and melts at 1200–1300 °C. Molten iron and slag drip down through the coke layer to the hearth where they reach their final temperature and composition.

1.1.1.4.2.4 Casting and Hot Metal Treatment

Hot metal and slag are tapped or casted 6–10 times per day. Blast furnaces with two or more tap holes tap hot metal and slag continuously. The tap hole is opened with a hydraulic drill and is closed with a hydraulic mud gun injecting fast setting tap hole clay. Slag and iron are separated in the main trough, where the melts settle, iron flows under the skimmer stone and slag stands behind the skimmer stone and is directed to granulating device or slag pit. The hot metal flows through the skimmer, which separates the slag from the hot metal to ladles or torpedo cars to be transported to hot metal treatment (e.g., desulfurization) and hot metal mixers at the steel plant.

Due to ecological and economic reasons, the conventional blast furnace process has changed within the past decades. A better burden distribution, increases in sinter and pellets quality, back pressure at the furnace top, and hot blast temperature of 1200–1300 °C, resulted in a rise of furnace productivity and drop in coke rate. Injection of auxiliary fuels such as oil, natural gas, and fine coal was started in order to further decrease the coke rate. The blast furnace process with pulverized coal injection (PCI) rate of up to 250 kg/THM and reduction of the coke rate from 500 down to 250 kg/THM has been realized. The reduced coke rate leads to a decrease in the carbon dioxide emission. Injection of plastic, iron-containing filter dust, and other waste has technological, economic, and environmental advantages.

1.1.2. THE IRONMAKING BLAST FURNACE

1.1.2.1. Construction and Profile

Generally speaking the blast furnace is a shaft furnace. The main parts are the top, throat, shaft, belly, bosh, tuyere belt, and the hearth. The charging equipment is located in the middle of the top cone. On the top cone there are also the four gas-off takes. Beneath the top is the throat, a short cylindrical part. The next part is the downward widening shaft (stack), then the short cylindrical belly (or bosh parallel). From the belly downward comes the bosh, a contracting conical part joining to the tuyere belt. Below the tuyere belt is the hearth with tap holes and the bottom. Figure 1.1.6 illustrates an outside view and internal structure of an industrial scale-operating blast furnace [14,15].

Dimensioning of a blast furnace is no simple mathematical task because the profile is an intermediate result of continuous evolution based on experience. Engineering companies are specialists on this field but for deeper understanding and planning of future revamps it is useful to understand the function of different parts of a blast furnace.

There are two characteristic dimensions describing the size of a blast furnace: hearth diameter and volume. The hearth dimension gives a more visual impression of the size but the volume is a more practical base for dimensioning. The dimensioning of a blast furnace starts from the specified output of hot metal. The next step is to estimate the specific productivity in t/m^3/day. Common values lie in range 2.5–4.0 t/m^3/day depending on the top pressure, oxygen enrichment, fuel rate, injection rate, burden properties, etc. Then the volume can be fixed. Guide values of the dimensions can then be calculated with a formula as expressed in Equation (1.1.16) [16]:

$$c_x = a \times V^b \tag{1.1.16}$$

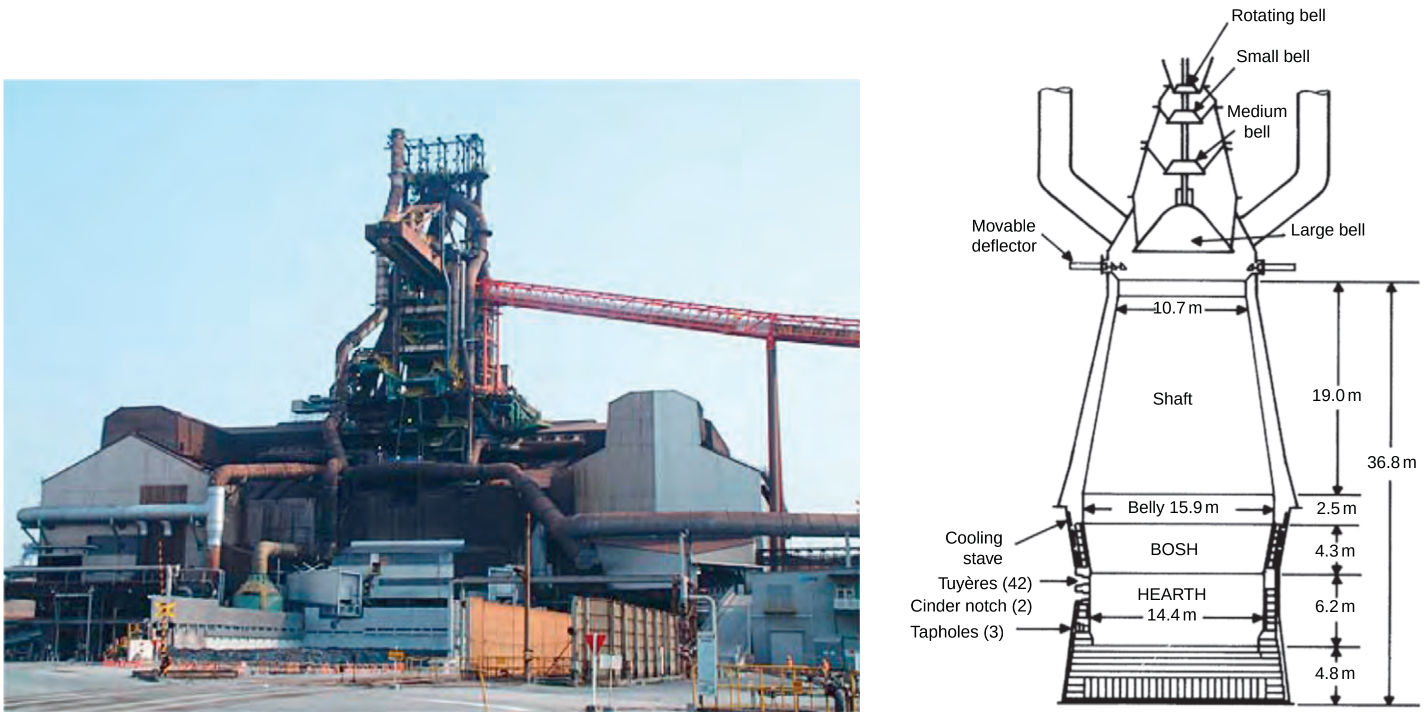

(a) (b)

Figure 1.1.6 A typical ironmaking blast furnace: Fukuyama No. 5 blast furnace of JFE Steel Corporation. (a) Overview (the third campaign: since March 2005) [14] and (b) structure of the furnace (first campaign: 1973–1983) [15].

where c_x is the dimension x, V is the furnace volume, a and b are constants obtained with regression analysis from published data [16].

All dimensions must then be checked with fluid dynamics calculations and empirical rules. The new volume can be calculated and if the new volume is too small to ensure production capacity, the dimensions must be adjusted (but keeping shaft and bosh angles unchanged).

1.1.2.1.1 Throat

The throat is a cylindrical, 2.5–3 m high part where the burden pattern takes its shape. Important parameters are the layer thicknesses, ore/coke distribution, slag former distribution, and distribution of particles with different size. It is important that the set value of the stock level is always above the lower end of the throat.

1.1.2.1.2 Shaft

The shaft is the highest part of the profile. Shaft angle is usually 82–86°. The better the burden materials are screened and sized, the bigger angle can be chosen. A too small angle leads to strong peripheral gas flow.

1.1.2.1.3 Belly

The belly is a relatively short, 1.7–2.0 m high cylindrical part. Its function is to make a smooth transition from a widening shaft to a tapered bosh, so that the bosh also gives a favorable increase in furnace volume.

1.1.2.1.4 Bosh

The bosh is a very important part of the blast furnace. It supports the root of the cohesive zone. The height of the bosh is about 2.7–3.7 m with a bosh angle of 74–82°. The bosh angle is critical with regard to lining durability. Also the rule of thumb is frequently used: 4′–4′ (4 ft. (1.2 m) upward from tuyere nose and 4 ft. from that point horizontally toward bosh wall) and 12′–5′ free space measured from the tuyere nose must be fulfilled.

1.1.2.1.5 Tuyere Zone

The tuyeres are installed in the tuyere belt, which is about a 1-m high cylindrical part in the upper end of the hearth. The number of tuyeres is 15–50 or more depending on the hearth diameter. Tuyeres of a modern blast furnace are equipped with special lances for injection of auxiliary fuel and reductants.

1.1.2.1.6 Hearth and Tap Hole

The hearth diameter can be calculated from the bosh geometry. The height of the hearth is 3.2–3.9 m from bosh to bottom [17]. The hearth provides the space for slag–metal separation, holds the remaining unreacted coke—deadman, where the hot metal gets saturated with carbon. The tap holes are located at 1/3 of the hearth height upward from the bottom. Number of tap holes depends on furnace productivity: one tap hole is good for up to 4000 t/day—four tap holes for 16,000 t/day.

1.1.2.2. Charging Equipment

The function of the charging equipment is to transmit the burden materials through the locks in the furnace to desired locations on the burden surface in the throat. For many years, the two-bell charging system with movable armor was the only proper charging equipment but nowadays the bell-less rotating chute is dominating. The advantages of the bell-less top is the more accurate filling of the furnace and better gas tightness with higher top pressures. The stock level is measured either with a mechanical stock rod or with a radar. Figure 1.1.7 illustrates the two types of charging systems. Charging "philosophy" and implementation are discussed more thoroughly in Section 1.1.5.1.2.

1.1.2.3. Lining and Cooling

The purpose of the refractory lining is to protect the steel shell of the furnace and the purpose of cooling is to keep the lining in shape. The old lining type was firebrick with water-cooling boxes. The latest state of this type of lining in the lower part of the blast furnace is graphite bricks in tight contact with copper cooling boxes and the graphite brick layers covered by silicon carbide bricks to prevent erosion on the hot surface. In the upper part of the furnace, fire brick with steel cooling plates are used.

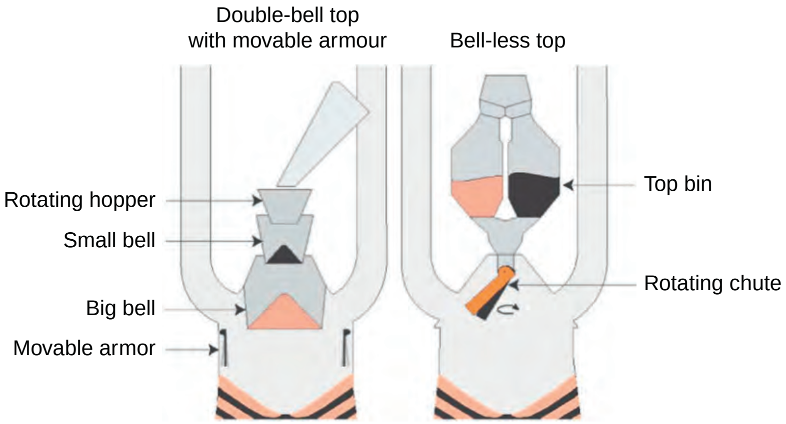

Figure 1.1.7 Illustration of blast furnace charging system: bell top and bell-less top charging [18].

Stave coolers were introduced in the 1950s. The staves were cast iron within cast steel pipes for circulating water. Copper staves were introduced in the 1990s and they are now the state of the art. Copper staves are used in the lower (hot) part of the furnace combined with cast iron staves in the upper part. The throat is lined with hard cast or hard welded armor plates. The hearth is lined with carbon bricks, sometimes with a ceramic cup inside. Cooling of the hearth is usually made by staves. Also spray cooling of the steel shell is applied on smaller furnaces.

Modern cooling water systems are closed because the water properties are under control and even small leakages can be indicated. Water leakages into the furnace are the principal causes of severe accidents in blast furnace plants.

1.1.2.4. Evolution of Blast Furnace Dimension

Blast furnaces have grown considerably in size during the twentieth century. In the early days of the twentieth century, blast furnaces had a hearth diameter of 4–5 m and were producing around 100,000 THM per year, mostly from lump ore and coke. At the end of the twentieth century the biggest blast furnaces had between 14 and 15 m in hearth diameter, and were producing 3–4 million tons of hot metal per year [18]. A typical development of blast furnaces is illustrated in Figure 1.1.8, showing the evolution of shape and dimensions of the ironmaking blast furnaces, from 1860s to 1980s. Since mid-1980s, the size of blast furnace remained more or less the same, at its optimal level (3000–5000 m^3) [19].

Presently, very big furnaces reach production levels of 12,000 tpd or more. For instance, the Oita No. 2 blast furnace (NSC) has a hearth diameter of 15.6 m and a production capacity of 13,500 tpd hot metal. The Thyssen-Krupp Schwelgern No. 2 blast furnace has hearth diameter of 14.9 m and a production capacity of 12,000 tpd hot metal [18].

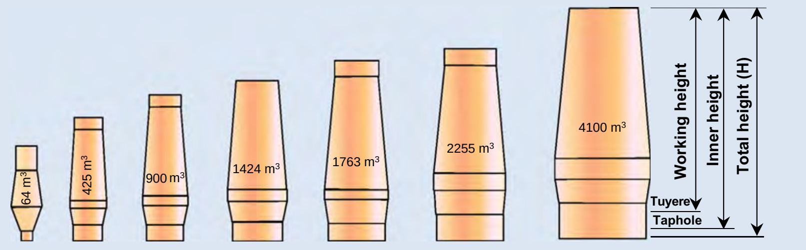

Shape and inner volume (m^3), calculated from taphole level above and 1 m below charging device	64 m^3	425 m^3	900 m^3	1424 m^3	1763 m^3	2255 m^3	4100 m^3
Hearth diameter (mm)	900	4500	6500	9000	9750	11,200	14,000
Total height H (mm)	15,300	20,300	24,000	26,075	29,400	31,450	36,000
Productivity: THM/day	25	450	1200	>2500	4000	6000	~10,000

Figure 1.1.8 Development of blast furnaces from 1860s to 1980s [19].

1.1.2.5. Auxiliary Units

In addition to the main structure of the blast furnace itself, there are the following auxiliary equipment:

- Belt conveyors for transporting raw materials (ore and coke) to the furnace top.
- Hoppers for temporarily storing these raw materials.
- PCI with equipment for pulverizing the coal and feeding it under pressure.
- With bell-type charging equipment. The raw materials enter the furnace through the gap created by lowering a small inverted bell. This bell closes and a larger bell (big-end-down) opens to allow material to fall into the shaft below.
- With bell-less charging equipment. The raw materials are dropped into the furnace through a rotating chute.
- Blowers for feeding the blast.
- The hot stove for heating the blast. This is a cylindrical furnace about 12 m in diameter and some 55 m in height, and has a chamber filled with checkered silica bricks. The hot stove is a type of heat exchanger in which the heat produced by combustion of the BF gas is stored in the checker-work chamber, after which cold air is blown through the hot checker-work to produce the preheated hot air blast to the furnace. Two or more stoves are operated on alternate cycles, providing a continuous source of hot blast to the furnace.
- BF top-pressure recovery turbine (TRT). A blast furnace is usually operated with a furnace-top pressure of about 250 kPa. To recover the energy from the large volume of high-pressure exhaust gas, the BF is equipped, after dust removal, with a TRT for generating electric power by utilizing the pressure difference between the furnace-top and gas-storing holder.
- Equipment for dust removal and recovery.

1.1.3. IRON-BEARING MATERIALS AND ADDITIVES

1.1.3.1. Types of Iron Ores

About 5% of the earth's crust is iron. Iron appears in many minerals and rocks. Iron findings contain frequently several iron minerals depending on their geological history and more or less gangue minerals, too. If the iron finding is commercially profitable to exploit, it is called iron ore. Iron ores can be classified into magnetite, hematite, goethite, limonite, siderite, ilmenite, pyrite, etc., according to the composition of minerals. Iron ore is typically classified also as high grade (+65% Fe), medium grade (+62–65% Fe), and low grade (−62% Fe). Typically, the integrated steel plants use medium/high grade iron ore, whereas the sponge iron plants require only high grade iron ore, preferably, with +67% Fe [20].

Iron ore production in 2009 was reported as 2,230 million metric tons (Mt), with a metal content of 1,090 million metric tons. Four main producers were China (880 Mt), Australia (394 Mt), Brazil (310 Mt) and India (225 Mt) [21]. However, the iron ore reported from China has lower iron content of an average of 33%, much lower than that of other countries as usable ore.

Mining takes place mainly in huge open pits, and few in underground (e.g., LKAB). The ore is crushed and sized to, e.g., 6.3–31.5 mm fraction if it is used as lumpy ore in blast furnaces. Pure, thoroughly sized and easily reducible lumpy ore is also used as a supplement with sinter and pellets. After mining, most of the iron ore is produced as fine concentrates through crushing, grinding, and screening. For low grade ore, various upgrading processes are used such as gravity separation, flotation, and magnetic separations for obtaining iron ore concentrates. For some iron ore mines, iron ore pellets are produced also on the mine sites and shipped directly to integrated steelmaking plants for blast furnace ironmaking and direct reduction plants such as LKAB in Kiruna, Sweden.

Hematite and magnetite are industrially two most important type of iron ores for ironmaking. Pure hematite Fe_2O_3 contains 69.94% iron. Hematite originates from sedimentation in archaic cratons. Hematite occurs in several varieties as kidney ore, specularite, martite, and iron rose. Hematite ores are the dominating type of iron ores today. They are easily reduced in the blast furnace. Pure magnetite Fe_3O_4 contains 72.36% iron. Magnetite originates mainly from sedimentation in archaic cratons, but volcanic occurrences are known, too. Dense magnetite lumps are not easily reduced in the blast furnace, but in some cases they are used if they contain manganese. Also the composition of their gangue can be useful to finetune the slag composition.

Siderite $FeCO_3$ with 48.2% Fe occurs in smaller amounts with other iron ores. Erzberg in Austria is an old (from the fourth century) and well-known siderite mine. Siderite must be roasted or nowadays sintered before charging in the blast furnace. Goethite $FeO\cdot(OH)\cdot nH_2O$ and limonite, a mixture of goethite and other minerals, were important ores in ancient times, but nowadays their importance is vanishing. Anyway, they must be agglomerated before use in blast furnace.

1.1.3.2. Agglomerates and Additives

Blast furnace process requires a good permeability of the burden materials for efficient gas–solid reactions. Only lumpy ores can be directly charged into the blast furnaces, and all fine iron ore concentrates require agglomeration processing before charging into the furnace. Two types of agglomeration technologies are commonly used in industry: sintering and pelletizing.

1.1.3.2.1 Sinter

1.1.3.2.1.1 Sintering Process

Sintering is a widely used method to agglomerate iron-containing fine-grained materials. In sintering the ore fines, concentrates, fluxes, and coke breeze are thoroughly weighed, moistened, and mixed. The sinter mix is fed on the grate of the sintering machine to make a 0.3–1 m high bed. The grate is an endless strand of slowly moving pallets. The surface is ignited in the ignition hood and air is drawn through the bed. Coke in the mix is ignited and the combustion zone descends slowly downward. The downward flowing air is preheated in the upper zones and together with combustion of the coke the temperature will rise up to about 1400 °C. At this temperature, the ore grains start to melt and stick together. When the combustion of coke ends, the half molten material starts to solidify and release heat to the downward flowing air. When the combustion zone reaches the grate, the pallet has reached the end of the strand where it turns over to the return rails and the sinter cake drops in a crusher for further processing. Figure 1.1.9a illustrates a typical sintering machine [22]. Figure 1.1.9b shows the emission optimized sintering (EOS) system for better environmental control [23]. The EOS system consists of a hood above the sinter strand, a fresh air fan with duct work and the respective control valves, a recirculating gas fan, and the corresponding control valves with bleed-in system, as well as a measuring and control system for the EOS unit.

1.1.3.2.1.2 Iron-Bearing Materials

Ore fines and iron concentrates make the main part of the sinter mix. The grain size of ore fines and concentrates is typically 0–8 and 0–3 mm, respectively. Grains smaller than 0.1 mm are not desired because they reduce the gas permeability of the bed and thus decrease the sintering efficiency. Recycled materials, such as mill scale, scrap fines, and dusts can also be used in the sinter mix. These materials must not contain oil or high amounts of zinc and other impurities.

1.1.3.2.1.3 Additives

Limestone, burnt lime, BOF slag, manganese ore, olivine, etc., are added in the mix to finetune the composition of blast furnace slag. These materials shall be ground to <3 mm grain size. Burnt lime has a strong positive effect on sinter plant productivity.

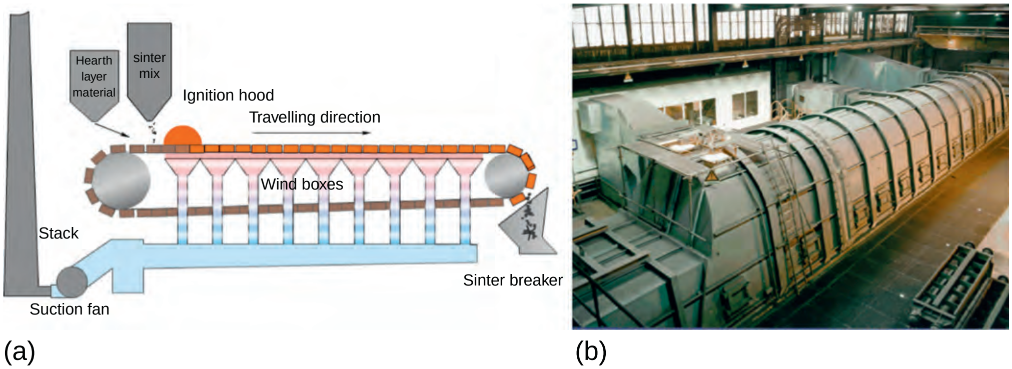

Figure 1.1.9 (a) Schematic view of a typical iron ore sintering plant [22] and (b) EOS hood on sinter strand in Tata Steel IJmuiden [23].

1.1.3.2.1.4 Fuel

Coke breeze is the most common fuel for sintering, and anthracite is used too. Fuel must not contain tar because it will damage the off-gas cleaning system. Fuel is ground to <3 mm grain size.

1.1.3.2.1.5 Return Fines

Return fines constitute 20–40% of the final mix. Return fines come from hot and cold screening and from screening at the blast furnace. Return fines have several advantages:

- hot returns elevate the mix temperature and prevent from over-moistening thus improving the bed permeability
- returns act as nuclei in the micro pelletizing phase

1.1.3.2.1.6 Moisture

Moisture content is used to synchronize the heat wave speed and combustion zone speed in order to reach maximum sintering temperature. Moisture is important also for good mixing and high permeability of the mix. Optimum moisture varies a lot depending on mix properties.

1.1.3.2.1.7 Sinter Handling

Sinter lumps from the primary crusher are hot screened and cooled in a rotary or belt cooler. The hot fines less than 5 mm are mixed with the raw mix. The cooled sinter is screened to desired fractions and transported to the blast furnace bins. The cold fines of less than 5 mm are returned in the raw mix to make up the final sintering mix.

1.1.3.2.1.8 Sinter Quality

Important properties of sinter for blast furnace process are reducibility, size and size distribution, cold and hot strength, and softening and melting behavior. Typical sinter suitable for blast furnace process is from 15 to 25 mm, as is illustrated in Figure 1.1.10 [22]. Another important property is the disintegration of sinter in reduction, which occurs during the transformation of hematite to magnetite, and is related to the fraction of secondary hematite. It is found that using fluxes with high MgO content (olivine or dolomite) can minimize the reduction–disintegration of the sinter [18].

1.1.3.2.2 Pellets

1.1.3.2.2.1 Pelletizing Process

Similar to sintering, pelletizing is another widely used process to agglomerate the iron ore. Sinter plants are usually located near the blast furnace plant, but pelletizing plants

Figure 1.1.10 Typical sinter for blast furnace process (size: ≤25 mm) [22].

are often located near the mining site. Some works have both pelletizing and sintering plants at the smelter sites.

1.1.3.2.2.2 Green Pellets

The ore is crushed, ground, and concentrated in several steps to very small grain size—e.g., over 75% less than 45 μm. Binder (bentonite or organic) and possible additives are fed in the slurry and mixed before filtering. The filter cake is transported to large balling drums or balling discs to be rolled to green pellets. The green pellets are screened to 9–11 mm diameter. The oversize is crushed and fed together with the undersize back to balling.

1.1.3.2.2.3 Induration

The process to harden pellets by heating them up to the sintering temperature is called induration. There are three induration processes: Grate-Kiln, Straight Grate, and Vertical Shaft furnace, of which the first two are dominating whereas the shaft furnace is retreating. Figure 1.1.11 illustrates a typical pellet firing process [22].

In Grate-Kiln process, green pellets are fed on oil or gas-fired endless Straight Grate machine where they are dried and preheated. The preheated pellets are then fed to a rotary kiln where their temperature is raised in oxidizing atmosphere to 1290–1400 °C. In induration, ore grains are sintered together with oxidation and slag-forming bonds. Pellets are cooled in a separate cooler. In Straight Grate process drying, preheating, induration, and cooling take place on the same endless grate machine. In both processes, heat from later process steps is circulated back to preceding steps by hot air with a duct and fan system.

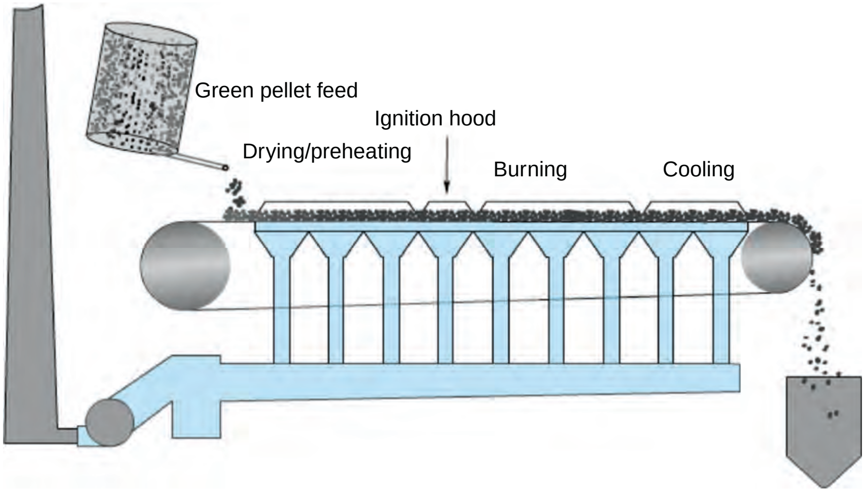

Figure 1.1.11 Illustration of pellet plant [22].

Figure 1.1.12 Iron ore pellets (size: 9–13 mm) [22].

1.1.3.2.2.4 Pellet Quality

Similar to sinter, the following properties are important for pellets: cold strength, reduction–disintegration, the swelling properties, melting, and softening. The reduction–disintegration property of pellets are of less concern compared to sinter. However, pellets have more tendency of swelling than sinter and lumpy ore. Swelling occurs during the transformation of wüstite to metallic iron. Figure 1.1.12 illustrates typical iron ore pellets [22].

1.1.3.2.3 Briquettes

At steel plants without a sintering plant, briquetting is one possible solution to process ore fines, mill scale, dusts, and other recycled materials. The materials are weighed, mixed with 10–15% cement, and moistened. The mix is pressed in a briquette press to 70 mm high and about 70 mm in diameter briquettes, which are left to harden in wet and warm atmosphere for a couple of days.

1.1.3.2.4 Slag Formers in Agglomerates

1.1.3.2.4.1 Limestone

Agglomerates are usually classified as acid or fluxed agglomerates. Acid agglomerates contain practically no added CaO. Their CaO/SiO_2 ratio is far below 0.8. Agglomerates with CaO/SiO_2 ratio ≥ 0.8 are called fluxed. If CaO/SiO_2 is so high (e.g., 1.2) that it together with coke ash gives desired final basicity to the blast furnace slag (e.g., 1.1), agglomerate is called self-fluxing.

Limestone must be crushed to <3 mm grain size to ensure dissolving of CaO in mineral matrix during agglomeration. Free CaO makes the product vulnerable to moisture, which causes cracking due to reaction $CaO + H_2O \rightarrow Ca(OH)_2$.

1.1.3.2.4.2 Burnt Lime

0.5–5% of burnt lime is frequently added in sintering mix because it has a strong positive effect on sinter productivity when it promotes micropelletizing in mixing drum, keeps the gas permeability good during the sintering process, and improves sinter strength.

1.1.3.2.4.3 BOF Slag

BOF slag can replace limestone in sinter mix to a certain degree. The main components of BOF slag are typically $CaO = 55\%$, $Fe + Mn = 15\%$, and $SiO_2 = 15\%$. The use of BOF slag recycles iron and manganese and replaces limestone to some extent thus reducing slag disposal. The contents of impurities (P, V, Ti, and Cr) can limit the use of BOF slag when they accumulate in recycled slag.

1.1.3.2.4.4 Olivine and Dolomite

Olivine $[(Mg,Fe)_2SiO_4]$ and dolomite $[CaMg(CO_3)_2]$ are used to adjust the MgO content in the final blast furnace slag. They also improve the metallurgical properties of pellets due to higher MgO content. Dolomite is decomposed during the agglomeration process releasing CO_2 and forming CaO and MgO, which then participate in mineralization reactions in sinter formation. As mentioned earlier, MgO as flux in the sinter can minimize the reduction–disintegration of the sinter.

1.1.3.2.4.5 Other Additives

To control the iron content (or to increase the mass of slag bonding phases), small additions of quartzite, sand, olivine, etc., can be applied. Manganese ore and manganese slag (from Mn alloy production) are used in the sinter mix instead of adding them as lumpy ore in the blast furnace.

1.1.3.2.5 Additives in Blast Furnace

The ideal burden consists of one kind of coke and one kind of self-fluxing sinter or pellets. In the real world, this is not possible. When small adjustments in the sinter or pellet chemistry cannot be done, certain additions are made in the burden. Burden adjustments are made also when rapid finetuning is needed. One required property, common to all additives, is that they must withstand decrepitating. "Decrepitation" is the breakage of iron ore, in particular lumpy ore, upon heating.

The most common burden additive is raw limestone. The size of limestone must not be too large because it is important that the decomposition of carbonate should take place as early in the shaft as possible. If the decomposition inside a large lump of limestone takes place below the zone where the Boudouard reaction, $CO_2 + C \rightarrow 2CO$, will possibly take place, coke consumption will increase.

BOF slag would be a better basic additive if the contents of P, V, Ti, or Cr do not limit its use. Manganese ore is a frequently used additive to get the desired Mn content in the hot metal.

Many other special additives can be used for other purposes, e.g., dolomite or olivine to improve slag properties, high silica lumpy ore to flush out alkalis, etc. Slag control by injecting finely ground slag through the tuyeres has been tried but this is still on experimental stage.

1.1.3.2.6 DRI and Scrap

DRI and hot briquetted iron (HBI) are normally used directly for EAF steelmaking process, but they can be used to boost blast furnace production. Scrap has the same effect and it is also used to recycle iron and steel scrap from slag handling. It must not contain fines of less than 5 mm and no pieces that can destroy conveyor belts.

1.1.4. REDUCING AGENTS

Blast furnace ironmaking is a multistep reduction of iron oxides at elevated temperatures. To obtain metallic iron in the form of hot metal from iron oxides (sinter, pellets, lumpy ores), considerable amount of reducing agent is required, and at the same time large amount of thermal energy is needed to raise the raw materials and the products to the required reaction temperatures and supply the thermal energy demanded by the endothermic reactions. In the blast furnace process, the reducing agents and fuels are provided by coke and various other less expensive fuels/reductants such as pulverized coal, hydrocarbons (oil or natural gas), and waste plastics as injectants. This chapter will describe the preparation and properties of coke and various injectants commonly used in the modern ironmaking blast furnaces.

1.1.4.1. Coke

Coke, as the main carbon source, has five important functions in blast furnace process:
(1) coke carbon is the main source of energy
(2) CO and carbon reduce iron oxides
(3) carbon carburizes the hot metal
(4) coke creates a permeable support for the burden
(5) coke layers act as a gas distributor

1.1.4.1.1 Coking

1.1.4.1.1.1 Raw Materials and Blending

Fossil carbon is found in many forms, starting from the youngest: peat, lignite, coal, and anthracite. Oil and natural gas are large carbon resources, too. All of them have been used for coke making, except anthracite and natural gas, but only a relatively few coal grades are considered as good coking coals for metallurgical coke. Large deposits of good coking coals are found in Australia, Canada, United States, South Africa, Russia, and China.

Coke is made of a blend of typically three to seven coking coal grades. Coal grades have different properties:

- physical properties (density, grain size, petrography, ash, volatiles, moisture)
- chemical properties (P, S, K and Na contents, ash composition)
- coking properties (plasticity, shrinking, swelling)
- stability of the quality

Sometimes small amounts of additives (e.g., oil) and recycled materials can be added to the coal mix.

The aim of blending is to get the best balanced properties of the coke and to ensure stable good operation of the coking plant. The blending starts with primary crushing and dosing. The blend goes through secondary crushing to 2.0–2.5 mm grain size and conveyed to the coal bin.

1.1.4.1.1.2 Coke-Oven Batteries

Vertical coke-ovens are arranged in two batteries side by side, e.g., 30 + 30 to 70 + 70 in number. Coal bin is located aside between the two batteries. Both batteries have usually two charging and pushing machines.

Typical dimensions of ovens are:

- Length: 15–20 m
- Height: 7–9 m

- Width: 40–60 cm
- Wall thickness: 10 cm

The ovens are heated with a mixture of blast furnace-top gas and coke oven gas (COG). Between each oven there are heating slots where hot flue gas flows and heats the walls of the ovens. Gas and air are preheated with flue gas from the ovens.

The ovens are filled one by one in a sequence, heated 12–14 h at about 1050 °C and emptied with the pushing machine. Coke is quenched conventionally with water in a quenching tower (wet quenching). Dry quenching is made with circulating nitrogen in a quenching chamber. Heat from nitrogen is recovered in a waste heat boiler. Coke dry quenching (CDQ) is environmentally and ecologically better than wet quenching. CDQ also improves the quality of coke and enables reduced coke consumption in the blast furnace. As the product quality is improved, CDQ may also allow for the use of lower-cost noncoking coal in the process, thereby reducing costs [24].

Raw gas from the batteries is cooled and washed with water sprays. Coal tar and many other components of the raw gas are mixed in the water. The treatment of gas, tar, and water takes place on site delivering many valuable byproducts, e.g., tar, benzene, ammonia, sulfur, and COG. A typical composition of COG is $H_2=60\%$, $CH_4=24\%$, $CO=6\%$, $CO_2=2\%$, $N_2=6\%$. COG is used as fuel in rolling mills and power plant. It can also be injected in the blast furnace through the tuyeres like tar as well.

After quenching, coke is screened in several fractions, e.g.:

- +40 mm: blast furnace base coke
- 20–40 mm: blast furnace small coke
- 8–20 mm: nut coke
- 3–8 mm: coke breeze
- 0–3 mm: coke fines (dust)

Figure 1.1.13 shows typical coke particles suitable for the blast furnace process.

Figure 1.1.13 Coke particles for blast furnace process [22].

The commercial cokemaking process can be classified into three categories: the byproduct process, the heat-recovery process, and the beehive process [25]. In "byproduct cokemaking," the off-gas is collected and sent to the byproduct plant for recovery of various byproducts. In nonrecovery cokemaking, the off-gas is not recovered as byproducts; however, when heat is recovered through a waste heat boiler it is also called "heat-recovery cokemaking." A beehive oven is a simple firebrick chamber built with an arched roof so that the shape inside is that of an old-fashioned beehive. Beehive coking is now an obsolete process with low productivity and high pollution.

1.1.4.1.1.3 Heat-Recovery Cokemaking

Heat-recovery cokemaking is a modern application (since 1960) as a modification of the old beehive process. Heat-recovery oven chambers have a horizontal 4 m × 15 m sole. The total height of the chamber is about 1.5–2 m with a vault roof. The preformed 0.5–0.7-m thick coal cake is pushed on the sole in the hot chamber. The hot surfaces start the cokemaking process and gasification of volatile components. Primary air is led above the coking bed oxidizing partly the volatiles and heating the bed. Partly oxidized hot gas is led through channels in the walls down to channels below the sole where final oxidation with secondary air takes place heating the sole. Flue gas is drawn through channels in the walls up to gas tunnel and further to boilers. This process will be more important when the resources of good coking coals are exhausted. Figure 1.1.14 illustrates the cross-section through a heat-recovery coke oven [25].

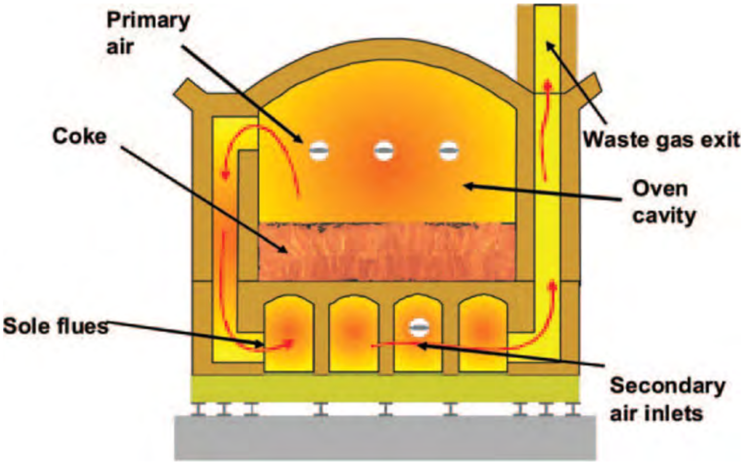

Figure 1.1.14 Illustration of the heat-recovery coke oven [25].

1.1.4.1.1.4 Byproduct Cokemaking

For byproduct cokemaking, the volatile matter evolved during the coking process is collected and refined into byproduct chemicals. The coking process is performed in narrow, tall slot ovens that operate under a nonoxidizing atmosphere. A positive pressure within the oven cavity prevents air ingress and subsequent combustion of the volatile matter. Ovens typically range in height from 4 up to 8 m in the latest plants. The main emission sources from the ovens occur during coke pushing, at which time the oven doors are opened and the coke is exposed to the atmosphere [25]. Volatiles driven off during the coking process pass through a collector main to the byproduct chemical plant. Tars are condensed by cooling the crude gas with flushing liquor and then in a primary cooler. An electrostatic precipitator removes the remaining tars. The gas is further treated, producing additional byproducts, including light oil, naphthalene, ammonium sulfate, and sulfur, depending on market demand. The cleaned gas, known as COG, is normally stored in a gas holder and boosted in pressure for use around the steel plant as a heating fuel or reducing gas [25].

Both byproduct and heat-recovery coke plant technologies are capable of producing high-quality coke suitable for high-productivity blast furnaces. The decision as to which type of plant to build, considered from the viewpoint of return on investment, comes down to how the coke plant is integrated into the overall steel plant and what external energy sources are available to the plant. From an environmental viewpoint, the heat-recovery technology had a smaller footprint than the byproduct technology. Due to its negative-pressure operation and incineration of all the volatile matter in the coal, the heat-recovery process is less susceptible to toxic gas releases. The coal bed configuration also means particulate emissions are reduced [25].

1.1.4.1.2 Coke Characterization

Basic properties are chemical composition, cold strength, and size. They are the first figures telling if a certain coke is suitable for blast furnace use.

1.1.4.1.2.1 Composition

The content of impurities (e.g., S, P, and alkalis) shall be low, as well as ash and moisture contents. Where the exact limits are, depends on local conditions, burden composition, steel grades, etc.

1.1.4.1.2.2 Cold Strength

Cold strength is measured with standard Micum test. Coke of defined size is tumbled 4 min within a test drum (rotation speed 25 rpm/min); screened with test sieves and the fractions are weighed. The test values are Micum 40 (M40) and Micum 10 (M10). Some other values are sometimes used, too. Good blast furnace coke has M40 value over 80% and M10 less than 10%.

1.1.4.1.2.3 Size

Blast furnace coke should be sized to ensure good gas permeability in the shaft. An old rule of thumb states that the upper limit of the coke fraction shall be two times the lower limit. The lower limit of base coke is usually 40 mm, which gives the upper limit 80 mm. Small coke can be charged as separate charges and nut coke mixed with pellets.

1.1.4.1.2.4 Metallurgical Properties

Metallurgical properties of blast furnace coke are measured by standard test methods. These tests try to simulate real blast furnace conditions thus telling the behavior of coke in different sections of the blast furnace.

CRI-Test (Coke Reactivity Index) 200 g of 19–22.4 mm coke pieces are placed in a test retort and heated up to 1100 °C in pure N_2. Then 5 l/min pure CO_2 is led through the sample during 1 h at 1100 °C. The loss in weight in % is the CRI.

CSR-Test (Coke Strength After Reaction with CO_2) CSR is measured from the same sample immediately after CRI test. The sample is tumbled in a 700-mm long, 130-mm diameter tube rotating 30 min around its middle with 20 rpm speed; CSR-index is the percentage of +10 mm grains after the tumbling. CSR and CRI have a strong negative correlation. High CSR and low CRI are desirable.

1.1.4.2. Injectants

1.1.4.2.1 Pulverized Coal

Pulverized coal can be used as a reducing agent by injecting it through the tuyeres. Coke has been replaced up to 250 kg/THM with pulverized coal [26]. Coals for PCI are usually cheaper noncoking thermal coals. Important properties of the coals are:

- content of volatiles and moisture
- chemical composition (S, P, alkalis, ash)
- grindability (Hardgrove Grindability Index)
- stability of the quality.

Coal is dried and ground to <0.1 mm grain size. Pulverized coal is carried pneumatically to a bin and further to weighing and distributing system to be injected in the blast furnace, as illustrated in Figure 1.1.15 [18].

1.1.4.2.2 Plastic, Fluff, and Other Solids

Waste materials, e.g., plastics and fluff, can be recycled by injecting in the blast furnace if they are ground to suitable grain size to be transported pneumatically and if they contain enough of carbon that can be oxidized. These materials must not contain too much of undesirable impurities such as Cl, Zn, P, S, etc.

Blast furnace dust can be recycled by injecting if its Zn content is not too high to accumulate in the process.

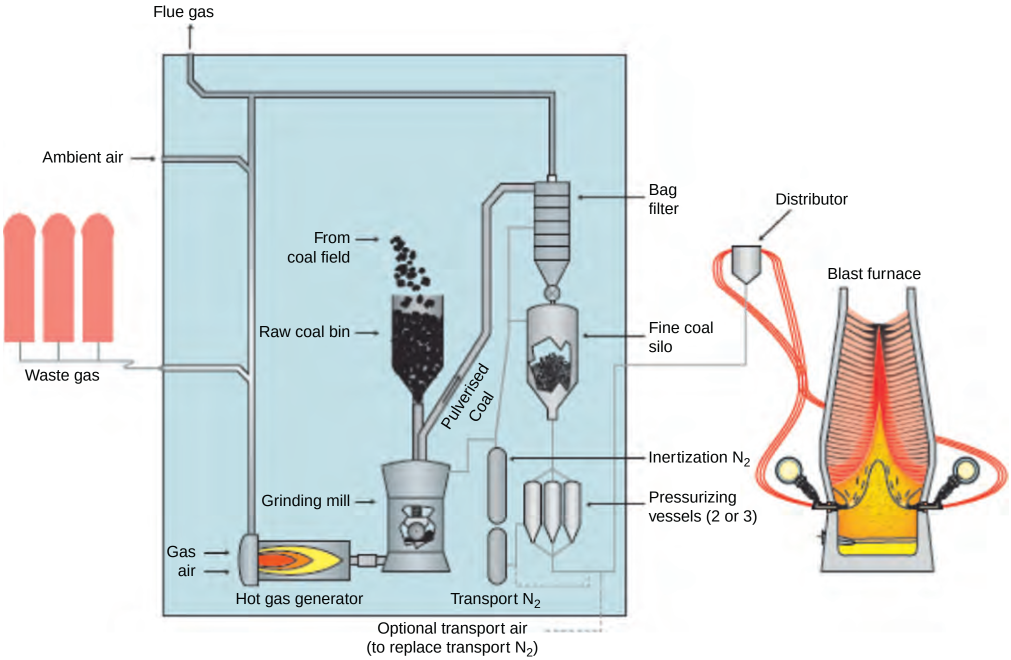

Figure 1.1.15 Illustration of pulverized coal injection (PCI) in the blast furnace [18].

1.1.4.2.3 Oil and Tar

Injection of oil was widely used before oil crisis in the 1970s. Since then PCI has been dominant. Equipment for oil injection is quite simple. Oil has been injected up to 150 kg/THM. The replacement ratio decreases from about 1.3 kg coke/1 kg oil with small oil rates down to 1 kg coke/1 kg oil with large oil rates. Light oil fractions are easier to inject and they have a better replacement ratio. The heaviest fractions, e.g., bottom oil must be preheated up to 220 °C before pumping and injection. The main disadvantages of oil are high sulfur content, strong soot formation with high injection rate, and the price. A typical composition of heavy bottom oil is C = 86.6%, H = 10.0%, S = 1.8%, N = 0.8%, and O = 0.8%.

Surplus tar from coke plant can also be injected like oil in the blast furnace. Tar is more abrasive for the pumps than oil. A typical composition of coal tar is C = 91.5%, H = 5.5%, S = 0.6%, N = 0.9%, and O = 1.5%. Tar contains also some 2–5% water.

1.1.4.2.4 Natural Gas

Natural gas is widely used where it is available at reasonable price. It consists mainly of methane (over 80% in volume) with a few percent of ethane and other alkanes. The main

Table 1.1.1 Constituents of the Natural Gas from Different Countries

Volume%	Russia Urengoi	Germany Goldenstedt	USA Kansas	Holland Groningen	Norway Troll
Methane	98.0	88.0	84.1	81.3	93.2
Ethane	0.8	1.0	6.7	2.8	3.7
Propane	0.2	0.2	0.3	0.4	0.4
Butane	0.02	0.0	0.0	0.4	0.5
Nitrogen	0.9	10.0	8.4	14.3	1.6
CO_2	0.1	0.8	0.8	0.9	0.6

impurity is nitrogen and the rest is small amount of carbon dioxide. Table 1.1.1 lists the constituents of the natural gases from different countries.

Natural gas is easy to inject and it is clean—practically without sulfur. It has a strong reducing effect on the adiabatic flame temperature. The lowest limit is claimed to be 2073 K (1800 °C). The price of natural gas is usually high.

The low sulfur content brings several benefits:

- Better working conditions in the cast house
- Higher carbon content in hot metal
- Less need for desulfurization

Higher H_2-content in top gas enables more electric power generation. Natural gas injection can decrease CO_2 emissions depending on replacement ratio and injection rate.

1.1.4.2.5 Coke Oven Gas

COG is a strong fuel but it is less useful compared to other injected fuels in the lower part of the blast furnace. COG contains $H_2=60\%$, $CH_4=24\%$, $CO=6\%$, $CO_2=2\%$, and $N_2=6\%$, but only carbon in CH_4 is oxidized in the raceway to CO releasing heat. CO_2 reacts with coke carbon to CO consuming energy, whereas H_2, N_2, and CO are only heated up in the raceway. The advantage of H_2 and CO as reducing gases comes in use in the upper part of the furnace. COG lowers the adiabatic flame temperature more than other injected materials.

1.1.5. COUNTER-CURRENT MOVEMENTS OF BURDEN AND GAS

1.1.5.1. Burden Descending

1.1.5.1.1 Different Zones in Blast Furnace

Blast furnace has a typical conical shape, and is subdivided into various zones according to either the mechanical structure (external) or the physical and chemical state of the feeding materials and products (internal). Figure 1.1.16 illustrates various zones (external and internal) and the temperature distribution from the top to the bottom of the blast furnace [18].

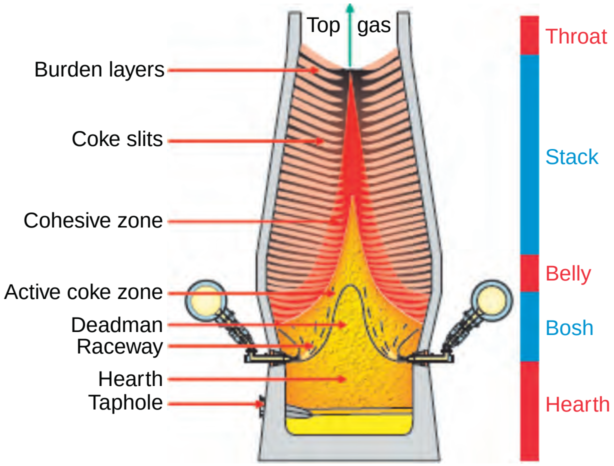

Figure 1.1.16 Different zones in blast furnace [18].

From the vertical direction the blast furnace could be generally divided into five zones (externally):

- *Throat*: it denotes the burden surface on the top of the blast furnace.
- *Stack or shaft*: where the ores are heated and reduction reactions start.
- *Belly or bosh parallel*: the short vertical section.
- *Bosch*: where the ore reduction completes, and the ores are melting down.
- *Hearth*: where the molten materials (slag and hot metal) are collected and tapped via the tap holes.

According to the internal state of the feed materials, various other zones could be denoted in the blast furnace:

(1) *Primary reduction zone*: the upper part of shaft, where higher valence iron oxides (hematite and magnetite: Fe_2O_3, Fe_3O_4) are reduced. The temperature ranges from 400 to 1000 °C.

(2) *Thermal reserve zone*: the lower part of the shaft zone, where the temperature is maintained at about 800–1000 °C. In this zone, reduction of wüstite (FeO) to metallic iron takes place.

(3) *Cohesive zone*: it extends from above bosh near the wall up to middle part of stack in the center of the blast furnace. In cohesive zone, the materials have reached about 1200 °C and start to soften and melt except coke particles.

(4) *Active coke zone/dripping zone*: beneath the cohesive zone, where final reduction to metallic iron completes, and melts of slag and hot metal form and drip through the coke layer.

(5) *Deadman*: a porous packed-bed of unreacted coke particles sitting or floating in the hearth. Carbon saturation of hot metal takes place within the deadman.

1.1.5.1.2 Charging

Charging is the important place where the furnace operation is controlled. Once the burden materials are dumped in the throat, there are minimal means to influence material positions in the furnace. The main idea is to get ore and coke components distributed in positions where gas and solids have optimal conditions for heat and material exchange. The main stream of gas must meet the main flow of ore. The shape of the cohesive zone is controlled mainly with ore to coke distribution (O/C) on the top: the higher O/C on a certain position on furnace radius in the throat—the lower is the cohesive zone on corresponding position lower in the shaft.

There are usually two mechanical stock rods or radar devices measuring continuously the height of the burden. The burden descends slowly and when it comes to stock level, a new charge is dumped in the furnace.

Size segregation is a phenomenon that must be taken into account in charging. The place where falling material hits the burden surface is here called the ridge. The smaller pieces will stay at the ridge and the bigger will continue to roll along the slope to the foot of the ridge. As a result the zones at the wall side and center consist of larger lumps and have good gas permeability. If the ridge is at the throat armor, the coarse pieces roll toward the furnace center where the gas permeability becomes good whereas the wall side becomes compact with small grains. The negative effects of size segregation can be minimized with sizing and/or fractioning of raw materials. A narrow size distribution contributes to good gas permeability whereas a wide size distribution gives a dense packing with poor gas permeability.

Another important material property in charging is the angle of repose. Typical values are: 35–38° for coke (steep), 29–33° for sinter, and 25–26° for pellets (more flat) as is shown in Figure 1.1.17 [18]. Moisture content can increase the angle of repose.

There are two principal designs of charging equipment: bell top and bell-less top. The bell-less top is the dominating design nowadays. Both of them have numerous variants.

1.1.5.1.2.1 Bell Top Charging

In bell top, there are two concentric bells making a gas-tight lock. The dump portions are fed on the upper (small) bell, the bell is rotated to a desired sector and the dump portions are dropped on the big bell. Depending on the charging program, one or more

Figure 1.1.17 The angle of repose of blast furnace burden materials [18].

portions are dropped on the big bell. When the order is complete, the pressure between the bells is equalized. Then the big bell goes down and dumps the materials in the furnace. The falling material can further be directed to a certain location on the furnace radius with a movable armor. A common way to describe a certain charging sequence is, e.g., OOCCC ↓ CCCOO ↓, etc., where O means one ore skip, C one coke skip, and ↓ means the big bell dump [27].

In addition to the charging sequence, the distribution can be adjusted by skip weight and stock level. With smaller skip weight O/C tends to increase on the wall side. Stock level is the distance between burden surface and open big bell. Stock level determines the place of the material ridge where the burden falls from the big bell edge or will the material hit the throat armor. The position of the ridge has a strong effect on segregation: the small size material will stay on the ridge and the coarser will run toward the wall side and to the center.

1.1.5.1.2.2 Bell-Less Top Charging

The bell-less top gives more freedom to place materials on desired places on furnace radius. In bell-less top, there are two material bins with gas-tight valves for filling the bins up and dosing valves in bottoms of the bins. The bins operate alternately: from one bin, burden material is flowing through the dosing valve to a rotating chute while the other bin is filled with burden material. The angle of the rotating chute is controlled to place the material as a ring on material surface at a desired distance from furnace center. Simulation model is used to find a charging program giving the desired O/C distribution [28].

1.1.5.1.3 Burden Descending and Physical–Chemical Changes

1.1.5.1.3.1 Throat and Shaft

The direction of the coke movement is mainly toward the raceways. A smaller part in the center and between the raceways is sinking toward deadman. In the cylindrical throat descending is even, but in the shaft the diameter is slightly widening to bosh parallel (belly). When the shaft widens, the burden layers become thinner. Coke moves slightly more to the wall side than ore components. If the grain size of the overlying layer is considerably smaller than in the underlying, mixing of the layers can take place. Especially pellets tend to percolate in coke layers.

The direction of ore component is mainly straight downward diverging slightly toward the walls.

1.1.5.1.3.2 Cohesive Zone

During descent, the burden is surrounded by ascending hot reducing gas. The iron oxides are reduced to a great extent when they reach the outer boundary of the cohesive zone where the temperature is about 1100 °C. At this temperature region, metalized grains start to sinter and the slag components separate. The above located burden weight compresses the softening metallic layer to a more compact ring and the slag is squeezing out. Coke layers are left between the metal rings and they are called coke windows. The ascending gas flows from the center horizontally through the coke windows through the cohesive zone and then upward again. The gas heats inner side of the metallic ring and when the temperature of the metal reaches 1200 °C, it starts to melt down. This is the inner boundary of the cohesive zone.

The bell-shaped cohesive zone is built up of sintered metal rings alternating with coke layers. The profile of ideal cohesive zone is like an upside down V building an arch that supports the burden in the shaft. The root of the cohesive zone should be located in the bosh. The profile can vary a lot depending on its thickness and height and also on the location of the root.

1.1.5.1.3.3 Dripping Zone

The space below the cohesive zone is the dripping zone. Molten iron and slag drip from the cohesive zone zigzagging through the voids between coke particles to the hearth. Molten materials avert strong gas flows from the raceways but on other sections they flow straight down. If the deadman is blocked, molten materials flow down along its surface.

1.1.5.1.3.4 Active Coke Zone

The active coke zone starts where the cohesive zone ends. In this zone, coke particles move toward the raceways. The active coke zone turns gradually into hearth coke. In the active coke zone, coke is in a semi-fluidized state flowing toward the raceways. To keep the burden descending smoothly, it is important to control the cohesive zone so that no narrow sections occur between the cohesive zone and the hearth coke.

1.1.5.1.3.5 Raceway

The raceway cavities are formed when the hot blasts through the tuyeres penetrate in the hearth coke bed. Coke flows from above in the cavity, circulates vigorously and crumbles during combustion. Finally the small pieces are packed to the end of the raceway and oxidized completely while new coke flows in the cavity.

1.1.5.1.3.6 Hearth Coke and Deadman

Hearth coke fills the hearth and stretches upward between raceways up to bosh or even lower shaft as an anthill-shaped coke bed. Hearth coke moves slowly in the hearth and is finally fading out while carbon dissolves in hot metal and coke ash in slag. At the same time, the hearth coke is renewed by new coke from the active coke zone.

Deadman is located inside the hearth coke. Its diameter is about 3 m smaller than the hearth diameter. Deadman can be either active or blocked. An active deadman floats in molten products or it can more permanently contact the hearth bottom. Hot metal and slag can flow through the active deadman though it is denser packed than hearth coke.

Coke in the deadman dissolves in hot metal like hearth coke. If deadman is blocked, it is in tight contact with the hearth bottom and its temperature is below 1000 °C [29]. The space between coke pieces is filled with solid iron, slag, Ti(C, N), spinel, CaS, CaO, and other compounds with high melting point. It is very difficult to get a blocked deadman active because it is cooled from hearth bottom.

1.1.5.1.3.7 Hot Metal and Slag

Hot metal casting is made through the tap hole 4–12 times per day, depending on the size and design of the blast furnace. If there are two or more tap holes, casting can be continuous. In a blast furnace with one tap hole only most of the hot metal comes out alone in the beginning of the tapping. Slag is floating on the hot metal and starts to come after 10–30 min after tap start. Hot metal surface lies almost horizontally in the hearth, but during the cast when slag starts to flow out, the slag surface begins to lean toward the tap hole because the viscosity of the slag is high and it takes time to flow through the coke bed to the tap hole. Slag level on the opposite side of the tap hole is higher than at the tap hole and the mass of slag presses the hot metal surface below the level of the tap hole. Both hot metal and slag flow out through the tap hole until the slag level is so low that also gas can burst out. The tap hole is closed with a mud gun and the casting is over.

1.1.5.2. Movement of Gas

Gases inside the blast furnace arise partly from the external hot blast and partly from the internal reactions of combustion, reduction, and coke gasification (Boudouard reaction). The gas temperature inside the furnace has a very steep gradient as was shown in Figure 1.1.16, starting at 2100–2300 °C of flame temperature in raceway and ending at 100–300 °C at the top of the furnace. Figure 1.1.18 shows the vertical gas profile in the operating blast furnaces [15].

1.1.5.2.1 Combustion

1.1.5.2.1.1 Hot Blast

The air before hot stoves, called "cold blast," is generated with a blower. Cold blast temperature is 80–200 °C depending on pressure and ambient temperature. The air blast is heated in hot stoves up to 1100–1350 °C. There are three or four stoves serving one blast furnace. Hot stoves are regenerative heat exchangers that are normally heated with blast furnace-top gas. If the number of stoves is three, one is on blast and two on heating. If the number of stoves is four, they usually operate staggered parallel: two on blast, two on heating. Oxygen-enriched blast is mixed in the cold blast before hot stoves, up to 29% total O_2 in the hot blast. If more oxygen is added it is injected through the tuyeres.

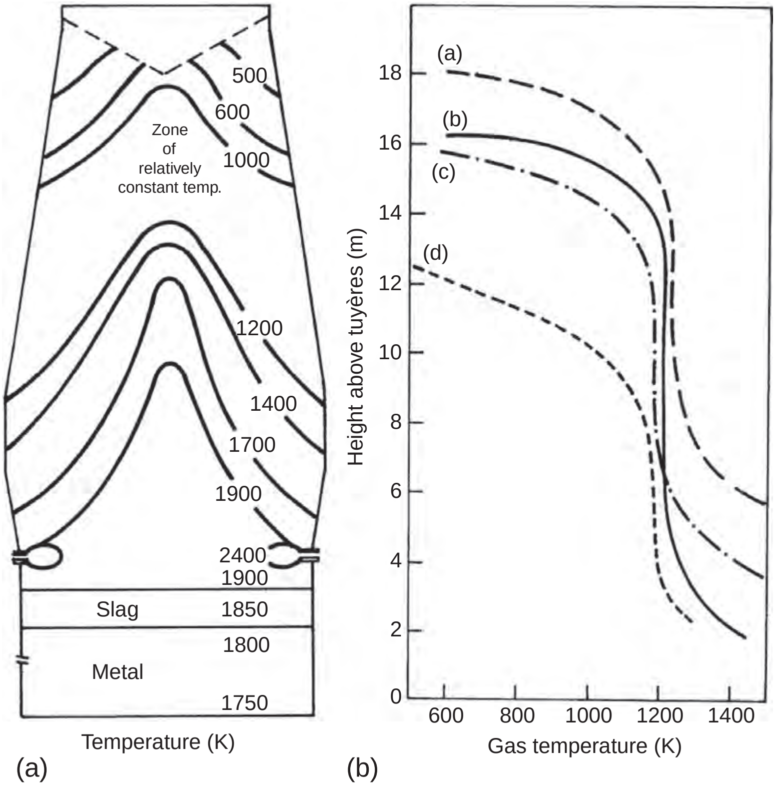

Figure 1.1.18 Vertical gas temperature profile of various operating blast furnaces [15]: (a) from a quenched furnace data and (b) from thermal couple probes.

1.1.5.2.1.2 Raceways

When the hot blast flows from the tuyere in the hearth coke, a cavity called raceway takes shape. The velocity of the hot blast jet at tuyere nose is 200–240 m/s. This velocity is calculated for total blast from hot stoves. A rough estimation can be calculated with Equation (1.1.17) as follows:

$$w = 22.414 \times V \frac{T + 273.15}{273.15} \times \frac{1}{1 + p} \times \frac{1}{n + A_t} \tag{1.1.17}$$

where w is the jet velocity, m/s, V is the hot blast volume, T is the hot blast temperature, °C, p is the hot blast pressure, bar (g), n is the number of tuyeres, A_t is the cross-sectional area of one tuyere, m^2.

Injected fuels and oxygen increase the velocity. A raceway is 0.8–2 m long, 0.5 m wide. The shape of raceway reminds of a pear with an upward bending end. Its bottom consists of fine-grained coke, which is called "birds nest." The penetrating jet expands, mixes with hearth gas and coke building a whirling cavity where coke carbon, injected fuel, and hearth atmosphere react with hot blast. Physical raceway is defined by stagnant coke and chemical raceway where neither CO_2 nor H_2O exist. Factors influencing the raceway length are

- jet velocity
- rate of injected fuel
- oxygen enrichment
- deadman

Jet velocity will increase the raceway length to a certain point, but too high velocity makes the raceway act like a jet mill grinding coke, which will block the birds nest and bend the raceway upward.

Increasing the rate of injected fuel moves the hottest point of raceway backward (as can be seen as increasing heat loads on bosh lining) thus shortening the raceway. Oxygen enrichment lengthens the raceway. If deadman is clogged (inactive), it bends the raceway upward and steers gas flow toward the bosh walls thus making the material and gas distribution still worse. Deadman grows larger and molten materials are forced to flow more close to hearth walls.

Physical conditions in the raceway are extremely severe due to high temperature and high gas velocity. Raceway adiabatic flame temperature is a common key figure.

The gas produced in the raceway is called bosh gas. This gas consists mainly of N_2, CO, and H_2 with small amounts of Ar, SiO, H_2S, and CS_2. Bosh gas leaves the vicinity of the raceway at about 1700 °C.

1.1.5.2.2 Ascending Flow

1.1.5.2.2.1 Raceway—Cohesive Zone

The bosh gas flows from the raceway up to the cohesive zone mainly along the active coke zone. In the active coke zone, also called dripping zone, gas is in an intensive counter current with coke molten metal and slag. Iron flows easily through the coke layer but large slag rates or slag with high viscosity may cause troubles by flooding. When flooding takes place, slag does not drip down. It is held up between coke particles by dynamic pressure of ascending gas resulting in hanging, in other words, the burden does not descend. Nowadays, with low slag rates and good slag viscosity control this rarely happens, but if the designed blast volume is exceeded this may take place.

1.1.5.2.2.2 Cohesive Zone

At the inner boundary of the cohesive zone, the gas stream bends sharply into the coke windows. Gas temperature is about 1300 °C. The iron layer between the coke windows is carburized a lot and the inner edge melts down. As the whole cohesive zone descends—the shape of the zone seems to stay even though the inner boundary melts away. A big portion of the total pressure drop in the furnace occurs in the coke windows of the cohesive zone. A narrow cohesive zone is favorable for the furnace operation.

The outer boundary of the cohesive zone is not as clear as the inner one. The gas turns up toward the throat. Gas temperature is about 1000 °C and its composition has changed slightly. Due to direct reduction of Fe, Si, Mn, P, Ti, and other elements CO content has increased.

1.1.5.2.2.3 Shaft

Gas temperature at the outer boundary is the same around the cohesive zone but is then cooled down quite fast to thermal reserve zone temperature of 800–1000 °C [27]. This temperature depends mainly on coke properties; when the solution loss reactions take place. 950 °C is a common value. Burden temperature is about 50 °C lower. This temperature depends on coke properties, the coke reactivity (the temperature at which Boudouard reaction comes in effect). The higher the CRI is, the higher coke consumption reduction of iron oxides goes on slowly and this gas temperature remains almost to the upper shaft. The thermal reserve zone is highest where the ore/coke ratio is highest on the furnace radius.

1.1.5.2.2.4 Upper Shaft and Throat

When the burden has been loaded in the furnace, moisture starts to evaporate. Temperature in the burden cannot rise above 100 °C until all moisture has evaporated. Then it starts to warm up and be heated rapidly by the ascending gas. Reduction of iron oxides is also delayed until the moisture has disappeared.

About 4–6 m below the stock level begins strong heat exchange between ascending gas and descending burden. Gas temperature decreases sharply from 950 to 100–300 °C. In the furnace center, the top gas temperature is higher, 300–600 °C and close to the wall down to about 120 °C.

The shape of gas temperature distribution responds quite well to the shape of cohesive zone. If the burden is cold and wet at the same time when oxygen enrichment is high (the specific amount of gas is low), top gas temperature can go down to 80 °C. In this case, the thermal reserve zone can disappear with severe consequences like chilled hearth.

1.1.6. BLAST FURNACE REACTIONS

Section 1.1.1 has outlined main chemical reactions taking place in the blast furnaces: combustion of the coke and other injected carbon-bearing fuels, and stage-wise reduction of iron oxides by carbon and hydrogen. Section 1.1.6 focuses on the thermochemical and thermodynamic analysis of these reactions and their influence on the blast furnace performance. Furthermore, efforts are also made to discuss the chemical behavior of minor elements and their effects on the product quality, including silicon, sulfur and phosphorus, zinc, and alkaline elements such as sodium and potassium.

The chemical reactions between iron ore (iron oxides) and reductant (coke and other injected fuels, and hydrogen from water vapor) and combustion of fuels fulfill the two important requirements of ironmaking process: reduction of iron oxides to metallic iron and forming liquid slag and hot metal; heating up the ferrous burden and coke to the required temperatures. Because of the counter-current flow and the solid burden and reducing gases, the analysis of these reactions could start from the entering of the solid burden from the top, or from the tuyeres of incoming hot blast and injected fuels. The reactions will be discussed according to different levels of the blast furnace, similar to the book written by Biswas [27], in three general zones:

(1) *the upper part*: temperature range 25–800 °C for preheating and preparation zone
(2) *the middle part*: temperature range 800–1000 °C for indirect reduction (thermal reserve zone, or chemical reserve zone)
(3) *the lower part*: temperature range 1000–1500 °C for direct reduction and melting.

As a general remark, all the thermodynamic calculations made in this section were made by using HSC Chemistry 6.1 [30].

1.1.6.1. Reactions in the Upper Zone

1.1.6.1.1 Water Removal and Volatilization

Drying of burden materials can be an important phase when burden materials are cold and their moisture content is high. The average moisture content of coke and ore is about 5% but can be as high as 15% in very moist ores. Evaporation of water (moisture) consumes about 1425 kJ thermal energy per kg water. A rule of thumb states that 1 kg of charged water will increase coke rate by 0.5 kg. This phenomenon comes pronounced with low fuel rate and high oxygen enrichment of hot blast. Too low heat content ratio may be identified when average top gas temperature drops to about 80 °C and the heat flux to the cooling system in upper shaft goes down. To help this situation, gas flow must be increased by increasing the coke rate or decreasing the oxygen enrichment.

Coke particles may contain up to 1.5–2% of volatiles. They volatilize in this zone but the amount being small, they do not change the top gas composition significantly.

Water occurs in the ore also as crystalline or hydrated water. The decomposition of the hydrates of iron oxides may start around 300 °C and continue to higher temperature levels of 400 °C. It needs 4035 kJ thermal energy per kg water, much higher for pure evaporation. However, for sinter and pellets, the crystalline water should have already been removed during sintering and firing of pellets. For lumpy ore, the removal of crystalline water is still important. It should be noted that the water vapor from drying or from removal of crystalline water may react with ascending CO gas to form CO_2 and H_2, the so-called "water–gas shift reaction" or simply "water–gas reaction."

The water–gas reaction as is shown in Equation (1.1.18) is highly exothermic. The reaction will shift to the left at higher temperatures. The equilibrium constant of the reaction is 0.59 at 1273 K (1000 °C), and will increase to 5.0 at 773 K (500 °C).

$$CO + H_2O = CO_2 + H_2 \quad \Delta H^{\circ}_{298} = -41.4\,\mathrm{kJ/mol} \tag{1.1.18}$$

Some iron ores (e.g., goethite) contain chemically bonded water. They decompose between 200 and 500 °C. Siderite, $FeCO_3$ begins to decompose at about 360 °C, although these are not the main iron ore components.

1.1.6.1.2 Preheating and Early Stage of Ore Reduction

Temperature region from 100 to 570 °C can be called preheating. It is a relatively rapid phase. Reduction of iron oxides starts during preheating. The stage-wise reductions of iron oxides with CO and H_2 are expressed as follows:

$$\begin{aligned} &3Fe_2O_{3(s)} + CO_{(g)} = 2Fe_3O_{4(s)} + CO_{2(g)} \\ &\quad \Delta G^{\circ}_{298\,K} = -58.739\,\mathrm{kJ},\ \Delta G^{\circ}_{843\,K} = -86.855\,\mathrm{kJ} \\ &\quad \Delta H^{\circ}_{298\,K} = -44.964\,\mathrm{kJ},\ \Delta H^{\circ}_{843\,K} = -30.050\,\mathrm{kJ} \end{aligned} \tag{1.1.19}$$

$$\begin{aligned} &Fe_3O_{4(s)} + 4CO_{(g)} = 3Fe_{(s)} + 4CO_{2(g)} \quad (T < 570\,°C) \\ &\quad \Delta G^{\circ}_{298\,K} = -16.393\,\mathrm{kJ},\ \Delta G^{\circ}_{843\,K} = -0.826\,\mathrm{kJ} \\ &\quad \Delta H^{\circ}_{298\,K} = -16.356\,\mathrm{kJ},\ \Delta H^{\circ}_{843\,K} = -44.478\,\mathrm{kJ} \end{aligned} \tag{1.1.20}$$

$$\begin{aligned} &3Fe_2O_3 + H_{2(g)} = 2Fe_3O_4 + H_2O_{(g)} \\ &\quad \Delta G^{\circ}_{298\,K} = -30.137\,\mathrm{kJ},\ \Delta G^{\circ}_{843\,K} = -78.865\,\mathrm{kJ} \\ &\quad \Delta H^{\circ}_{298\,K} = -3.826\,\mathrm{kJ},\ \Delta H^{\circ}_{843\,K} = +6.440\,\mathrm{kJ} \end{aligned} \tag{1.1.21}$$

$$\begin{aligned} &Fe_3O_4 + 4H_{2(g)} = 3Fe + 4H_2O_{(g)} \\ &\quad \Delta G^{\circ}_{298\,K} = +98.016\,\mathrm{kJ},\ \Delta G^{\circ}_{843\,K} = +31.312\,\mathrm{kJ} \\ &\quad \Delta H^{\circ}_{298\,K} = +148.196\,\mathrm{kJ},\ \Delta H^{\circ}_{843\,K} = +101.482\,\mathrm{kJ} \end{aligned} \tag{1.1.22}$$

In the upper part of blast furnace, coke does not participate in reduction of iron oxides, and the temperature is so low that Boudouard reaction can be neglected. Therefore, oxygen removal from iron oxides takes place only through "indirect reduction," which arises from the gas–solid reactions. Especially reductions of Fe_2O_3 and Fe_3O_4 with CO (1.1.19) and (1.1.20) are highly exothermic, whereas reduction with H_2 is more endothermic. The equilibrium CO/CO_2 and H_2/H_2O for the reduction of iron oxides at different temperatures can be well represented in Figure 1.1.19. It is very obvious that reduction of Fe_2O_3 to Fe_3O_4 is thermodynamically very easy. At temperatures below 843 K (570 °C), Fe_3O_4 would be directly reduced to metallic iron with either CO or H_2 gas. This equilibrium diagram will be discussed further for reductions at higher temperatures above 843 K. Compared to CO gas, H_2 reduction required more reducing power (high H_2/H_2O ratio).

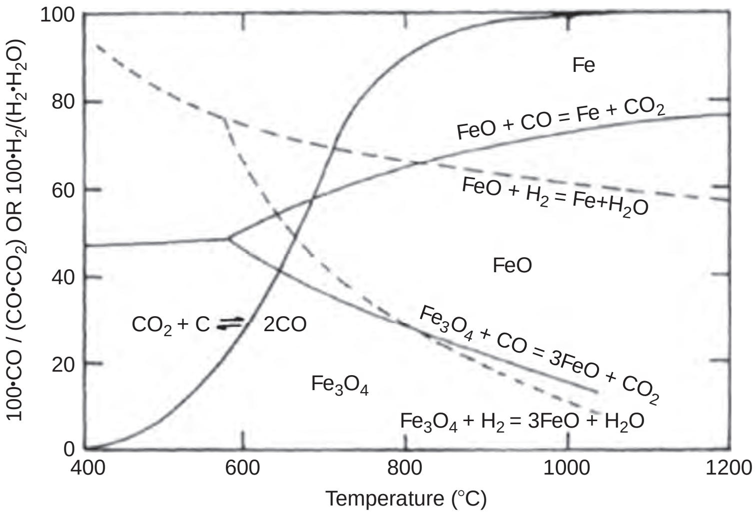

Figure 1.1.19 Equilibrium diagram of iron oxide reduction with CO and H_2 with imposed Boudouard reaction [27].

At temperatures above 843 K, reduction of magnetite with CO and H_2 will only lead to the formation of wüstite, and the formation of metallic iron can only go through the reduction of wüstite. The reactions are listed in Equations (1.1.23)–(1.1.25).

$$\begin{gathered}
Fe_3O_{4(s)} + CO_{(g)} = 3FeO_{(s)} + CO_{2(g)} \quad (T > 570°C) \\
\Delta G^\circ_{298\,K} = 17.986\,kJ, \;\; \Delta G^\circ_{1073\,K} = -4.046\,kJ \\
\Delta H^\circ_{298\,K} = +30.726\,kJ, \;\; \Delta H^\circ_{1073\,K} = +9.706\,kJ
\end{gathered} \tag{1.1.23}$$

$$\begin{gathered}
Fe_3O_4 + H_{2(g)} = 3FeO + H_2O_{(g)} (T > 570°C) \\
\Delta G^\circ_{298\,K} = +46.588\,kJ, \;\; \Delta G^\circ_{1073\,K} = -3.522\,kJ \\
\Delta H^\circ_{298\,K} = +71.864\,kJ, \;\; \Delta H^\circ_{1073\,K} = +43.822\,kJ
\end{gathered} \tag{1.1.24}$$

It can be seen that at about 1073 K (800 °C), the equilibrium ratios of $CO/(CO + CO_2)$ and $H_2/(H_2 + H_2O)$ are very close to each other. As can be seen in Figure 1.1.19, the hydrogen reduction and CO reduction lines cross at 821 °C; below this temperature, CO is a stronger reducing agent and above this temperature, H_2 is a stronger reducing agent [27]. This is true for both Fe_3O_4 and FeO reductions. Again it is obvious that H_2 reduction is much more endothermic than CO reduction.

1.1.6.1.3 Decomposition of Carbonates

Carbonates exist in the ferrous burden partially in the iron ore, and partially as added flux for slag forming. Calcium carbonate (limestone) and dolomite ($CaMg(CO_3)_2$) are typical fluxing agents. When they are added directly to the blast furnace, the strongly

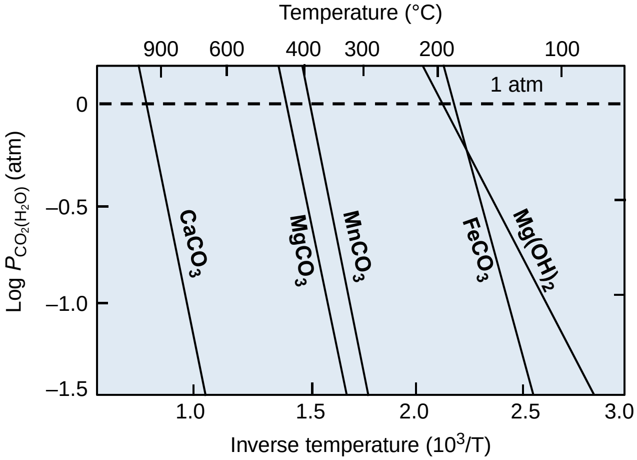

Figure 1.1.20 Equilibrium partial pressure of CO_2 (H_2O) of decomposition of some carbonates and hydroxide as a function of inverse temperature; re-drawn from reference [31].

endothermic decomposition (calcination) reactions will have significant effect on the energy consumption and local temperature in the furnace. Furthermore, the released CO_2 gas will tend to react with coke at temperatures above 900 °C to generate CO gas, which is again a strong endothermic reaction. Figure 1.1.20 shows the equilibrium decomposition partial pressure of CO_2 as function of temperature for a number of carbonates that are relevant to the blast furnace process [27]. The carbonates in the ore and the added limestone or dolomite to the sinter or pellets would have already decomposed during sintering and/or firing of pellets, and will not have influence on the blast furnace process.

1.1.6.1.4 Behavior of Volatile Compounds and Metals

The volatile metals that accompany the charge materials are lead, zinc, and alkalis in the form of their compounds. These compounds have very detrimental effects on the blast furnace lining and burden properties, and the operation. Lead oxide is very easily reduced and the metal does not get reoxidized in the shaft. However, its vapors may penetrate the brickwork. The oxides of zinc and alkali metals are reduced in the lower part of the furnace. The volatile metals are carried to the upper part of the furnace by the fast ascending gases, get reoxidized at lower temperatures by gases having higher oxygen potential (CO_2 or H_2O). A part of the vapors may leave the furnace with the top gas or penetrate the brickwork. The rest is carried down and gets reduced; the metals vaporize and the process is repeated. Thus, a zinc and alkali cycle builds up in the furnace [27].

More detailed discussion about the volatiles will be given in Section 1.1.6.5 together with behavior of other minor elements and impurities including silicon, sulfur, and phosphorus.

1.1.6.2. Reactions in the Middle Zones

The middle zone of the blast furnace follows the upper zone downward to 3–5 m above the tuyere level. It has a temperature range of 800–1000 °C. However, the height of this zone may account for 50–60% of the shaft height (about 75% of the shaft volume). This part is often called "thermal reserve zone" or "chemical reserve zone."

1.1.6.2.1 Chemical and Thermal Reserve Zone

In most part of this zone, the iron-bearing raw material is essentially all wüstite. In the "chemical reserve zone," very little reactions take place and the temperature is kept roughly constant and thus it is also called "thermal reserve zone." At temperatures above 570 °C, reduction of magnetite will generate only wüstite according to thermodynamics, and formation of metallic iron can only be through the reduction of wüstite. Figure 1.1.21 illustrates the temperature and reducing gas profiles of an operating blast furnace along the furnace height [32]. The presence of the chemical and thermal reserve zones are obvious.

The existence of this chemical reserve zone is mainly caused by the insufficient gas-reducing power (CO or H_2) coming from the lower zone of the blast furnace. The real gas composition of the operating blast furnace within this temperature range lies in the wüstite stable zone. Figure 1.1.22 illustrates an example of blast furnace working line (gas temperature profile) in relation to the Fe–O–C stability diagram. It can be seen that at the temperatures between 600 and 1000 °C, only FeO is the stable product, and above 1040 °C the reduction of FeO to metallic iron takes place.

1.1.6.2.2 Indirect Reduction of Wüstite

At the lower part of the thermal reserve zone, where the temperature is around 1000 °C, "indirect reduction" of wüstite (1.1.25) by the uprising CO gas from the lower zone takes place. Due to the kinetic limitation, the Boudouard reaction hardly takes place at this temperature and below. Thus, the required CO gas for wüstite reduction comes only from the lower part of the high-temperature zone.

$$\begin{aligned} &FeO_{(s)} + CO_{(g)} = Fe_{(s)} + CO_{2(g)} \\ &\qquad \Delta G^\circ_{298\,K} = -11.460\,kJ,\ \ \Delta G^\circ_{1273\,K} = +8.993\,kJ \qquad (1.1.25) \\ &\qquad \Delta H^\circ_{298\,K} = -15.694\,kJ,\ \ \Delta H^\circ_{1273\,K} = -15.653\,kJ \end{aligned}$$

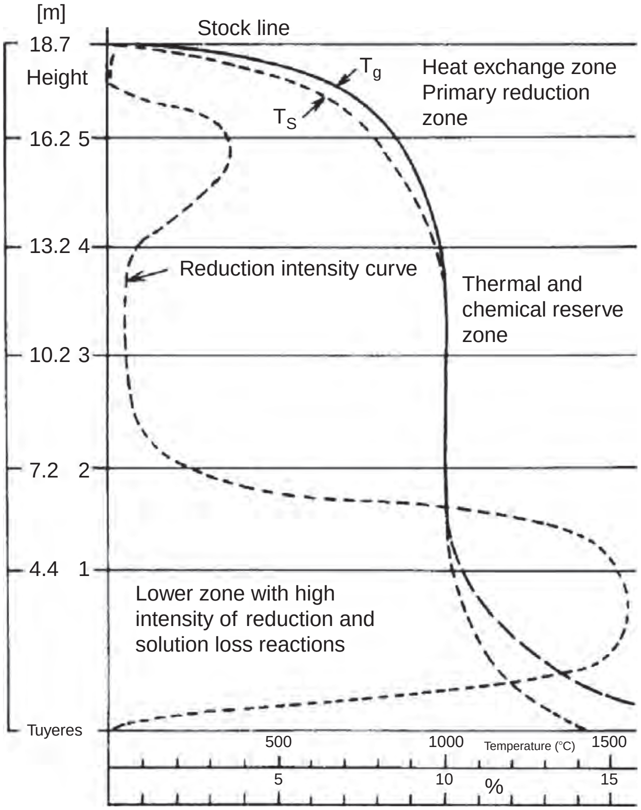

Figure 1.1.21 Distribution of the estimated temperature of the burden and gas and the reduction intensity of industrial scale blast furnace [32].

Due to the exothermic nature of the indirect reduction, the gases do not cool during their ascending flow, and thus the "indirect reduction" of wüstite forms the bottom portion of "thermal reserve" zone. On the contrary, the reduction of magnetite with both CO and H_2 are endothermic as is shown in reactions (1.1.23) and (1.1.24).

Thermodynamically speaking, the minimum CO/CO_2 ratio for the indirect reduction of wüstite at 1000 °C is 2.34, i.e., about 70% CO and 30% CO_2. In other words, the "gas utilization efficiency," defined as the ratio of $CO_2/(CO+CO_2)$, should be below 30%. The indirect reduction is very important for the blast furnace operation, and is preferred over the "direct reduction," i.e., the overall reduction of wüstite by carbon in the coke. In normal blast furnace operation, "direct reduction" removes about 1/3 of the total oxygen in the iron oxide, while "indirect reduction" removes the 2/3 of the oxygen from the iron oxides [18]. Comparison of "indirect reduction" and "direct reduction" is made in Section 1.1.6.3.

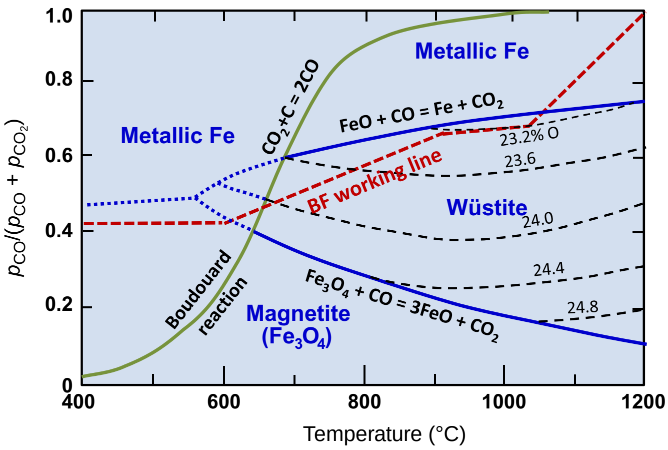

Figure 1.1.22 Fe–O–C equilibrium diagram [27] superimposed with a blast furnace working line (broken line), re-drawn from reference [33].

1.1.6.3. Reactions in the Lower Zones

In the lower zone of the blast furnace, the temperature extends from about 1000 °C near the “cohesive zone” to about 1500 °C near the hearth of the furnace. In this zone, the following physical and chemical changes take place [27]:

(1) calcination of limestone
(2) direct reduction of iron from unreduced wüstite and silicates
(3) direct reduction of impurities (silicon, manganese, phosphorus, sulfur, alkaline metals, lead, zinc, chromium, titanium, etc.)
(4) melting of slag and metal; carburization of iron
(5) combustion of coke; oxidation of elements before the tuyeres

1.1.6.3.1 Calcination of Limestone

Calcination of limestone takes places essentially at about 1000 °C. The reaction is highly endothermic and consumes large amount of thermal energy (1.1.26) that comes from the burning of coke. Furthermore, limestone decomposition releases CO_2 gas, and the CO_2 gas will react further with coke through Boudouard reaction (1.1.27), leading to extra solution loss of carbon.

$$\begin{aligned} &CaCO_{3(s)} = CaO_{(s)} + CO_{2(g)} \\ &\Delta G^{\circ}_{298\,K} = 130.423\,kJ, \quad \Delta G^{\circ}_{1273\,K} = -16.169\,kJ \\ &\Delta H^{\circ}_{298\,K} = 178.175\,kJ, \quad \Delta H^{\circ}_{1273\,K} = 163.207\,kJ \end{aligned} \tag{1.1.26}$$

$$\begin{aligned}&C+CO_{2(g)}=2CO_{(g)}\\&\quad\Delta G^{\circ}_{298\,K}=120.004\,kJ,\ \ \Delta G^{\circ}_{1273\,K}=-52.268\,kJ\\&\quad\Delta H^{\circ}_{298\,K}=172.422\,kJ,\ \ \Delta H^{\circ}_{1273\,K}=167.744\,kJ\end{aligned}\tag{1.1.27}$$

According to a rough estimate by Biswas [27], for every 100-kg limestone charged to the blast furnace, the coke rate increases by approximately 25–35 kg/THM. Therefore, fluxing of the iron ore (using prefluxed sinters and pellets) and calcination of limestone outside the blast furnace is preferred to avoid extra consumption of coke.

1.1.6.3.2 Direct Reduction of Wüstite

Direct reduction of wüstite and other forms of iron oxide takes place in the following order. First the reduction of FeO with CO gas (1.1.28), and then the formed CO_2 gas reacts with coke generating CO gas again (1.1.27):

$$\begin{aligned}&FeO+CO_{(g)}=Fe+CO_{2(g)}\\&\quad\Delta G^{\circ}_{1273\,K}=+8.993\,kJ,\ \ \Delta G^{\circ}_{1473\,K}=+12.929\,kJ\\&\quad\Delta H^{\circ}_{1273\,K}=-15.653\,kJ,\ \ \Delta H^{\circ}_{1273\,K}=-16.484\,kJ\end{aligned}\tag{1.1.28}$$

$$C+CO_{2(g)}=2CO_{(g)}\tag{1.1.27}$$

The total reaction can be written as (1.1.29) shown below:

$$\begin{aligned}&FeO+C_{(g)}=Fe+CO_{(g)}\\&\quad\Delta G^{\circ}_{1273\,K}=-43.275\,kJ,\ \ \Delta G^{\circ}_{1473\,K}=-73.731\,kJ\\&\quad\Delta H^{\circ}_{1273\,K}=+152.091\,kJ,\ \ \Delta H^{\circ}_{1273\,K}=+151.169\,kJ\end{aligned}\tag{1.1.29}$$

Although the total reaction of the “direct reduction” of wüstite is very much thermodynamically in favor with very negative Gibbs energy of reaction, the reaction is highly endothermic, mainly caused by the Boudouard reaction. In reality, most of the unreduced iron in the lower zone is in the form of fayalite ($2FeO\cdot SiO_2$) or intermixed in the primary slag. Reduction of FeO in the slag is more difficult than free FeO.

At this high-temperature zone, reduction of wüstite by hydrogen can also regarded as “direct reduction,” since the formed water vapor will react with coke and form H_2 and CO, as is shown in reactions (1.1.30) and (1.1.31) [19]:

$$\begin{aligned}&FeO+H_{2(g)}=Fe+H_2O_{(g)}\,(\text{indirect reduction})\\&\quad\Delta G^{\circ}_{1273\,K}=+3.417\,kJ,\ \ \Delta G^{\circ}_{1473\,K}=+1.551\,kJ\\&\quad\Delta H^{\circ}_{1273\,K}=+16.543\,kJ,\ \ \Delta H^{\circ}_{1473\,K}=+13.976\,kJ\end{aligned}\tag{1.1.30}$$

$$\begin{aligned}&H_2O_{(g)}+C=H_{2(g)}+CO_{(g)}\,(\text{water}-\text{gas reaction})\\&\quad\Delta G^{\circ}_{1273\,K}=-46.692\,kJ,\ \ \Delta G^{\circ}_{1473\,K}=-75.283\,kJ\\&\quad\Delta H^{\circ}_{1273\,K}=+135.548\,kJ,\ \ \Delta H^{\circ}_{1273\,K}=+134.987\,kJ\end{aligned}\tag{1.1.31}$$

The sum of reactions (1.1.30) and (1.1.31) leads to the same reaction (1.1.29) for "direct reduction" of wüstite.

$$\begin{aligned} &\mathrm{FeO} + \mathrm{C}_{(g)} = \mathrm{Fe} + \mathrm{CO}_{(g)} (\text{total reaction : direct reduction}) \\ &\Delta G^{\circ}_{1273\,\mathrm{K}} = -43.275\,\mathrm{kJ},\ \Delta G^{\circ}_{1473\,\mathrm{K}} = -73.731\,\mathrm{kJ} \\ &\Delta H^{\circ}_{1273\,\mathrm{K}} = +152.091\,\mathrm{kJ},\ \Delta H^{\circ}_{1273\,\mathrm{K}} = +151.169\,\mathrm{kJ} \end{aligned} \tag{1.1.29}$$

Two important disadvantages of "direct reduction" are: (1) excessive consumption of coke and generation of extra CO, which is more than needed in the upper zone of the furnace and (2) excessive energy requirement, which consumes more coke or fuel in the combustion zone. However, the "direct reduction" guarantees a more complete reduction of iron oxide in the lower zone, which prevents the loss of ferrous materials or their reduction in the hearth of the blast furnace. In practice, it is the combination of "indirect reduction" in the upper zone and the "direct reduction" in the lower zone that makes the total reduction of iron oxide an efficient process.

Reduction of various impurities in the blast furnace may take place in the upper, middle, and lower zones. They will be discussed separately in Section 1.1.6.4.

1.1.6.4. Deadman and Hearth

Deadman and hearth phenomena play key roles in hot metal quality. The condition of the deadman has a strong influence on hot metal temperature and composition. When hot metal can flow freely toward the tap hole and the deadman is a porous coke bed, then conditions are good for desulfurization and carbonization of hot metal. The deadman has also a significant effect on lining wear and campaign length by controlling hot metal flow in the hearth [34].

1.1.6.4.1 Functions of Deadman

The renewal of deadman coke proceeds mainly by dissolving in hot metal and also by direct reduction of FeO in the slag with coke. According to an old rule of thumb, the renewal is estimated to take about 4 weeks. Data from a tracer (radioactive Sc_2O_3) test gives more detailed information:

(1) Coke in the peripheral zone of the deadman is consumed in 2–3 days due to larger hot metal flow dissolving coke carbon.

(2) Coke in the middle zone of the deadman is consumed very slowly—in 15–19 days.

Even longer lag times have been reported. When the hearth coke is renewed and the porosity between coke lumps increases, the slag starts to run out earlier than with clogged coke. Hot metal flows more at the wall side of the hearth when the center is clogged and the heat loads are higher compared to the operation with an open center.

The time for renewal depends also on the shape of the cohesive zone. For a V-shaped cohesive zone, the coke in the center is consumed faster, and floating up toward the raceway also renews the coke in the periphery. This kind of cohesive zone is formed when the production rate of the furnace is strongly reduced. An old rule of thumb states the descending speed of hearth coke to 1 m/day.

1.1.6.4.2 Floating Deadman

Deadman normally sits on the bottom of the hearth under normal operating conditions. However, a floating deadman is also a common phenomenon. Deadman floating occurs when the buoyancy of the submerged coke encumbers the descent of burden material. The floating of the deadman can be anticipated when the charging frequency and gas utilization decrease before tapping.

Floating has desirable features but also some disadvantages. If the deadman floats, it is not stuck to the cold bottom and it will sooner or later open and become active if it has been clogged. The negative effects are the unsteady burden descent, which disturbs the burden distribution and gas utilization, and the faster flow of the hot metal through the gap from the hearth bottom, which will cause more severe erosion of the refractory at the bottom region.

1.1.6.4.3 Inactive Deadman

If the deadman becomes clogged it will cause poor hot metal quality, irregular burden descent, abnormal hearth erosion (so-called elephant foot), etc. An inactive deadman is caused by different factors: low coke strength, low production rate, too long maintenance stop, water leakage into the furnace, improper burden distribution, hearth erosion, peeling scaffolds, etc.

An inactive deadman is "sitting" on the hearth bottom and usually not floating in the hot metal. It is perhaps more common in large blast furnaces but occurs also in smaller ones, depending on the furnace construction and operation. The coke in the deadman is closely packed and the space between coke particles is filled with coke breeze, solid metal, solid slag, and unreduced ore. Calcined lime can also be found if it is used in the burden.

Heat to the deadman is carried by dripping hot metal and slag. Heat is flowing out through the hearth wall and bottom cooling. Heat is also consumed by the "direct reduction" of FeO in slag. When the deadman has become inactive it is very difficult to get heat into it and melt the solidified slag and metal because the deadman is like a solid rock in the middle of the hearth. Hot metal and slag cannot trickle through it so that they flow along the crust down to the active cylinder-shaped annulus part of the hearth. The operating part of the hearth is thus strongly reduced.

In some blast furnaces, there are special tuyeres for a probe for sampling and/or temperature measurement. These measurements show the thermal state of the deadman. The deadman is inactive if the temperature is below 1400 °C, and the temperature of an inactive deadman can drop down to 1200 °C and even lower. In a normal deadman, the temperature is above 1400 °C, and up to 1700 °C at the tuyere level.

Inactive deadman is a harmful phenomenon because the hot metal quality is poor with low carbon and high sulfur contents. There is also a great risk of an elephant foot formation, which will reduce campaign life. Therefore it is important to get the deadman activated as soon as possible. Proper control of coke size (avoiding small-sized coke in the charge) and high deadman temperature are important for maintaining a porous and open deadman structure.

Interesting dependence between deadman condition, reduction of iron, hot metal sulfur, and carbon and hot metal temperature has been found. This knowledge has been used in practice resulting in remarkable improvement of hot metal quality and hearth condition.

1.1.6.5. Behavior of Minor Elements and Impurities

Impurities, metallic or nonmetallic, determine the hot metal quality required by the converter steelmaking process such as silicon, sulfur, and phosphorus. On the other hand, reduction of certain impurities in the raw materials (ferrous or reducing agents) can affect significantly the blast furnace performance such as alkali metals (Na and K) and volatile metals (Zn). The behavior of the impurities and their effect on the process and the product quality are briefly described below. For detailed knowledge and proper control of these impurities, please refer to Biswas [27] and Babich *et al.* [19].

Blast furnace charge (both iron ore and coke) contains other impurities besides iron oxides. Many of them can be reduced *to a certain extent* at high temperatures under strong reducing atmosphere in the lower zone of the blast furnace. They can be dissolved into the product—hot metal (Si, Mn, P, S, Ti), escape together with the top gas or circulate within the furnace, or be absorbed by the refractories. Furthermore, coke also contains a number of impurities, in particular sulfur, which contributes to the sulfur in the hot metal. According to Babich *et al.* [19], the *metallic impurities* could be classified into the following three groups according to their affinity to oxygen (chemical stability), which can be illustrated with the Ellingham diagram as shown in Figure 1.1.23.

- Less stable metal oxides above the FeO line: Cu_2O, NiO, PbO. These metal oxides are more easily reduced with CO and H_2 gases in the upper part of the blast furnace through "indirect reductions."
- Metal oxides below but close to FeO lines: ZnO, Cr_2O_3, MnO, SiO_2, TiO_2. These metal oxides are slightly more stable than FeO, but can be partially reduced by carbon in the higher temperature zones through "direct reduction." These metals can be distributed between metal phase and slag phase depending on the local oxygen potential. Zn has very low boiling point (907 °C) and will become vapor at the lower zone of the furnace, and will be partially circulating in the furnace and partially carried out with the top gas.

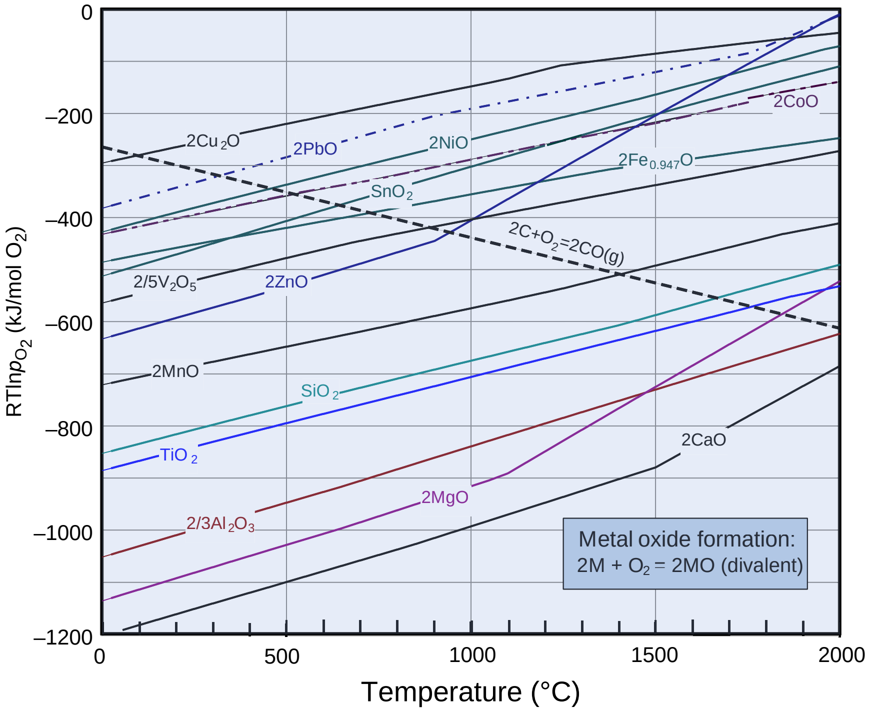

Figure 1.1.23 Ellingham diagram (showing the oxide stability and thermodynamic reducibility with carbon) plot based on calculation with HSC Chemistry [30].

- Very stable oxides far below the FeO line: Al_2O_3, MgO, CaO. These oxides are generally not reduced in the blast furnace, and are the major slag-forming components.

Furthermore, the following two groups of impurities have special impact on the product quality and operation of the blast furnace.

- Nonmetallic impurities: P and S. Phosphorus and sulfur originated from ore, flux, and coke are critical to the hot metal quality. Control of sulfur and phosphorus has always been an important issue in ironmaking and steelmaking.
- "Circulating elements": K, Na, Zn. They are very harmful for the blast furnace operation due to their high vapor pressure and oxidizing–reducing circle along the blast furnace and their aggressive nature to the burden and refractories.

Table 1.1.2 summarizes the source and destination of the major impurities in the blast furnace, in reference to the average compositions of hot metal and slag [18].

1.1.6.5.1 Behavior of Metallic Impurities

1.1.6.5.1.1 Silicon

Silicon is one of the main impurities in the hot metal to be removed in steel converter, which should be controlled at the level of about 0.5%, but normally in the range of

Table 1.1.2 Impurities in the Blast Furnace Processes [18]

Element	**Input**	**Output Iron**		**Output Slag**	
	kg/THM	**kg/THM**	**%**	**kg/THM**	**%**
(a) Source and destination					
Silicon	46	5	11	41	89
Manganese	6	4.5	75	1.5	25
Titanium	3	0.7	23	2.3	77
Sulfur	3	0.3	10	2.7	90
Phosphorous	0.5	0.48	96	0	0
Potassium	0.15	0	0	0.11	73
Hot Metal		**Typical (%)**	**Slag**	**Typical (%)**	**Range (%)**
(b) Composition of hot metal and slag					
Iron	Fe	94.5	CaO	40	34–42
Carbon	C	4.5	MgO	10	6–12
Silicon	Si	0.40	SiO_2	36	28–38
			Al_2O_3	10	8–20
Manganese	Mn	0.30			
Sulfur	S	0.03	Sum	96	
Phosphorous	P	0.07	Sulfur	1	

0.3–0.9% in the hot metal. Silicon content in the hot metal is used as the measure of thermal state of the hearth, due to the strong endothermic nature of the SiO_2 reduction.

Silicon comes into the furnace in the form of silica or silicate partially in the ore (gangue: about 3/4) and partially in coke (coke ash: about 1/4). Generally silicon is thought to be transferred to the hot metal through two routes:

(1) from coke ash (and coal) through formation of SiO gas in the raceway via carbothermic reduction at very high temperatures. The SiO gas ascends to the belly and disproportionate to SiO_2 (to join slag) and silicon metal (dissolving into metallic iron). Another possible way is that SiO gas will be reduced by the dissolved carbon in the liquid iron droplets.

$$SiO_2 + C = SiO_{(g)} + CO_{(g)} \tag{1.1.32}$$

$$2SiO_{(g)} = (SiO_2)_{slag} + [Si]_{Fe} \tag{1.1.33}$$

$$SiO_{(g)} + [C]_{Fe} = [Si]_{Fe} + CO_{(g)} \tag{1.1.34}$$

However, the hot metal silicon so formed can be reoxidized when the hot metal droplets flow through the slag layer by the FeO in the slag (if present) as below:

$$[Si]_{Fe} + 2(FeO)_{slag} = (SiO_2)_{slag} + [Fe] \tag{1.1.35}$$

(2) Direct reduction of SiO_2 in the slag with dissolved carbon in the hot metal as shown in reaction (1.1.36).

$$(SiO_2)_{slag} + 2[C]_{Fe} = [Si]_{Fe} + 2CO_{(g)} \tag{1.1.36}$$

The freshly reduced iron (dissolved with carbon) is thought to be a catalyst for the direct reduction of SiO_2, and could decrease the initial reduction temperature down to 1050–1100 °C [19]. Figure 1.1.24 illustrates the path of the Si formation and distribution between metal and slag.

1.1.6.5.1.2 Manganese

Manganese occurs in the burden as oxides (MnO_2, Mn_2O_3, Mn_3O_4) and carbonate ($MnCO_3$) or silicate and phosphate if converter slag is charged. Reduction of manganese oxides are also stage-wise similar to iron oxides, and until MnO the reduction reactions take place in the upper and middle zone of the blast furnace via "indirect reduction" with

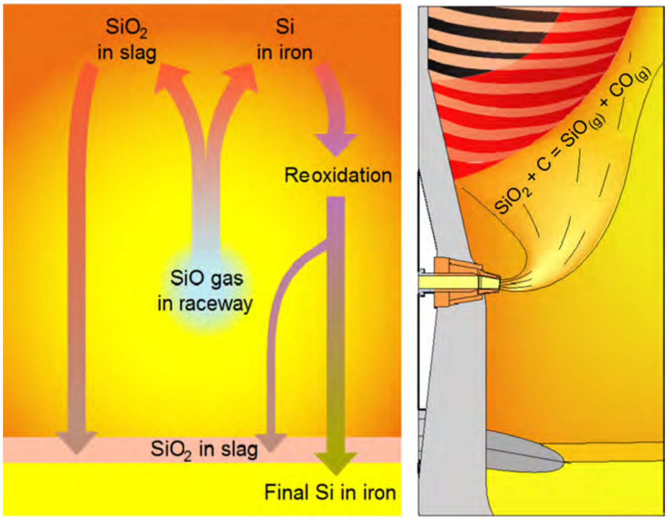

Figure 1.1.24 Illustration of silicon reduction in the blast furnace [18].

CO gas. MnO is more difficult to be reduced with CO, and is mostly through direct reduction in the lower zone (bosh or belly) via Boudouard reaction. Further reduction of MnO by silicon in the hearth can also take place. High Mn recovery is preferred in most cases and it is an alloying element in steelmaking. Normally about 50–70% of manganese is recovered in the blast furnace to produce hot metal for steelmaking.

1.1.6.5.1.3 Titanium

Titanium is present in the blast furnace as ilmenite ($FeO{\cdot}TiO_2$) in the burden, and is very difficult to reduce. Most of the oxide is reported into slag causing very high viscosity. Reduction of TiO_2 in the slag can partially take place in the hearth by carbon and silicon. The reduced Ti metal can form titanium carbide, nitride, or carbonitride, which all have very high melting temperatures and will precipitate as solid from the melt. Deliberate charging of ilmenite to the blast furnace is used for the protection of the hearth refractories and for repair of the damaged area in the hearth [19].

1.1.6.5.1.4 Chromium

Chromium occurs in the burden as chromite ($FeO{\cdot}Cr_2O_3$). Reduction of chromite is difficult and highly endothermic. Carbothermic reduction of chromite takes place in the hearth by direct reduction and the Cr that is formed dissolves in liquid hot metal. Recovery of chromium in the blast furnace can reach about 90% [27].

1.1.6.5.2 Behavior of Nonmetallic Impurities P and S

1.1.6.5.2.1 Phosphorus

In the blast furnace, phosphorus originates from coke, iron ore, and flux in the form of P_2O_5, $3(CaO){\cdot}P_2O_5$, and $3(FeO){\cdot}P_2O_5$. Silica helps in breaking of the phosphate bond and releasing free P_2O_5 gas, and thus promotes the reduction indirectly. P_2O_5 vapor will react with carbon via Boudouard reaction or be directly reduced with carbon when it passes through the coke.

$$3CaO{\cdot}P_2O_5 + 3SiO_2 = 3(CaO{\cdot}SiO_2) + P_2O_5 \tag{1.1.37}$$

$$P_2O_{5(g)} + 5C = 2P_{(g)} + 5CO_{(g)} \tag{1.1.38}$$

The reduction of P_2O_5 is almost complete, and no physical or chemical condition can influence it. More than 90% of the phosphorus load enters the iron and the rest is lost either in the slag or in the flue gas or is absorbed in the refractory linings [27]. Therefore, production of low P hot metal is only possible by using low P-bearing coke and ore. Dephosphorization requires oxidizing conditions, and cannot be conducted in the blast furnace. All phosphorus is removed during oxygen steelmaking in most of the steelmaking operation. In Japanese steel plants, dephosphorization of hot metal before converters is a common practice. This process as well as other post blast furnace treatments are described in Chapter 1.3.

1.1.6.5.2.2 Sulfur

Hot metal sulfur comes mainly from coke and auxiliary reductant such as coal and oil (80–90%), and the rest from the ferrous burden and fluxes. The total input of sulfur into blast furnaces is typically 2.5–3.5 kg/THM [18]. In the coke, sulfur occurs in organic compound but after combustion sulfur occurs in the ash as sulfides and sulfates. In the ore and fluxes, sulfur occurs in the form of sulfates ($CaSO_4$ or $BaSO_4$) and sulfides (FeS or FeS_2). During the descent of the stock, the sulfur in the charge materials is absorbed in the shaft and the bosh by the metal and the slag and the final transfer of sulfur from the metal to slag occurs in the hearth [27]. Furthermore, a small proportion of sulfur escapes from the top gas as SO_2 and H_2S gases. The bulk of the coke sulfur is transformed to hot metal by chemical reactions, mainly during the combustion of coke in front of the tuyeres.

Table 1.1.3 illustrates the balance of sulfur from the raw materials to the product streams [19]. It can be seen that in this case more than 96% of S comes from coke and pulverized coal. As a result, about 68% (or 85% if error is not counted in the total output) of S is reported to the slag, and 9% (11.5%) of the S is reported to hot metal, and only less than 3% is reported to off-gas. On average, the sulfur content in the hot

Table 1.1.3 Sulfur Balance of Ironmaking Blast Furnace [19]

	Consumption (kg/THM)	**S (%)**	**S (kg/THM)**
Input			
Sinter	924	0.009	0.084
Pellets	529	0.004	0.021
Lump ore	153	–	0
Scrap	–	–	–
Flux	7	–	0
Coke	392	0.591	2.319
PC	109	0.753	0.821
Total			3.245
Output			
Hot metal	1000	0.030	0.300
Slag	241	0.92	2.217
Flue dust	13	0.692	0.09
Total			2.607
Error			0.638

metal is in the range of 0.025–0.050%. Normally sulfur will be further removed externally through desulfurization in ladles before entering into the steelmaking converters.

1.1.6.5.2.2.1 Transfer of Sulfur to the Hot Metal Sulfur in the hot metal may be assumed in the form of dissolved FeS or S. Sulfur enters the metal from the raw materials (as sulfides or sulfates), through one or more of the following reactions [27].

(1) Transformation of metal sulfides in the burden into hot metal as [FeS]. This can be direct dissolution of burden FeS to hot metal FeS (1.1.39), or through SO_2 formation–reduction of SO_2 to elemental S_2 and sulfidation of Fe to FeS in the hot metal (1.1.40).

$$(\mathrm{FeS})_{\mathrm{burden}} = [\mathrm{FeS}]_{\mathrm{Fe}} \tag{1.1.39}$$

$$\left\{\begin{array}{l} \mathrm{FeS} + 10\mathrm{Fe_2O_3} = 7\mathrm{Fe_3O_4} + \mathrm{SO_{2(g)}} \\ \mathrm{SO_{2(g)}} + 2\mathrm{C} = 0.5\mathrm{S_{2(g)}} + 2\mathrm{CO_{(g)}} \\ [\mathrm{Fe}] + 0.5\mathrm{S_{2(g)}} = [\mathrm{FeS}] \end{array}\right\} \tag{1.1.40}$$

(2) Transformation of metal sulfates into [FeS] in the presence of carbon and Fe or FeO, or through SiO gas:

$$\mathrm{CaSO_4} + [\mathrm{Fe}] + 3\mathrm{C} = [\mathrm{FeS}] + \mathrm{CaO} + 3\mathrm{CO_{(g)}} \tag{1.1.41}$$

$$\left\{\begin{array}{l} \mathrm{CaSO_4} + 4\mathrm{C} = \mathrm{CaS} + 4\mathrm{CO} \\ \mathrm{CaS} + \mathrm{FeO} = [\mathrm{FeS}] + \mathrm{CaO} \end{array}\right\} \tag{1.1.42}$$

$$\left\{\begin{array}{l} \mathrm{CaS} + \mathrm{SiO_{(g)}} = \mathrm{SiS_{(g)}} + \mathrm{CaO} \\ \mathrm{SiS_{(g)}} + 2[\mathrm{Fe}] = [\mathrm{Fe-Si}] + [\mathrm{FeS}] \end{array}\right\} \tag{1.1.43}$$

1.1.6.5.2.2.2 Transfer of Sulfur from Hot Metal to Slag It is important to notice that the affinity of metals to sulfur increases in the following order: FeS, MnS, MgS, Na_2S, CaS [19]. Thus, the best option to remove sulfur in the hot metal is to use calcium or magnesium (in the form of oxides in the blast furnace) to form CaS or MgS. Fortunately, CaS has certain solubility in the slag, and this forms the fundamentals of sulfur removal from hot metal to slag in the blast furnace. The main hot metal desulfurization reaction can be expressed with Equation (1.1.44):

$$[\mathrm{FeS}] + (\mathrm{CaO})_{\mathrm{slag}} = (\mathrm{FeO})_{\mathrm{slag}} + (\mathrm{CaS})_{\mathrm{slag}} \tag{1.1.44}$$

The equilibrium constant is expressed in Equation (1.1.45):

$$K = \frac{a_{(\mathrm{CaS})} \cdot a_{(\mathrm{FeO})}}{a_{[\mathrm{FeS}]} \cdot a_{(\mathrm{CaO})}} \tag{1.1.45}$$

The sulfur distribution ratio expressed as $L_s = (\mathrm{S})_{\mathrm{slag}}/[\mathrm{S}]_{\mathrm{Fe}}$ is closely linked to the equilibrium constant K (1.1.45). A lower activity of FeO and a higher activity of CaO in the slag are in favor of a higher L_s at a given temperature (constant K). Slag basicity (proportional to CaO activity in the slag) is a very important parameter for sulfur removal. In practice, the sulfur content of hot metal is determined by the sulfur distribution ratio L_s, sulfur input to the hot metal and slag (sulfur load: S), and the slag volume (n) as expressed in Equation (1.1.46) [19]:

$$[\mathrm{S}] = \frac{0.1 \times \mathrm{S}}{1 + 0.001 \times L_s \times n} \tag{1.1.46}$$

where S is the sulfur load (kg/THM), n is slag volume (kg/THM).

In contrast to the phosphorus control, the blast furnace conditions (slag properties) are in favor of sulfur removal from hot metal to slag. The control of sulfur in the hot metal could be achieved through the following measures [19]:

- Decrease the sulfur load by reducing the coke rate, using low S coke and injectants
- Increase the slag basicity through a higher CaO and MgO content in the slag
- A higher temperature in the dripping zone and hearth (desulfurization reaction is highly endothermic)
- Lower (the FeO) content in the slag to reduce its activity
- Increase the contact time between hot metal and slag though more frequent metal tapping
- Optimize the hot metal composition (C, Mn, Si having influence on S content in hot metal)
- Increase the slag volume (but this will have side effect on the blast furnace process).

The remaining sulfur in hot metal (0.025–0.050%) will be removed in hot metal desulfurization station through use of soda ash (Na_2CO_3), lime (CaO), Mg metal, or calcium carbide (CaC_2) in ladles. Hot metal desulfurization will be treated in a separate book in this book series "Hot metal refining processes." For more detailed chemistry of sulfur removal and metal and the hot metal sulfur control, please refer to Biswas [27] and Babich *et al.* [19].

1.1.6.5.3 Behavior of Circulating Elements

1.1.6.5.3.1 Zinc

Zinc comes into blast furnace from ore in the form of oxide or ferrite, silicate or sulfide, it can also be brought in through the use of recycled secondary materials such as flue dust or sludge in the form of oxide or ferrite. At high temperatures (above 1000 °C) in the lower zone of blast furnaces, these zinc-bearing compounds (mostly transformed to the oxide form) can be reduced by CO and carbon to zinc vapor [27,19]. The following reactions illustrate the possible formation route of zinc through reduction of free zinc oxide and zinc ferrite ($ZnO{\cdot}Fe_2O_3$) with CO gas and carbon.

$$\begin{gathered}ZnO + CO_{(g)} = Zn_{(g)} + CO_{2(g)}\\ \Delta G^{\circ}_{1473\,K} = 13.643\,kJ,\ \ \Delta H^{\circ}_{1473\,K} = 185.317\,kJ\end{gathered} \tag{1.1.47}$$

$$\begin{gathered}ZnO + C = Zn_{(g)} + CO_{(g)}\\ \Delta G^{\circ}_{1473\,K} = -73.017\,kJ,\ \ \Delta H^{\circ}_{1473\,K} = 345.858\,kJ\end{gathered} \tag{1.1.48}$$

$$\begin{gathered}ZnO{\cdot}Fe_2O_3 + 4CO_{(g)} = Zn_{(g)} + 2Fe + 4CO_{2(g)}\\ \Delta G^{\circ}_{1473\,K} = 21.274\,kJ,\ \ \Delta H^{\circ}_{1473\,K} = 163.003\,kJ\end{gathered} \tag{1.1.49}$$

$$\begin{gathered}ZnO{\cdot}Fe_2O_3 + 4C = Zn_{(g)} + 2Fe + 4CO_{(g)}\\ \Delta G^{\circ}_{1473\,K} = -325.366\,kJ,\ \ \Delta H^{\circ}_{1473\,K} = 824.791\,kJ\end{gathered} \tag{1.1.50}$$

It could be seen that reduction of ZnO and zinc ferrite by carbon is more thermodynamically in favor than the reduction by CO gas, although both are more difficult to be reduced compared to FeO. Both types of reactions are highly endothermic (reduction by carbon is more endothermic), and this also means that higher temperature will be in favor of both types of reactions. In practice, the extent of reduction depends on activity of ZnO in the compound or the formed initial slag. A higher activity of ZnO is in favor of the formation of Zn vapor.

The problem of zinc vapor formation in the lower zone of the furnace is that it will condensate in the upper part of the furnace when the temperature is lower than the boiling point of Zn (907 °C), normally starting at 520–580 °C [27]. In addition, zinc vapor will be reoxidized back to ZnO in the upper part when temperature is below 900 °C, and the formed ZnO becomes part of the flue dust, which is carried by the top gas, which may form the build-ups in the throat and off-takes. The condensation of zinc and ZnO may take place on the burden and coke surfaces, which block the pores and reduce the gas permeability. This will cause an increase in coke rate and decrease in productivity [19]. Some zinc vapor may seep through the brick joints in the lining and condense around the cooling plates as metal. The other part of the reoxidized zinc descends to the high-temperature zone and gets reduced again. The formed zinc circulation zone is well illustrated in Figure 1.1.25 [19]. The circulation zone occupies the entire dry part of the shaft and part of the cohesive zone. Thus, a zinc cycle similar to the alkali cycle forms in the furnace [27].

Zinc circulation within the blast furnace causes disturbances in the blast furnace operation, the generation of low zinc-concentration flue dust imposes another environmental and technological challenge for disposal and re-utilization. Different technological measures are suggested to reduce the detrimental effect of zinc circulation when the input of zinc cannot be avoided [19].

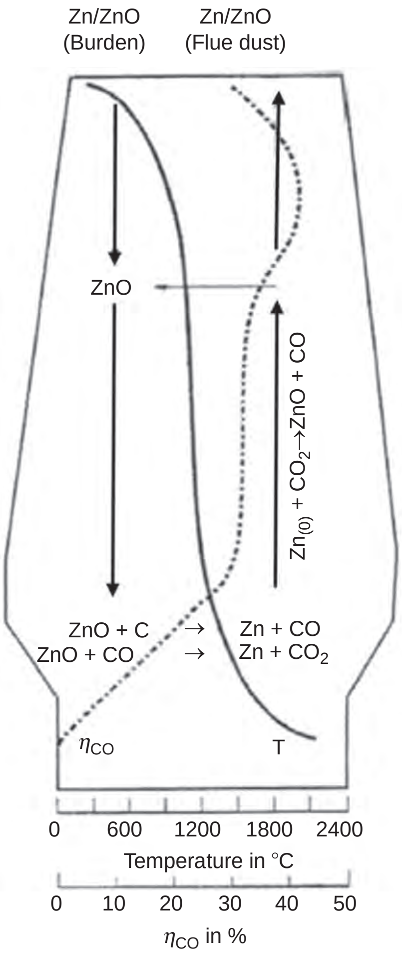

Figure 1.1.25 Illustration of zinc circulation in the blast furnace [19].

1.1.6.5.3.2 Alkali Metals: Potassium and Sodium [19]

Potassium and sodium come into the furnace from coke and ore in the form of oxides, silicates, and carbonates. Alkali input is in the range of 1.5–5 kg/THM. Tables 1.1.4 and 1.1.5 illustrate the alkali input and circulation within the commercial operating blast furnaces[19]. In the lower part of the furnace, they are reduced to metal vapor and the metal vapor reacts with carbon and nitrogen to form cyanides (NaCN and KCN). The formed cyanides ascend to the upper zone and react with CO_2-forming carbonates (Na_2CO_3 and K_2CO_3). The formed carbonates descend to lower zone and are reduced to metal vapor again, leading to the recirculation of the alkali metals. As can be seen in Table 1.1.5, the amount of circulating alkali metals is 5–10 times as high as the input alkali metals in terms of unit hot metal production. As an example, the distribution

Table 1.1.4 Alkali Metal Input and Its Share from Coke to Ferrous Materials [19]

Company	Share of Total Alkali Input (%)			Alkali Input (kg/THM)
	Coke	Sinter	Pellets	
Voest Alpine Stahl	28	45	19	4.95
EKO Stahl	49	31	18	2.70
Thyssen-Krupp Steel	48–59	21–28	4–6	2.55–2.79
	Coal 10–17	Ore 2–7		

Table 1.1.5 Examples of Alkali Metal Input and Circulation [19]

BF/Company	BF Volume (m^3)	Amount of Circulating Alkali (kg/THM)	Input of Circulating Alkali (kg/THM)
Ougree (CRM)	8.5	30	5
Hirokata BF 1 (NSC)	1407	13.1	2.29
Kokura BF 2 (Sumimoto)	1350	17–18	4.43
Amagasaki BF 1 (Kobe)	1976	22–23	2.14

of the alkali metals is illustrated as follows: slag 69.1%, washing water 24.2%, flue dust 5.3%, and sludge 1.4%.

As is summarized by Babich *et al.* [19], alkali metals reduce the strength of the coke and pellets, they worsen the gas distribution and drainage of liquid products, and promote scaffold formation. This causes disturbances of smooth operation of the furnace and a higher coke rate, decrease in productivity and furnace service life, and corrosion of gas turbine shovels. Different technological measures are suggested to reduce the harmful effects of the circulating alkali metals in the blast furnace [19].

1.1.6.6. Formation of Hot Metal and Slag

1.1.6.6.1 Formation of Hot Metal

Metallic iron is mainly formed through gas–solid reduction, approximately 2/3 through indirect reduction and 1/3 through direct reduction. Carburization of iron can start at relatively low temperatures in contact with CO gas. Dissolution of carbon in solid iron or sponge lowers the melting point of iron significantly. In the shaft, the carbon content in the iron does not exceed 1 wt% due to the slow kinetics of solid–solid reaction [19]. At high temperatures above 1000 °C, coke becomes a stronger carburization agent. However, in the liquid phase, carbon content can increase to 3.0–3.5 wt% in the belly of the blast furnace. The lowest melting temperature of 1153 °C can be reached at the eutectic point of 4.3 wt% of carbon, which is a large temperature drop from the melting point of pure iron of 1536 °C. In the dripping zone, the partially carburized liquid iron flows through the coke bed, and drips into the hearth. In the hearth, the hot metal picks up more carbon, reaching the saturation of about 4.5 wt% at the temperature of 1500 °C.

Liquid iron will also absorb certain amount of sulfur, phosphorus, silicon, and manganese, which need to be controlled in the sufficiently low level suitable for subsequent oxygen steelmaking. These have been discussed previously in the behavior of minor elements.

1.1.6.6.2 Formation of Slag

Slag is formed from the gangue materials of the burden and the ashes of the coke and other auxiliary reductants. During the blast furnace process, slag is formed in two stages: first "primary slag," and "primary slag" develops then to a "final slag." Four main components (SiO_2, CaO, MgO, and Al_2O_3) make up about 96% of the slag. Typical blast furnace slag compositions and the ranges are illustrated in Table 1.1.2. The minor components are MnO, TiO_2, K_2O, Na_2O, S, and P [18].

The primary slag is formed during the melting process of the burden prior to the solution of coke ash components into the slag, and the amount is relatively small. The liquidus temperature is much lower due to the high content of FeO (about 1200 °C). The primary slag formation together with the carburization of the iron determines the softening and melting of the burden, the "cohesive zone." The temperature or the range of softening–melting transformation is important for the cohesive zone permeability. If the transformation of solid to liquid is quick, and occurs in a high and narrow range of temperature, the cohesive zone will be more permeable, leading to higher furnace productivity [19].

The final slag is formed after the direct reduction of FeO in the primary slag and the dissolution of SiO_2 and other oxides from the ash, and the amount increases. The melting temperature of final slag is around 1300 °C. The formation of final slag is more or less complete in the combustion zone. The final slag runs along with the molten iron into the hearth. Iron droplets pass through the slag layer to form the molten hot metal pool. During this passage, the slag reacts with the metal, and transfer of Si, Mn, and S occurs between the metal and the slag, tending to attain equilibrium. The properties (melting temperature (range), slag basicity, viscosity, and sulfide capacity), composition, and amount of the final slag in the hearth control the composition/quality of the hot metal and the productivity of the blast furnace [22]. Slag volume in the modern blast furnace is about 150–300 kg/THM depending on the burden composition [19].

1.1.7. ENERGY CONSUMPTION AND BLAST FURNACE PERFORMANCE

1.1.7.1. Energy Consumption in Blast Furnace Ironmaking

1.1.7.1.1 A Global Picture on Energy Consumption

Iron and steelmaking process is energy intensive. Generally speaking, energy constitutes a significant portion of production cost, from 20% to 40%, according to the estimation from world steel association [7]. About 95% of energy for an integrated steelmaking plant comes from solid fuel (mainly coal), 3–4% from gaseous fuel and 1–2% from liquid fuel. Figure 1.1.26 illustrates the total energy consumption of various steelmaking processes.

It can be seen that blast furnace–BOF steelmaking route consumes 19.8–31.2 GJ energy per ton crude steel, while the EAF route using 100% steel scrap consumes 9.1–12.5 GJ energy per ton steel. For the integrated steel production with blast furnace–BOF route, responsible for almost 2/3 of the total steel production, about 75% of the energy arising from coal is attributed to the blast furnace process.

Blast furnace ironmaking makes use of coke as the major source for both energy and reduction of iron oxides. In the blast furnace process, coke has multifunctions and plays an important role as reductant, burden support, and fuel. On the other hand, more and

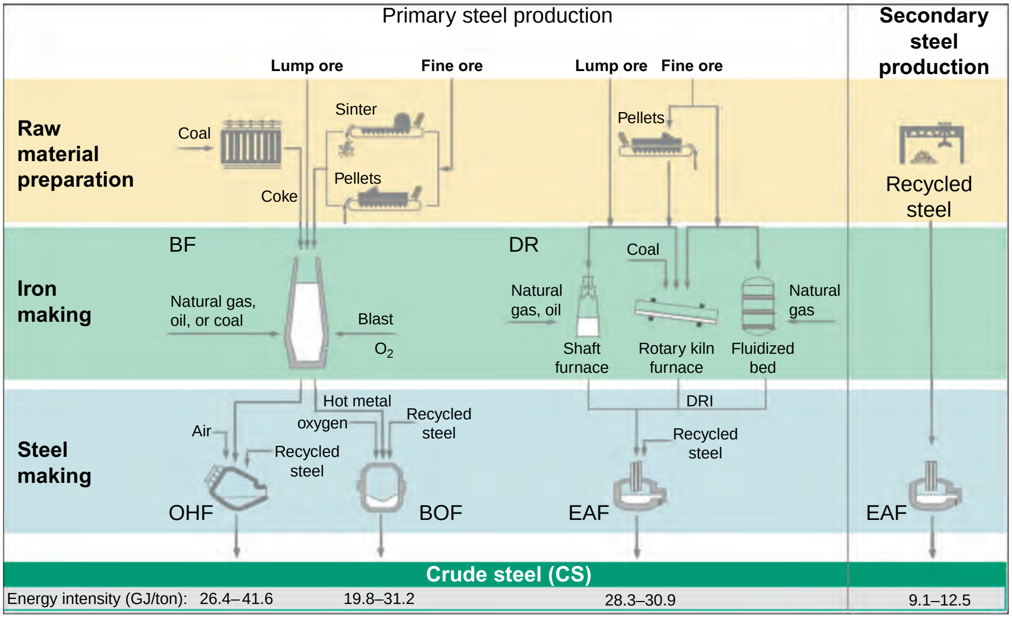

Figure 1.1.26 Energy consumption of different steel production routes [7].

more coke is being replaced with PCI and injection of oil and other secondary fuels such as waste plastics and biomass. Along with the technology development, the coke and overall fuel consumption for blast furnace ironmaking has been reduced significantly and more and more alternative fuels and reductants are replacing expensive metallurgical coke. Figure 1.1.27 shows the historical development in energy consumption of blast furnace ironmaking in German steelmaking industry [35].

It can be seen that in 1950s only coke was used for blast furnace process, and coke consumption was as high as 950 kg/THM. Along the technology development, the coke consumption has been reduced to 500–550 kg/THM during 1970s. Since mid-1980s, PCI was implemented gradually to replace part of the coke, and the coke consumption was reduced to below 400 kg/THM, with a total injection of coal and other fuel of approximately 100 kg/THM. Nowadays, PCI rate at 130–160 kg/THM is a common practice, and PCI rate up to 250 kg/THM is possible to reduce the coke consumption down to 250 kg/THM. The modern blast furnace practice can be operated at the total combined fuel rate of about 500 kg/THM [36], which is very close to the minimum theoretical value under the classical blast furnace operation (as commonly accepted to be 465 kg/THM). However, even lower total fuel rate has been reached in some steel plants. In Japan they were running BF at about 400 kg/THM in 1980s but they had scrap in burden. The theoretical value depends on raw materials, practice, and final products. In the best cases, they are above 10% from the “minimum.”

The minimum blast furnace fuel rate is determined by an optimum balance of chemical and thermal input to the energy and mass balance [36]. Generally speaking, higher indirect reduction will increase the productivity, but too much indirect reduction increases the fuel requirement for heating the reducing gases. It is the combination

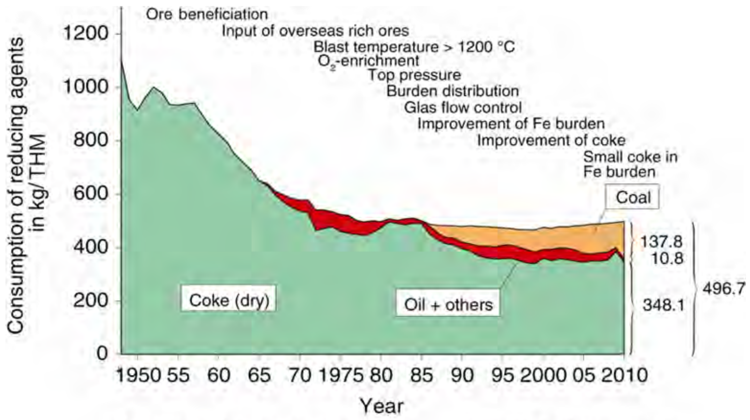

From 1991 on including new countries (Source: VDEh Blast Furnace Committee)

Figure 1.1.27 Consumption of reducing agents and fuel in German blast furnace ironmaking [35].

of indirect and direct reduction that makes the blast furnace an efficient process for ironmaking. Heat and mass balance models based on favorable operating conditions and metallurgical thermal and chemical boundaries have estimated the lowest possible fuel rate of 403–410 kg C/THM (roughly 465 kg coke/THM). However, low levels of fuel rate around this level could not be consistently maintained with problems of instability, heat balance, and production problems.

Figure 1.1.28 illustrates the use of PCI for blast furnaces in the Japanese steelmaking industry [37]. It can be seen that by the end of the twentieth century and beginning of the twenty-first century, an average PCI rate in Japan was approximately 120 kg/THM, but some individual operations could have reached more than 250 kg/THM (266 kg/THM at Fukuyama No. 3 blast furnace). But the higher PCI rate was compromised by the increased total reducing agent consumption. This is bound to the minimal requirement of the reduction of iron oxides and energy requirement to maintain the thermal state for the blast furnace as well as the temperature of the liquid products of hot metal and slag. This is very well illustrated in Table 1.1.6 for the Japanese steelmaking industry.

Table 1.1.7 shows the evolution of blast furnace operation, regarding coke consumption, and use of substitutional fuels [38].

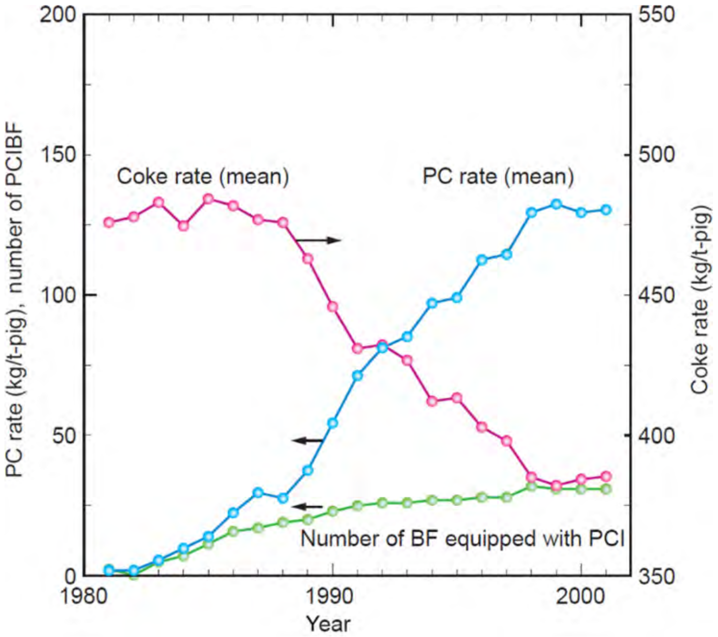

Figure 1.1.28 Increased PCI installations for blast furnace technology in Japan [37].

Table 1.1.6 Highest Japanese Operational Indices for Blast Furnaces with PCI [37]

	Month and Year	Steel Works, Blast Furnace	Coal Dust Ratio (kg/t)	Coke Ratio (kg/t)	Reducing Material Ratio (kg/t)	Tapping Ratio (t/day/m^3)
Maximum pulverized coal ratio (PCR)	6/98	Fukuyama No. 3 blast furnace	266	289	555	1.84
Minimum coke ratio (CR)	3/99	Kobe No. 3 blast furnace	214	288	502	2.06
Minimum reducing material ratio (RAR)	3/94	Oita No. 1 blast furnace	122	342	464	1.95
Maximum tapping ratio	1/97	Nagoya No. 1 blast furnace	137	350	487	2.63

Table 1.1.7 Progressive Reduction in Blast Furnace Coke Consumption in the World [38]

Year	Coke Rate (kg/THM)	Injectant (kg/THM)	Total Reductant (kg/THM)	Comments on BF Operation Including Major Changes Made
1950	1000	0	1000	Lean local ores were used
1965	600	0	600	Rich seaborne ores began to be used
1970	525	50	575	Oil injection, high blast temperature operation, oxygen enrichment were practiced
1980	500	50	550	High top-pressure operation along with improved burden distribution facilities and permeability control
1990	400	125	525	Increased coal injection as well as improved sinter, coke quality
2000	325	175	500	Increased coal/gas/oil/tar injection
2010	250	250	500	Continued use of metallics like DRI in the burden

1.1.7.1.2 Energy and Materials Balance, and Energy Recovery

1.1.7.1.2.1 Materials Balance

Figure 1.1.29 shows a general materials balance of a modern large scale ironmaking blast furnace [12]. To produce 1 THM with about 4.5 wt% C, it consumes about 1630 kg of ferrous materials as mixed charge (sinter, pellet, and lumpy ore), 380 kg of coke and 120 kg of pulverized coal, and 995 Nm^3 of O_2-enriched air at about 1180 °C. At the same time, it generates about 300 kg slag (consisting of mainly SiO_2, CaO, Al_2O_3,

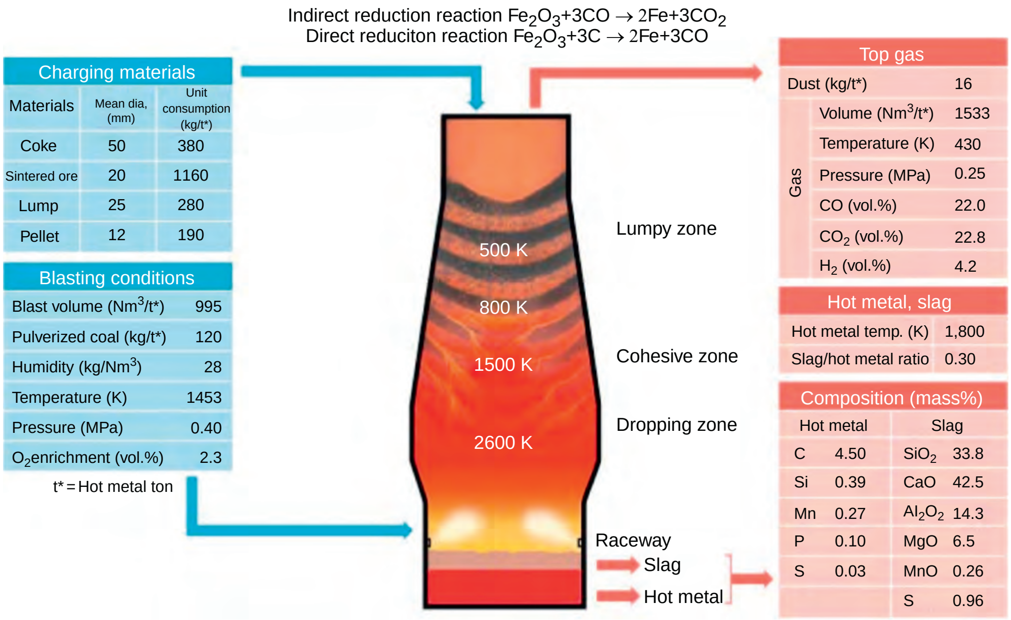

Charging materials

Materials	Mean dia. (mm)	Unit consumption (kg/t*)
Coke	50	380
Sintered ore	20	1160
Lump	25	280
Pellet	12	190

Blasting conditions

Blast volume (Nm^3/t^*)	995
Pulverized coal (kg/t*)	120
Humidity (kg/Nm^3)	28
Temperature (K)	1453
Pressure (MPa)	0.40
O_2enrichment (vol.%)	2.3

t* = Hot metal ton

Top gas

Dust (kg/t*)		16
Gas	Volume (Nm^3/t^*)	1533
	Temperature (K)	430
	Pressure (MPa)	0.25
	CO (vol.%)	22.0
	CO_2 (vol.%)	22.8
	H_2 (vol.%)	4.2

Hot metal, slag

Hot metal temp. (K)	1,800
Slag/hot metal ratio	0.30

Composition (mass%)

Hot metal		Slag	
C	4.50	SiO_2	33.8
Si	0.39	CaO	42.5
Mn	0.27	Al_2O_2	14.3
P	0.10	MgO	6.5
S	0.03	MnO	0.26
		S	0.96

Figure 1.1.29 Mass balance of a typical ironmaking blast furnace [12] (reference: 1 t hot metal).

and MgO), 16 kg flue dust, and about 1500 Nm^3 top gas (CO, CO_2, H_2, H_2O, and N_2) at about 160 °C and 2.5 bar pressure.

1.1.7.1.2.2 Energy Balance

Heat balance of a blast furnace can be made for total furnace balance or multistage thermal balance. The total balance of the blast furnace can give an overall picture of the energy input and output, while the multistage balance (often two-stage balance) takes into account the temperature effect on the heat flow according to the second law of thermodynamics. In practice, a two-stage heat balance is used, at a temperature of 900 °C as the boundary. Table 1.1.8 shows a general energy flow for a typical ironmaking blast furnace [39]. The calculation is made according to the production of 1 THM.

In the total energy balance, the heat input comes from the combustion of coke (may also include other fuels and injectants), and sensible heat of hot blast. Here heat from coke combustion was used as 100%, and sensible heat of hot blast was regarded additional, so that the total heat input is 112.81%. The normalized percentage based on total input or output is listed in parenthesis. It is very clear almost 60% of the total energy (or 67% from fuel/reductant input) is used for reduction reactions (including heating value of dissolved carbon). About 25% of the total energy is carried out by the top gas (mainly the chemical energy–latent heat). The sensible heat carried by slag and hot metal is relatively small (about 12%). The furnace heat loss is very small at about 1%, but normally at a level of 3–5%.

Table 1.1.8 Total Energy Balance of the Blast Furnace

	H_i (GJ/THM)	Base LHV_C (%)		
1. Supplied enthalpies				
Coke, LHV, m_c incl. $C_{dissol.}$[a]	12.6647		100.00	Input
Hot blast	1.6220		12.81	
Sum	14.2867	(100%)	112.81	
2. Reaction enthalpies				
Reduction of Fe_2O_3–FeO	6.7698		53.45	Output
Heating value $C_{dissol.}$	1.5922		12.57	
Reduction SiO_2, MnO	0.1597		1.26	
Sum	8.52I7	(59.65%)	67.29	
3. Enthalpy of the top gas (latent enthalpy)				
Heating value CO less the preheating of the blast	3.3596		26.53	
Sum		(23.52%)	26.53	
4. Enthalpy of the hot metal and slag (sensible enthalpy)				
Hot metal	1.0531		8.31	
Slag	0.6465		5.10	
Sum	1.6996	(11.90%)	13.42	
5. Enthalpy of the top gas (sensible enthalpy)				
CO	0.0537		0.42	
CO_2	0.0878		0.69	
N_2	0.1662		1.31	
Sum	0.3077	(2.15%)	2.43	
6. Losses in the furnace	0.1480	(1.04%)	1.17	
Sum 2–6	14.0366	(98.25%)	110.83	
7. Variance	0.250	(1.75%)	1.97	

Adapted from Ref. [39].

[a] LHV, lower calorific value; $C_{dissol.}$, carbon dissolution.

Although the latent heat of the top gas cannot be used directly in the reduction of iron oxides, it is normally used in the hot stoves to preheat the air blast, and the chemical energy is coming back as part of the hot blast. New development is being undertaken

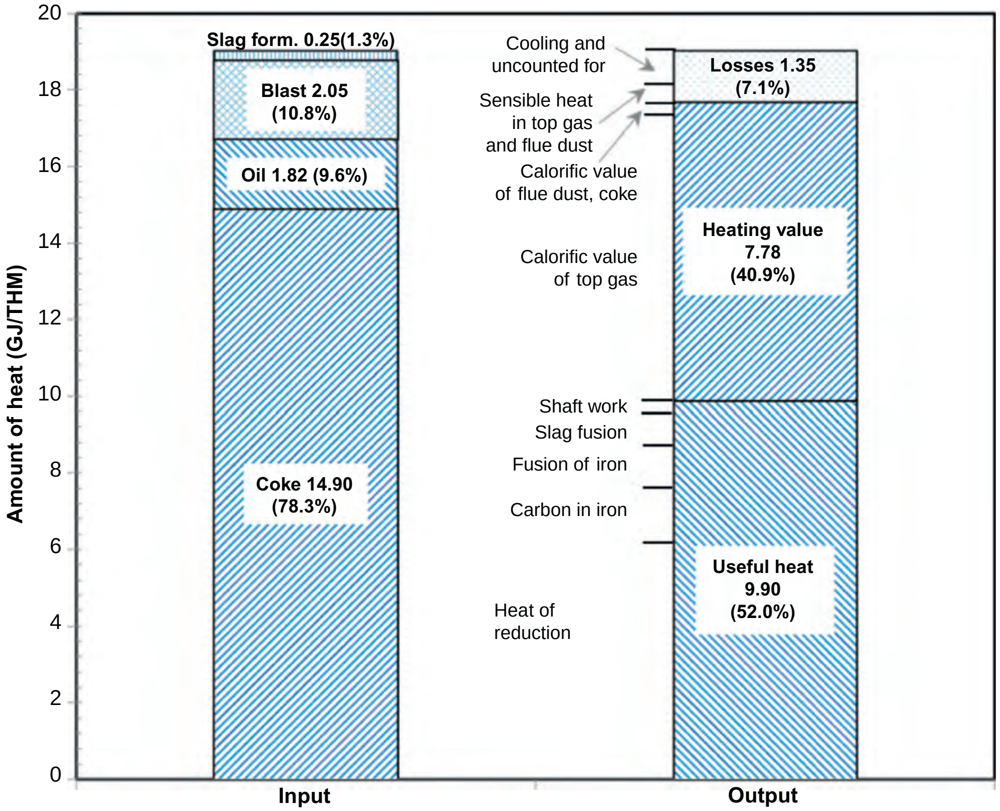

Figure 1.1.30 Example of heat balance of an ironmaking blast furnace. *Redrawn based on Ref. [27].*

to better utilize the chemical energy of the top gas as reducing agent, the so-called "top gas recycle blast furnace (TGRBF)," as a part of Ultra–Low Carbon dioxide (CO_2) Steelmaking (ULCOS) program supported by the European Union.

Figure 1.1.30 illustrates the energy balance of typical ironmaking blast furnaces [27], which is more or less corresponding to the values shown in Table 1.1.8. However, the reported useful heat for reduction reaction and melting ore and iron is a lot lower, and heating value in the top gas is much higher, mainly due to the lower fuel efficiency in the past.

1.1.7.1.2.3 Energy Recovery

An ironmaking plant consists of blast furnace, coking plant, sintering, and/or pelletizing plant. Both coking plant and blast furnace generate significant amount of extra heat in the form of COG and blast furnace-top gas. Both gases are secondary fuels, and are utilized in most cases internally (within ironmaking and steelmaking plants) for providing energy sources in other unit operations. Energy recovery of the whole ironmaking plant is illustrated in Figure 1.1.31 [39].

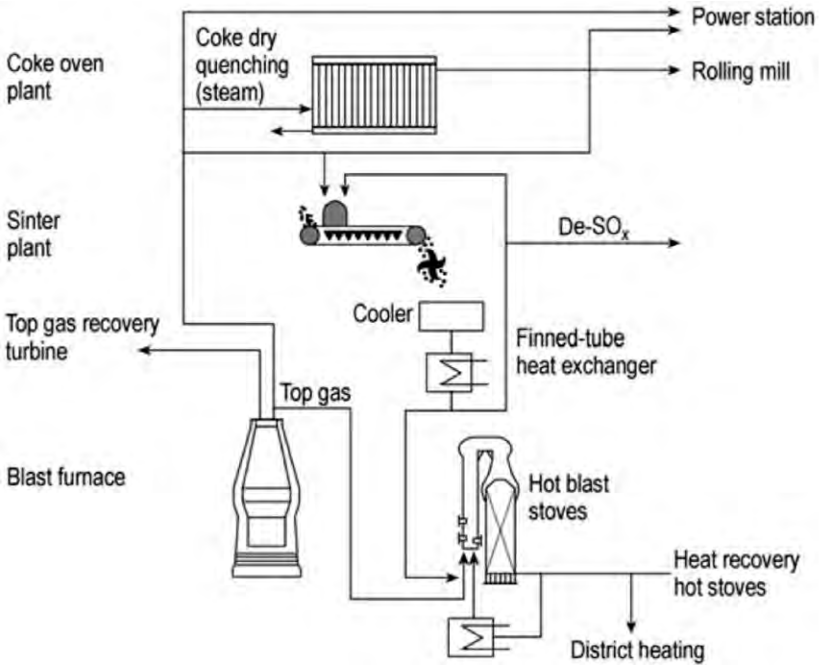

Figure 1.1.31 Energy recovery and utilization at coke plant, sinter plant, and blast furnace [39].

According to above energy balance analysis for blast furnace, the energy leaving blast furnace, which could be reutilized, may include the chemical and sensible heat of the top gas (up to 30%) as well as the sensible heat of slag (~5%). The top gas consists mainly of N_2, CO_2, CO, and H_2, with a heating value of 2850 and 3560 kJ/m^3 (STP). In the current industrial practice, the chemical energy (latent heat or heating value) of the top gas is used to preheat the air blast from room temperature to about 1250 °C through combustion. Blast furnace gas can also be used to generate electricity through using its higher pressure, and it can provide approximately one-third of electricity required for blast compression. The COG from coking plant is used as gaseous fuel in the sintering plants, the rolling mill furnaces, and sometimes in the power station. The sensible heat of slag is so far not being used in the industry, but there are active R&D efforts for recovery of sensible heat of blast furnace slag.

1.1.7.2. Mass and Energy Balance: Blast Furnace Operating Conditions

The thermal or enthalpy requirements in the blast furnace must be high enough to melt the iron and slag and to maintain a large reduction zone. Energy needs to be introduced to the blast furnace to make up the net enthalpy deficit caused by the transformation of hematite into iron, the heating and melting of the raw materials, and heat loss of the furnace. The energy comes from the hot blast introduced at the tuyeres and the gasification of carbon in the raceway.

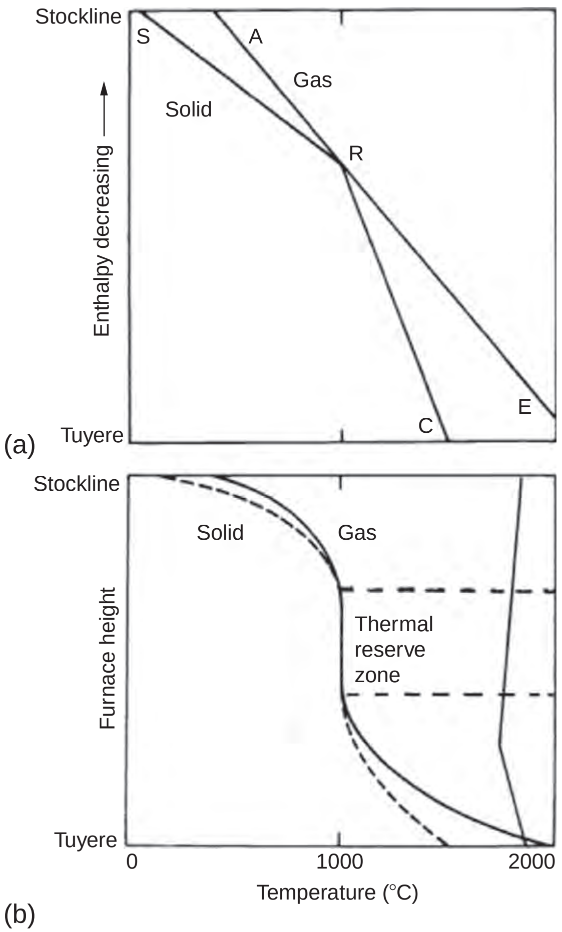

Figure 1.1.32 Illustration of Reichardt diagram; (a) Enthalpy of the gas and solid as a function of temperature; (b) Temperature of the gas and solid along the furnace height [40].

The heat requirement of the blast furnace can be graphically displayed with the Reichardt diagram [40]. Figure 1.1.32 illustrates a simplified version of the Reichardt diagram. The Reichardt diagram shows a plot of enthalpy of the gases and the burden against temperature along the stack. As a result of heat transfer, the enthalpy of the gas decreases with decreasing temperature of the ascending gas, where the enthalpy of the solids increases with increasing temperature during the descent in the blast furnace bed. In the lower part of the furnace, the heat capacity of the burden increases because of the heat required for the direct reduction of wüstite, softening and melting of the ferrous burden materials, and due to greater heat losses.

The carbon and hot blast needed to produce the required heat for the production of iron from iron ores can be described in a mass balance. The calculation of the quantities of

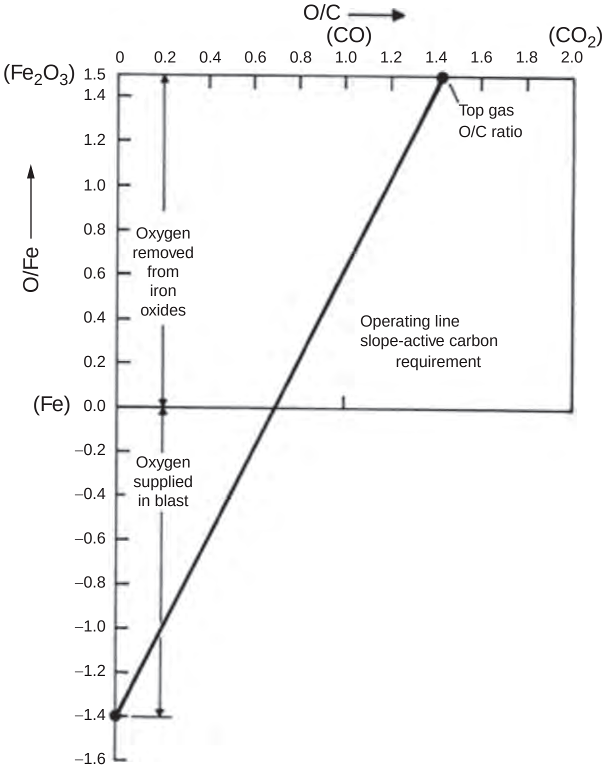

Figure 1.1.33 Illustration of Rist diagram [15].

reactants and products from the chemical reactions inside the blast furnace is called blast furnace stoichiometry.

The combination of stoichiometry and heat requirement of the furnace makes it possible to calculate the quantities of coke and blast air needed to produce iron from any given ore. When changes are made to operation conditions, the effect of the changes on coke and blast requirements can be determined [15].

The Rist diagram is designed to give a graphical representation of a heat and mass balances in the blast furnace [40]. Figure 1.1.33 illustrates the Rist diagram [15]. In the Rist diagram, the operating line is given based on stoichiometry of the blast furnace. The operating line is fixed by enthalpy requirements and process data.

The graphical representation of the heat and mass balance makes it easy to get basic information of the blast furnace process. The degree of reduction at which the direct reduction starts can be determined from the Rist diagram. The intersection of the operating line with the line O/C = 1 gives the O/Fe ratio at which the direct reduction starts. The composition of the gas that has passed through the blast furnace bed, top gas, can be determined. The top gas ratio can be read from the intersection of the operating line with

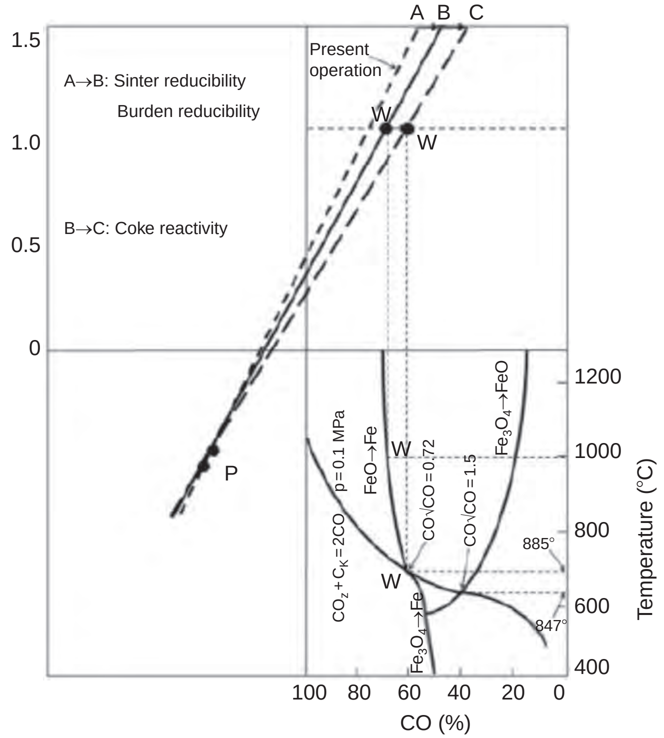

Figure 1.1.34 RIST operating diagram combined with Bauer–Glaessner equilibrium diagram and Boudouard reaction at 1 atm [41].

O/Fe = 1.5. In Figure 1.1.33, the O/C line between 1 and 2 is expressed in the CO utility of the top gas. The top gas utility is a parameter to express the efficiency of the blast furnace operation.

Furthermore, the Bauer–Glaessner equilibrium diagram is sometimes embedded into the lower right corner of the Rist diagram to show the constraints of Fe–O–C equilibrium temperature, as is illustrated in Figure 1.1.34 [41].

The diagram given in Figures 1.1.33 and 1.1.34 assumes that the iron ore is pure hematite. The oxygen removed from the iron ore is presented in the top part of the diagram. The amount of oxygen in the hot blast is given in the bottom part of the diagram.

Figure 1.1.35 shows the Rist–Schurmann diagram [27]. The left figure shows oxygen removal from pure Fe_2O_3 to metallic iron based on 1000 kg iron, according to countercurrent principle. The figure on the right illustrates the influence of CO gas utilization efficiency on the oxygen removal (the Rist–Schurmann diagram). The vertical shaded lines are determined by the equilibrium constant for the reduction reactions. The horizontal shaded lines are based on the weight of the different iron oxide configurations and the amount of oxygen needed to be removed. Hematite is represented by line d–d′,

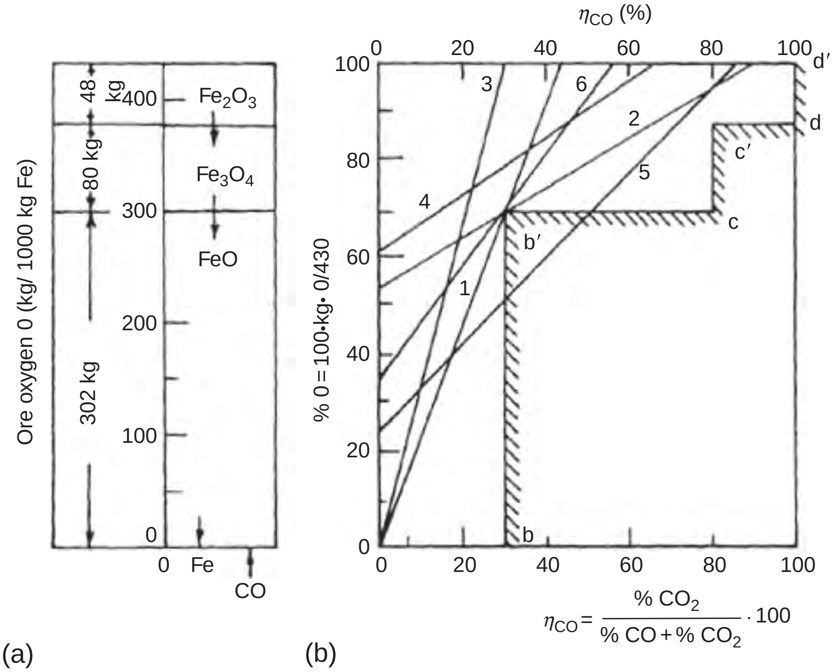

Figure 1.1.35 Rist–Schurmann diagram [27]: the removal of oxygen from pure Fe_2O_3 to 1000 kg Fe according to counter-current principle (left) and indirect reduction and CO-utilization for the various oxide phases (right).

magnetite is represented by line c–c′ and wüstite by line b–b′. From Figure 1.1.35, it can be seen that most of the oxygen needs to be removed from wüstite by the reduction reaction to produce iron. Therefore most coke is consumed by the reduction of wüstite in respect to hematite and magnetite.

In Figure 1.1.35, six operating lines are drawn. Line 5 crosses the shaded lines, which means the reduction reaction of wüstite does not take place. The ideal operating line approaches point b′ as close as possible and has a relative small proportion of its wüstite reduced to iron via direct reduction. In practice, the operating line will never hit point b′.

1.1.7.3. Blast Furnace Performance

The performance of ironmaking blast furnace can be characterized in different ways. Specific coke or fuel consumption (equivalent coke rate: kg/THM), fuel efficiency, smelting rate or output–productivity, are commonly used to evaluate the blast furnace performance. Blast furnace coke and fuel rate has been discussed extensively in the previous section. In this section, fuel efficiency and productivity will be briefly discussed.

1.1.7.3.1 Fuel Efficiency

Fuel efficiency is defined as the utilization percentage of reducing gas (CO and H_2): their conversion to CO_2 and water vapor (H_2). Since H_2 is present in the blast furnace together with carbonaceous fuel, the fuel efficiency should be defined as (η_{CO,H_2}) in Equation (1.1.51) [27]:

$$\eta_{CO,H_2} = \frac{CO_2 + H_2O}{CO + H_2 + CO_2 + H_2O} \tag{1.1.51}$$

Or quite often it is simplified as CO and CO_2 ratio in practice.

$$\eta_{CO} = \frac{CO_2}{CO + CO_2} \tag{1.1.52}$$

The determination of fuel efficiency is made through the measurement of chemical compositions of the top gas, and thus the top gas analysis gives a reasonably accurate indication of the fuel efficiency as well as the furnace efficiency. As can be seen clearly that the less CO and H_2 remaining in the top gas, the higher the fuel efficiency. Although the CO and H_2 in the top gas can still be used as secondary fuel, they have lost their reducing function in the blast furnace process, unless it is reintroduced back to the blast furnace again. This is the basis of the concept of TGRBF, which will be discussed later in Section 1.1.9. Modern blast furnace can reach a fuel efficiency of about 50%, according to the top gas composition, is illustrated in Figure 1.1.29.

Fuel efficiency is influenced by the proportion of direct and indirect reduction of iron oxides. As described in Section 1.1.6, direct reduction has only 50% use of the reducing power of carbon, at the same time is more endothermic and thus requires more thermal energy. Figure 1.1.36 illustrates a clear dependency of the fuel efficiency on the indirect reduction ratio [27].

1.1.7.3.2 Blast Furnace Productivity and Performance

Blast furnace productivity depends on the fuel efficiency and flow of materials and gases through the dry and wet zones of the furnace. Therefore, good gas permeability of the burden and proper control of direct reduction are important for obtaining a high furnace productivity.

Productivity (THM/day) depends on the amount of carbon burned in unit time at the tuyeres and the tuyere carbon (coke) consumed for producing a unit of iron, i.e., productivity is a function of the gas generated at the tuyeres in unit time and that required to produce a unit of iron [27]. The modern large blast furnace can reach a productivity of 10,000–13,000 THM/day with an inner volume of 4500–5500 m^3. However, the productivity from this definition depends very much on the size of the furnace, and cannot be used to measure the furnace performance, the specific productivity.

Other used performance indices are [27]:

- *area efficiency*, THM/m^2 day in the range of 65–70, specific hot metal production per unit area of the hearth per day (used mostly in Europe and America).

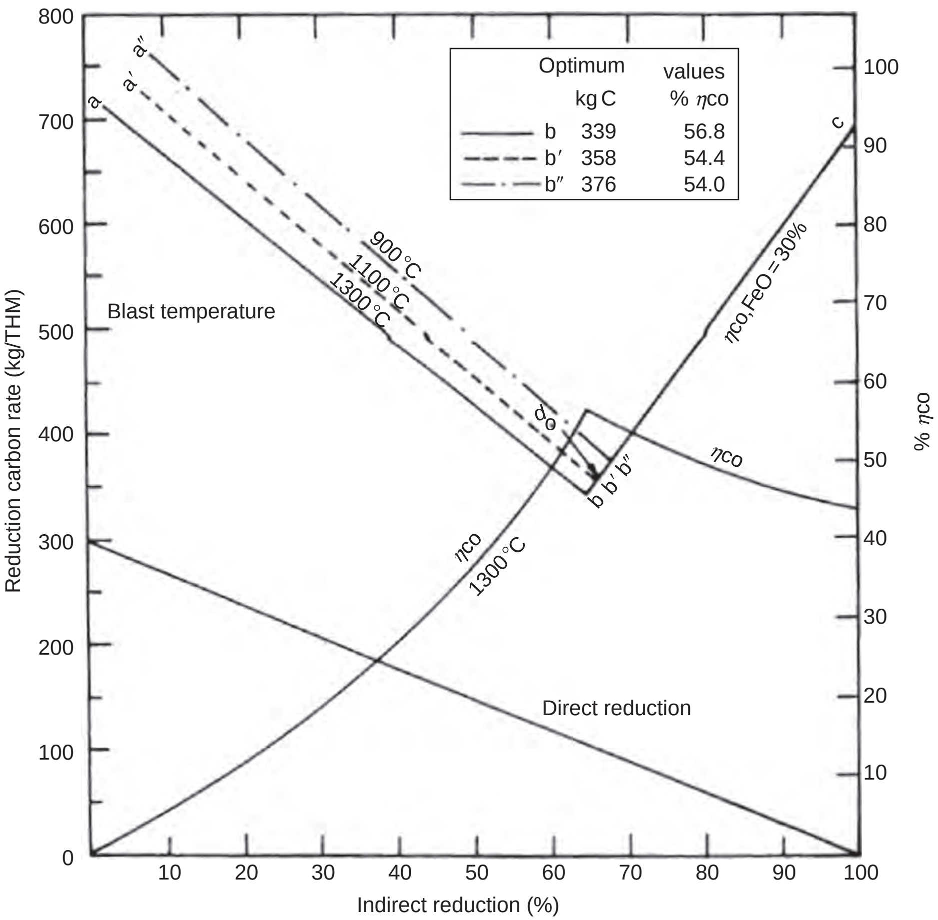

Figure 1.1.36 Variation of reduction carbon rate and fuel efficiency with indirect reduction for three blast temperature levels [27].

- *volume efficiency*, THM/m^3 day in the range of 1.4–3.5 (used mostly in America and former USSR), based on furnace volume calculated from the height taken from tuyere axis to 1 m below the tip of the bell in open position (America) or from the iron notch to the tip of the bell in open position (former USSR).
- *furnace volume utilization coefficient* (KIPO), m^3/THM day (used in the former USSR) in the range of 0.7–0.3.

The above characterization does not take into account specific coke (carbon) consumption, and in combination of coke rate, the performance of blast furnace can be evaluated. Tables 1.1.9 and 1.1.10 list the characteristics and operating conditions of some modern ironmaking blast furnaces in the world.

Table 1.1.9 Characteristic Data for Modern Large Ironmaking Blast Furnaces [39]

	Japan		**Germany**	**France**
	No. 2 Oita NSC	**No. 1 Kakogawa Kobelco**	**No. 2 Schwelgern Thyssen-Krupp Stahl AG**	**No. 4 Dunkerque SOLLAC**
Year of construction	1976	1970	1993	1973
Blown in date after last relining (month/year)	12/88	1/88	10/93	11/87
Hearth diameter (m)	14.9	14.1	14.9	14.0
Inner volume (m^3)	5245	4550	5513	4333
Number of tuyeres	40	40	42	40
Number of tap holes	4	4	4	4
Bell and hopper arrangement[a]	2 B+V	4 B	PW	PW
Top gas pressure (bar)	3.5	3.0	3.8	3.1
Hot blast stoves (number-type)[b]	4/ECS	4/ECS	3/ECC	4/ECC
Blast blower	Electr.	Electr.	Electr.	Electr.
Gas cleaning[c]	DC/ 2VS	C BF	DC C VS	DC VS C
Production (t/day)	11,800	9000	11,573	8640
Productivity on hearth area ($t/m^2/day$)	67.7	57.7	66.4	56.1
Net burden weight (kg/THM)	–	1570	1596	1614
Slag volume (kg/THM)	307	260	262	290
Coke rate (dry) (kg/THM)	331	315	341	309
Pulverized coal injection (dry) (kg/THM)[d]	142	230	131	179
Blast temperature (°C)	1196	1195	1170	1221
Blast volume (standard conditions) (m^3)	980	1010	924	914
Oxygen enrichment (%)	2.6	2.9	3.7	3.5

[a] B, bell; V, valves; PW, Paul Wurth top without a bell.
[b] ECS, external combustion stack; ECC, external combustion chamber.
[c] DC, dust catcher; VS, venturi scrubber; BF, bag filter; C, cyclone.
[d] THM, ton of hot metal.

Table 1.1.10 Operational Characteristics of Some Blast Furnaces in the World [38]

Parameter	Posco (Korea) BF 6	Tata Steel Europe (Netherlands) BF 6	Kimitsu 3 (Japan)	Nippon Steel (Japan)	G Blast Furnace (Tata Steel)
Production (t/day)	8600	7586	10,233	10,051	5150
Inner volume (m^3)	3800	2678	4450	4063	2648
Working volume (m^3)	3225	2328	3790	NA	2308
Productivity (t/m^3/day)[a]	2.66	3.37	2.7	2.47	2.2
Top pressure (kg/cm^2)	2.5	1.64	2.25	2.2	1.3
Oxygen enrichment (%)	106/2.0	13.2	4.0	2.4	4.6
Burden, % sinter (S)	85(S)	48.2(S)	50(S)	93(S)	70(S)
Ore (O), pellets (P)	15(O)	48.8(P)	50(P)	7(P)	30(O)
Al_2O_3 in sinter (%)	1.85	1.24	1.54	1.84	2.4
Coke ash (%)	11	11.3	9.5	10.2	15.4
Coke rate (kg/THM)	390	268	365	392	410
PCI rate (kg/THM)	100	233	125	71(oil)	120
Slag rate (kg/THM)	320	203	236	286	300
Al_2O_3 in slag (%)	14	15.1	16.7	15.3	19.2
Blast temperature (°C)	1200	1162	1180	1278	1080

[a] Productivity is based on working volume.

Remark: The code and name for blast furnace in Netherlands have been updated and corrected as "Tata Steel Europe (Netherlands) BF 6" by the current author.

1.1.8. PROCESS INSTRUMENTATION AND CONTROL

1.1.8.1. Process Control Structure

Blast furnace instrumentation has advanced dramatically in the past 50 years. As productivity demands on blast furnace increased and the fuel rates decreased, it became critical to monitor and understand more data for the process. New and improved instrumentation devices were invented and installed throughout the industry. The shared knowledge has enabled blast furnace operators and engineers to accomplish dramatic production increases, to lower the reductant rate, to introduce new types of energy sources (for better economy and environmental issues), and ultimately lead to better designs and control of the blast furnace process.

The modern blast furnace control system can be divided into several discrete layers to effect information and control of the blast furnace process, as is illustrated in Figure 1.1.37, and can be further described below [42]:

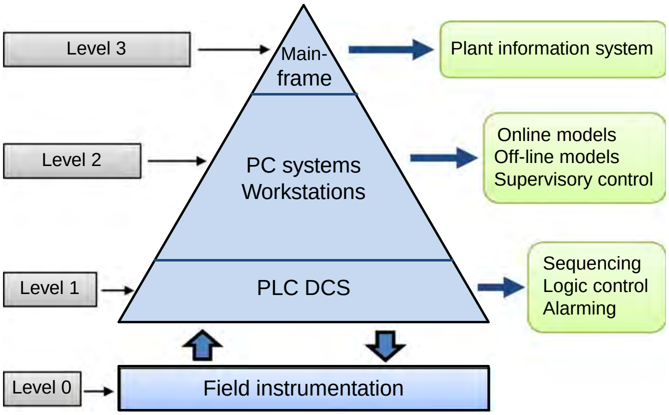

Figure 1.1.37 Process control structure [42].

- The first layer of the architecture comprises the field devices, referred to as Level 0. These are actual instruments, valves, motors, etc., which measure and control the pressures, flows, temperatures, positions, and analyses of the process.
- The second layer is the programmable logic controller and/or distributed control system, referred to as Level 1. On this level, the raw field data is initially processed. The information to and from the field devices is interfaced with this area where sequencing, logical control, instrumentation monitoring, alarming, first level diagnostics, and operation of the different areas of the blast furnace process are accomplished. The operators communicate with Level 1 via man–machine interface (MMI), which is typically personal computers and control panels. The MMIs are sometimes referred to as Level 1.5 as they could interface with both Level 1 and Level 2 systems. With PC- or workstation-based MMIs, supported by modern control software and the widely used TCP/IP as well as UDP/IP (User Datagram Protocol) networking, the operators can access all areas of the blast furnace plant via graphical screens that allow the operation and monitoring of the process in the remote control rooms.
- The third layer, referred as Level 2, is where the basic knowledge of the process is located. Models for controlling and optimizing the process through rule-based algorithms and parameter changes are located in this area. Typical process models found in Level 2 systems in blast furnaces include burden distribution, burden charging calculation, silicon prediction, hearth iron level prediction, refractory wear analysis, stove optimization, and heat and mass balances.
- The highest level associated with the blast furnace is Level 3, which forms part of the entire plant information system. The primary function is for business functions such as record keeping, order entry, quality requirements, order status, and management functions. Furthermore, artificial intelligence and expert system have been developed for online diagnosis of actual state of the furnace, which gives recommendations to maintain the blast furnace at its optimum operating point.

1.1.8.2. Blast Furnace Instrumentation

Figure 1.1.38 illustrates the instrumentation of modern blast furnaces, with sensors for temperature of solid feed, gas, refractory walls, pressure of blast at various levels, and instruments for burden profile and stock movement [42].

- Thermocouples are installed in the refractories at various locations to minor the conditions of the refractory.
- Pressure taps are located in the bustle pipe to monitor blast pressure and at different elevations of the furnace shaft to add in monitoring the permeability of the burden and the location of the cohesive or melting zone.
- A retractable below-burden probe is inserted for monitoring the temperature and composition of the gas in the shaft of the furnace. These data are used for modifying burden distribution changes and monitoring furnace efficiency.
- Fixed above-burden probes are employed to measure gas temperature to monitor gas patterns through the burden.
- A transverse radial profile meter measures the top surface of the burden material after initial charging to the top of the furnace.

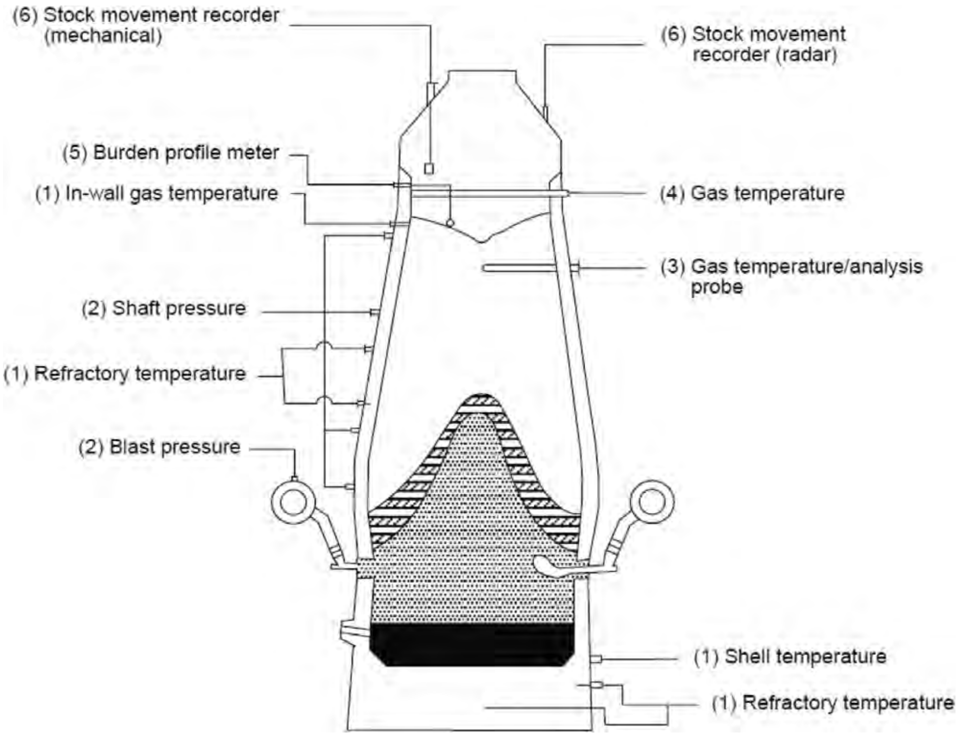

Figure 1.1.38 Blast furnace instrumentation [42].

- Stock movement sensors, either mechanical weights or radio wave type sensors, monitor the descent of the burden and essentially give the room for charging additional material into the furnace.

A blast furnace plant is a collection of unique subsystems: the raw materials handling and charging system, the furnace refractory condition and cooling system, the stove system, the cold and hot blast system, the gas cleaning and distribution system, the casting system, and the smelting process system.

The advance of technology, coupled with the increasing acceptance of the reliability of the instrumentation and control logics, is moving the process control of ironmaking to greater and greater levels of systems. These advanced systems not only monitor the process, but also change parameters, alert operators to undesirable conditions and potential area for inspection, and recommend changes to the process.

1.1.9. FUTURE TRENDS IN IRONMAKING

1.1.9.1. Challenges in Blast Furnace Process

Iron has been made in blast furnaces for more than 500 years. During that time, the blast furnaces have evolved into highly efficient reactors. At present, the blast furnace is still the dominant pig iron production unit, with several hundred units in operation worldwide. The blast furnace has a long history, and modern blast furnaces are highly effective and energy-efficient reactors.

However, blast furnaces require coke, and coke plants are expensive and have many environmental problems associated with their operation. Therefore, other techniques are now available which present a challenge to the blast furnace route for pig iron production, such as direct reduction and smelting reduction processes.

The injection of carbon-bearing reductants at the tuyere level has given new impetus to blast furnace operational practice to reduce the coke consumption significantly. Not only pulverized coal can be injected, gaseous reductants such as natural gas and waste plastics and biomass are used as reductants injected through tuyeres. Furthermore, oxygen-enriched air can be used to increase the efficiency and maintain relatively high temperature of the raceway. However, coke can never be fully replaced in a blast furnace because of its burden supporting function. The minimum blast furnace coke rate is assumed to be approximately 200 kg/t hot metal.

The following aspects put pressure on the blast furnace production route of steelmaking:

- Environmental aspects of sinter plants;
- Environmental and economic aspects of the coke oven plant;
- Relative inflexibility and scale of the pig iron production and massive integrated steel plants, in general;

- Increasing competition by the scrap- or DRI-based EAF steelmaking route, due to the pressure caused by global warming to decrease CO_2 emissions from iron/steelmaking.

A detailed evaluation of blast furnace ironmaking can be found in a recent review [43].

1.1.9.1.1 New Developments in Blast Furnace Ironmaking

1.1.9.1.1.1 Top Gas Recycle Blast Furnace

TGRBF is one of the research subprojects in the ULCOS program [44]. TGRBF uses oxygen instead of air, enabling the unwanted nitrogen compound to be eliminated and hence concentrating the top gas with CO_2. The mix of CO_2, CO, and H_2 from the top gas is sent to the gas separation plant to remove CO_2 and to recover CO and H_2, which can be recycled back into the furnace and reused as reducing agents. This would reduce the amount of coke needed in the furnace. In the framework of the ULCOS subproject, this concept has been successfully tested in 2007 at the LKAB's Experimental Blast Furnace in MEFOS Lulea, Sweden [45]. Vacuum pressure swing adsorption (VPSA) process was provided by Air Liquide to separate CO_2 from the top gas. VPSA unit operated successfully and reliably for the period of 7 weeks. From the first ULCOS campaign there was a CO_2 reduction of 24% in the BF due to CO_2 removal and top gas recycling. If CO_2 storage is applied, the emissions could be halved [46]. For further scaling up of TGRBF, the first operation in the mode with CO_2 storage is expected in 2016 at Florange and in the mode without CO_2 storage in 2014 at Eisenhüttenstadt during the second phase of ULCOS program.

1.1.9.2. New Ironmaking Processes

Two main types of commercial alternative ironmaking processes are available:

(1) *Direct reduction (DR)*: Direct reduction involves the production of solid iron from iron ores and a reducing agent (e.g., natural gas). The solid product is called DRI and is mainly applied as feedstock in EAF. The direct reduction process has been commercialized since the 1970s and a variety of processes have been developed.

(2) *Smelting reduction (SR)*: This involves combining iron ore reduction with smelting in a reactor, without the use of coke. The product is liquid pig iron, which can be treated and refined in the same way as hot metal from the blast furnace. Today, only one variant of SR is commercially proven (COREX), but a number of variants are in an advanced stage of development.

1.1.9.2.1 DRI Processes

Several methods have been used over the past 50 years to produce DRI [43,47,48]. In practice, two major processes are currently operating in large production namely MIDREX and HyL/Energiron (HYL III), which are based on (natural) gas reduction in shaft furnaces. Approximately 92% of the DRI is produced by using (reformed) natural gas as a fuel. Furthermore, in a significant number of sites, coal is used as a fuel in rotary kiln or rotary hearth furnaces (for example, SL/RN and iron dynamics). Additionally, lot of efforts have been put to develop fluidized-bed technologies to directly reduce fine ore concentrate by gas (FINMET, CIRCORED), which is the most advanced principle but has met serious practical problems due to sticking tendency in the final stage of reduction.

World DRI production has seen continuous growth since the year 1970, and by 2011 the total production reached 73.3 million tons [49]. Among various DRI processes, MIDREX dominates the market accounting for almost 60% of the total DRI production (MIDREX 44.4, HYL/EnergIron 11.1, Finmet 0.5, Coal-based 17.3 million tons in 2011, respectively). The total share of the DRI in the world crude steel production is about 5%, while the blast furnace hot metal account for 60% and steel scrap for the rest.

1.1.9.2.1.1 The MIDREX Process

Gas-based direct reduction processes are particularly suitable for installation in those areas where natural gas is available in abundance and at economical prices. The MIDREX process is a shaft-type direct reduction process where iron ore pellets, lump iron ore or a combination are reduced in a Vertical Shaft (reduction furnace) to metallic iron by means of a reduction gas (see Figure 1.1.39) [9].

The reducing gas is produced from a mixture of natural gas (usually methane) and recycled gas from the reduction furnace. The mixture flows through catalyst tubes where

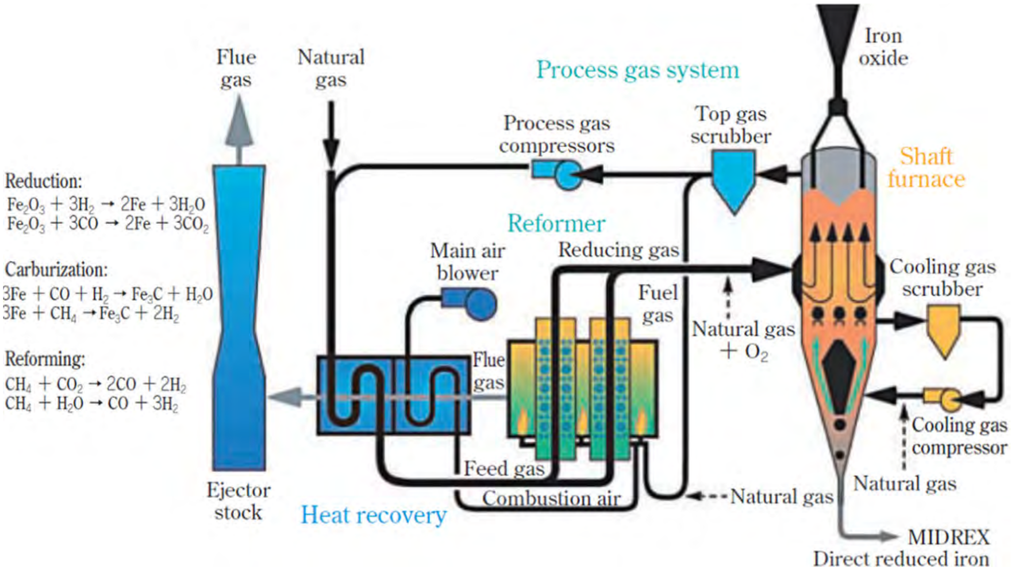

Figure 1.1.39 Process flow sheet of the MIDREX process [9].

it is chemically converted into a gas containing hydrogen and carbon monoxide. The desired reducing-gas temperature is typically in the range of 900 °C. The gas ascends through the reduction shaft in the counter-current direction and removes oxygen from the iron carriers. The product, DRI, typically has the total iron content in the range of 90–94% Fe. After the DRI exits from the bottom of the shaft, it can be compressed in the hot condition to HBI for safe storage and transportation. DRI or HBI are virgin iron sources free from tramp elements and are increasingly being used in EAF to dilute the contaminants present in the scrap.

The first commercial-scale MIDREX Direct Reduction Plant began operation in 1969 at Oregon Steel Mills in Portland, Oregon. There are now over 60 MIDREX Modules operating, under construction, or under contract in 20 countries. The scale of MIDREX plants continues to grow and today MIDREX has built the largest single module DR Plant in the world at Hadeed in Saudi Arabia, with a rated capacity of 1.76 million tons/year. A more detailed description of direct reduction processes can be found in Chapter 1.2.

1.1.9.2.2 Smelting Reduction Processes

Several smelting reduction processes are in development and only one process is currently operating on a commercial basis: COREX. Other process variants differ in the number of reactors, the amount of calorific gas produced, the ore feed (pellet, lump ore, or fines), and examples are HIsmelt, DIOS, ROMELT, AISI-DOE/CCF, and HIsarna [43,50].

1.1.9.2.2.1 COREX Process [50]

The COREX process is a two-stage process, as is shown in Figure 1.1.40. In the first step, iron ore is reduced to sponge iron in a shaft furnace by means of reducing gas. In the second step, the reduced iron is melted in the melter–gasifier vessel. Reducing gas (CO and H_2) used in the reduction shaft is supplied by gasification of coal by means of oxygen, forming a fixed or fluidized bed in the melter–gasifier. The partial combustion of the coal in the melter–gasifier generates the heat to melt the reduced iron. Liquid iron and slag are discharged at the bottom, by a conventional tapping procedure similar to that used in blast furnace operation.

Because of the separation of iron reduction and iron melting/coal gasifying in two steps, a high degree of flexibility is achieved and a wide variety of coals can be used. The process is designed to perform at elevated pressure, up to 5 bar. Charging of coal and iron ore is performed through a lock hopper system. The reducing gas contains 65–70% CO, 20–25% H_2, and 2–4% CO_2. After leaving the melter–gasifier, the hot gas is mixed with cooling gas to adjust the temperature to approximately 850 °C. The gas is then cleaned in hot cyclones and fed into the shaft furnace as a reducing gas. When the gas leaves the shaft furnace, it still has a relatively high calorific value and may be used as an export gas where the opportunity exists.

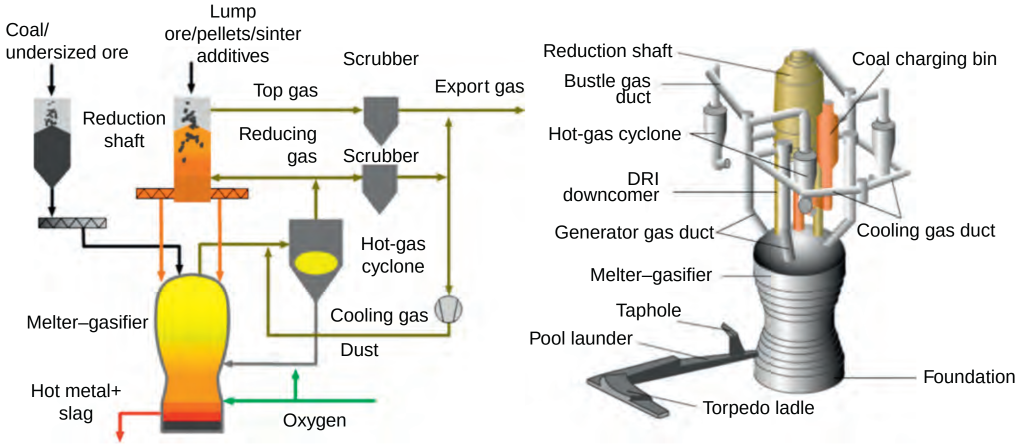

Figure 1.1.40 Process flow sheet of the COREX process (left) and schematic view of the COREX reactor (right) [22].

The COREX process was developed in the late 1970s at Alpine Industrieanlagenbau (VAI, now Siemens-VAI), and its feasibility was confirmed during the 1980s. Following the first industrial application of a COREX C-1000 plant (nominal production of 1000 THM/day) at Iscor Pretoria, South Africa, four C-2000 plants (nominal production of 2000 THM/day) were subsequently put into operation at Posco/Korea, Mittal Steel/South Africa and at JSW Limited/India. In early November 2007, the first COREX C-3000 plant was started up at Baosteel, China. It has a nominal production capacity of 1.5 million THM/year.

Recently a variant of COREX process, FINEX, is codeveloped by VAI and Posco for the production of hot metal based on the direct use of iron ore fines and noncoking coal. Fine iron ore is charged into a series of fluidized-bed reactors together with fluxes. The iron ore fines pass in a downward direction through four reactors where they are heated and reduced to DRI by means of a reduction gas—derived from the gasification of the coal—that flows in the counter-current direction to the ore. The first commercial FINEX plant with a capacity of 1.5-million-ton/year started operation at the Pohang Works since early 2007.

Figure 1.1.41 shows the comparison of raw materials and process steps for COREX and FINEX with conventional blast furnace process [10].

1.1.9.3. New Developments of Ironmaking Technologies

In Europe and Japan, active developments take place for new generation of ironmaking technologies, aiming at drastic CO_2 reduction: European program ULCOS and Japanese program COURSE 50.

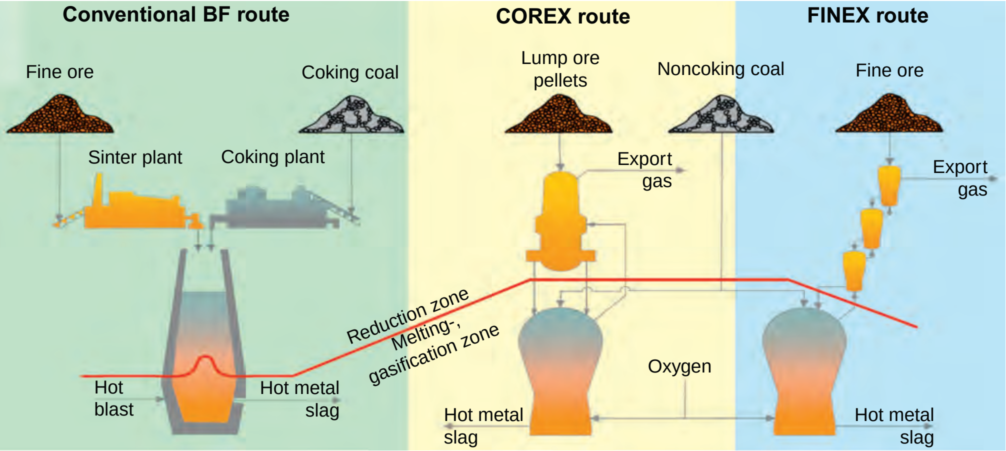

Figure 1.1.41 Comparison of COREX and FINEX with blast furnace process [10].

1.1.9.3.1 ULCOS: Ultra–Low Carbon Dioxide (CO_2) Steelmaking (EU)

ULCOS stands for Ultra–Low Carbon dioxide (CO_2) Steelmaking [44]. It is a consortium of 48 European companies and organizations from 15 European countries that have launched a cooperative research and development initiative to enable drastic reduction in carbon dioxide (CO_2) emissions from steel production. The consortium consists of all major EU steel companies, of energy and engineering partners, research institutes, and universities and is supported by the European commission. The aim of the ULCOS program is to reduce the carbon dioxide (CO_2) emissions of today's best routes by at least 50%. The ULCOS program consists of a series of coordinated projects launched in 2004 and is likely to continue into the 2020s.

The program has examined about 80 different process routes and selected four families of ULCOS solutions based on fossil fuel (coal or natural gas) and CCS or on the direct use of electricity [51]:

- *Top gas recycling blast furnace*: TGRBF, or ULCOS-BF. This is introduced in Section 1.1.9.1.
- *HIsarna*, a smelting reduction process based on a cyclone (CCF) and a bath smelter (close to HIsmelt), has been implemented on an 8 t/h pilot erected in IJmuiden.
- *ULCORED* is a direct reduction CO_2-lean process concept, fully evaluated at modeling level that will be tested on a pilot in a few years.
- *Two electrolysis processes: ULCONWIN* and *ULCOLYSIS*. Both are still at laboratory level. ULCOWIN reduces hematite at 110 °C in a water-based soda electrolyte. ULCOLYSIS is a molten oxide electrolysis process, where iron ore is dissolved in a molten oxide mixture at 1600 °C. Oxygen (O_2) evolves as a gas at the anode and iron is produced as a liquid metal at the cathode.

1.1.9.3.2 COURSE 50 (Japan)

COURSE 50 project was proposed by IISI with six major steel industries and related company in Japan. COURSE 50 stands for "CO_2 Ultimate Reduction in Steelmaking Process by Innovative Technology for Cool Earth 50." Basic idea of COURSE 50 is the use of hydrogen for iron ore reduction and development of cheap hydrogen production technology, as well as CO_2 separation and recovery [52]. COURSE 50 program consists of two major research activities [53].

(1) Development of technology to reduce CO_2 emissions from blast furnaces, involving□ □
  - development of reaction control technology to reduce iron ore by using hydrogen,
  - reforming technology of COG that increases the amount of hydrogen produced, and
  - technology to manufacture high-strength and high-reactivity coke for hydrogen reduction blast furnaces.

(2) Development of technology to separate and recover CO_2, involved with development of a high-efficiency CO_2 absorption method and technology to utilize unused waste heat in steelmaking plants for CO_2 separation and recovery.

REFERENCES

[1] R.F. Tylecote, History of Metallurgy, third ed., The Metals Society, London, 1984, p. 182.
[2] I. Bohm, Den svenska masugnen under 1800-talet (Swedish Blast Furnace in the 19th Century), Jernkontorets forskning, Stockholm, 1972.
[3] M. Weissenbacher, Sources of Power: How Energy Forges Human History, Praeger, Santa Barbara, CA, 2009, p. 194.
[4] W.K.V. Gale, British Iron and Steel Industry, David and Charles, Newton Abbot, 1967, pp. 55–58.
[5] G.R. Bashforth, The Manufacture of Iron and Steel, vol. 1, Chapman & Hall, London, 1957.
[6] M. Asanuma, et al., ISIJ Int. 40 (2000) 244.
[7] World Steel Association, World Steel Fact Sheet: Energy, www.worlsteel.org (accessed in 2012).
[8] AIST, Technology roadmap research program for the steel industry, Final Report, 2011.
[9] M. Atsushi, H. Uemura, T. Sakaguchi, MIDREX Processes, Kobelco Technology Review No. 29, December 2010, p. 50.
[10] W. Grill, The SIMETAL Corex and Finex Process, Siemens VAI—Ironmaking, 2009
[11] World Steel Association, Statistics Archive (Production Figures), www.worldsteel.org (accessed in 2012).
[12] JFE 21st Century Foundation: An Introduction to Iron and Steel Processing, http://www.jfe-21st-cf.or.jp/index2.html (accessed in 2012).
[13] M. Ito, S. Matsuzaki, K. Kakiuchi, M. Isobe, Development of visual evaluation and numerical analysis system of blast furnace, Nippon Steel Technical Report No. 89, January 2004, p. 38.
[14] JFE Steel Corporation, No. 5 Blast Furnace at West Japan Works (Fukuyama) Blown In, http://www.jfe-steel.co.jp/en/release/2005/050331.html.
[15] J.G. Peacey, W.G. Davenport, The Iron Blast Furnace: Theory and Practice, Pergamon Press, Oxford, 1979, p. 251.
[16] V.V. Poltavets, Domennoje proizvodstvo, Metallurgija, Moskva, 1972, p. 283 (in Russian: Blast furnace production).

[17] EBFC—European Blast Furnace Committee, Constructional Features of Blast Furnaces, 2004 (Confidential).
[18] M. Geerdes, H. Toxopeus, C. Van Der Vliet, Modern Blast Furnace Ironmaking—An Introduction, IOS Press, Amsterdam, 2009, p. 164.
[19] A. Babich, D. Senk, H.W. Gudenau, K. Th, Mavrommatis, Ironmaking, RWTH Aachen, Aachen, 2009, p. 402.
[20] SBMA—Mining and Construction Machinery, Iron Ore (iron-ore.shibang-china.com/iron-ore/index.html) (accessed in 2012).
[21] Index Mundi, Iron Ore: World Production by Country, www.indexmundi.com/en/commodities/minerals/iron_ore/iron_ore_table16.html (accessed in 2012).
[22] Y. Yang, A.T. Adema, R. Boom, Blast Furnace Ironmaking, World Steel Association, steeluniversity.org; http://www.steeluniversity.org (accessed in 2012).
[23] T. Leuwerink, A. van der Panne, in: NOXCONF 2001: International Conference on Atmospheric Pollution NO_x and N_2O Emission Control-Panel of Available Techniques, Paris-La Défense, France, March 21–22, 2001, 2001.
[24] Nippon Steel & Sumikin Engineering, Coke Dry Quenching (CDQ), http://www.jase-w.eccj.or.jp/technologies/pdf/iron_steel/S-10.pdf (accessed in 2012).
[25] P.S. Towsey, I. Cameron, Y. Gordon, Iron Steel Technol. 8 (3) (2011) 42.
[26] D. Sert, R. Godijn, Low coke rate and coal injection in excess of 200 kg/THM, Final Report, European Commission, 2002.
[27] A.K. Biswas, Principles of Blast Furnace lronmaking: Theory and Practice, Cootha Publishing House, Brisbane, 1981, p. 528.
[28] Y. Yu, Experimental and Discrete Element Simulation Studies of Bell Less Charging of Blast Furnace, Doctoral Thesis, Åbo Akademi, Åbo, Finland, 2013, p. 60.
[29] R. Nicolle, et al., in: Proceedings of the Sixth International Iron and Steel Congress, ISIJ, Nagoya, 1990, pp. 430–438.
[30] A. Roine, HSC Chemistry 6.1, Outotec Research Oy, Pori, Finland, 2007.
[31] L.C. Woollacott, R.H. Eric, Mineral and Metal Extraction—An Overview, South African Institute of Mining and Metallurgy, Johannesburg, 1994, p. 412.
[32] Y. Omori, Blast Furnace Phenomena and Modelling, The Iron and Steel Institute of Japan (ISIJ) Elsevier, London, 1987.
[33] T. van de Winckel, Reduction Kinetics in the Blast Furnace, M.Sc. Thesis, Department of Geotechnology, TU Delft, The Netherlands, 2008, p. 72.
[34] K. Raipala, On Hearth Phenomena and Hot Metal Carbon Content in Blast Furnace, Doctoral Thesis, Helsinki University of Technology, Espoo, Finland, 2003, p. 83.
[35] H.J. Kerkhoff, in: Welcome to Dusseldorf, Challenges and Opportunities of CO_2 Capture & Storage in the Iron and Steel Industry, Steel Institute VDEh Auditorium, Dusseldorf, Germany, 8–9 November 2011, 2011, (Power Point Presentation).
[36] S. Gupta, V. Sahajwalla, The Scope for Fuel Rate Reduction in Ironmaking: Technical Note 16, CCSD: Cooperative Research Centre for Coal in Sustainable Development, The University of New South Wales, Sydney, January 2005.
[37] NEDO, Clean Coal Technologies in Japan: Part 3A2—Pulverized Coal Injection for Blast Furnaces (PCI), 2006, http://www.nedo.go.jp/content/100080251.pdf.
[38] A. Ghosh, A. Chatterjee, Ironmaking and Steelmaking: Theory and Practice, Prentice-Hall, New Delhi, 2008, p. 472.
[39] H.B. Lüngen, J. Yagi, Iron 2—Blast Furnace Process, Ullmann's Encyclopedia of Industrial Chemistry, Wiley-VCH Verlag GmbH & Co. KGaA, Weinheim, 2012.
[40] P. Grieveson, Pure Appl. Chem. 54 (1982) 1313.
[41] A. Babich, D. Senk, H.W. Gudenau, Ironmaking Steelmaking 36 (2009) 222.
[42] AISE, in: R.J. Fruehan, D.H. Wakelin (Eds.), The Making, Shaping and Treating of Steel—Ironmaking Volume, 11th ed., The AISE Steel Foundation, Pittsburgh, PA, 1999, p. 780.
[43] J. Poveromo, in: Paper for 22nd Blast Furnace Ironmaking Course, McMaster University, Hamilton, May 13–18, 2012, 2012.

[44] ULCOS, Ultra-Low Carbon Dioxide (CO_2) Steelmaking, http://www.ulcos.org (accessed in 2012).

[45] G. Zuo, A. Hirsch, in: Proceedings of the 4th ULCOS Seminar, October 1–2, 2008, 2008.

[46] J. van der Stel, D. Sert, A. Hirsch, N. Eklund, L. Sundqvist Ökvist, in: SCANMET IV—4th International Conference on Process Development in Iron and Steelmaking, vol. 1, Swerea|MEFOS, Luleå, Sweden, June 10–13, 2012, 2012, p. 51.

[47] A. Sawada, T. Miyamoto, Overview of Market for Direct Reduced Iron, Kobelco Technology Review No. 29, December 2010, p. 47.

[48] Industry Efficiency Technology Database, Direct Reduced Iron, www.ietd.iipnetwork.org/content/direct-reduced-iron (accessed in 2012).

[49] MIDREX, 2010 World Direct Reduction Statistics, 2010, http://www.midrex.com (accessed in 2012).

[50] B. Anameric, S.K. Kawatra, Miner. Process. Extract. Metall. Rev. 30 (2009) 1.

[51] J.P. Birat, J. Borlée, H. Lavelaine, P. Négro, K. Meijer, J. van der Stel, P. Sikström, in: SCANMET IV—4th International Conference on Process Development in Iron and Steelmaking, vol. 1, Swerea|MEFOS, Luleå, Sweden, June 10–13, 2012, 2012, p. 35.

[52] S. Matsuzaki, K. Yonezawa, K. Saito, M. Naito, CAMP-ISIJ 22 (2009) 268.

[53] S. Matsuzaki, K. Higuchi, A. Shinotake, K. Saito, in: SCANMET IV—4th International Conference on Process Development in Iron and Steelmaking, vol. 1, Swerea|MEFOS, Luleå, Sweden, June 10–13, 2012, 2012, p. 45.